

TGC2: 00321

Non-Print Items

Abstract:

Subducted crust refertilizes the subarc mantle wedge as well as the deep convecting mantle. In the subarc region, mass transfer occurs mainly through fluids, melts, or supercritical liquids. Experiments show that devolatilization reactions may occur at almost any depth in the chemically complex subducting lithosphere. Extreme temperature gradients across the slab lithosphere, the subduction channel, and the mantle hanging wall promote diachronous fluid production. Fluids are dominated by H₂O, and the temperature of melting is controlled by the availability of H₂O and CO₂. The exact nature of the transfer agent and its composition depends on the source lithologies and the temperature regime, which vary significantly between different subduction zones. Nevertheless, *P-T* paths calculated from mechanical subduction-zone models suggest that, in most subduction zones, the subducted crust remains at subsolidus conditions in the subarc regime. In a few, the pelitic solidus is overstepped, and fluid-saturated melting may be induced by flushing of H₂O derived from more deep-seated metamorphic reactions. A steady volatile flow into the subarc wedge does not imply a steady supply of most trace elements, because low temperatures prevent diffusive equilibration, and, thus, the reactive volumes, in combination with the residual minerals formed through the devolatilization reactions, determine the efficiency of trace element transfer to the mantle wedge.

Three main lithologies contribute to the devolatilization signal: peridotites, the mafic oceanic crust, and pelitic sediments + eroded continental crust, all three of which may contain carbonates that were added through hydrothermal or sedimentary processes. Most of the subducted CO₂ survives the subarc regimen, while most of the H₂O is lost to the subarc mantle, making CO₂ the dominant volatile that is transported into the deeper mantle. At > 200–250 km depth, a fairly high temperature stability of hydrous phases relative to a typical subduction *P-T* path, in combination with relatively low melting temperatures for carbonated lithologies, leads to the possible formation of carbonatites within the subducting crust.

Finally, examination of volcanic arcs worldwide reveals that their position is controlled not by devolatilization from the slab, but mainly by convection in the mantle wedge, which generally does not reach steady state, and to a minor extent by the structure of the overriding plate.

Keywords: Devolatilization; Lithosphere; Subduction

Author and Co-author Contact Information:

Au6

M.W. Schmidt
ETH Zürich
Zürich
Switzerland
E-mail: max.schmidt@erdw.ethz.ch

S. Poli
Università degli Studi di Milano
Milan
Italy
E-mail: stefano.poli@unimi.it

Au5 a0010

321 Devolatilization During Subduction

Au1,29

MW Schmidt, ETH Zürich, Zürich, Switzerland
S Poli, Università degli Studi di Milano, Milan, Italy

© 2013 Elsevier Ltd. All rights reserved.

321.1	Introduction	1
321.2	Setting the Scene	3
321.2.1	The Oceanic Lithosphere Before Subduction	3
321.2.2	Accretion Versus Erosion	4
321.2.3	Rock Hybridization at the Slab–Mantle Interface	5
321.2.4	Continuous Versus Discontinuous Reactions	5
321.2.5	Fluid Production	6
321.2.6	Fluid Availability Versus Multicomponent Fluids	7
321.2.7	Real-World Effects	8
321.3	Devolatilization Regimes in MORB	9
321.3.1	High Dehydration Rates and Fluid Production (Typically to 600 °C, 2.5 GPa)	9
321.3.2	Low Dehydration Rates and Little Fluid Production (2.5–10 GPa and 500–800 °C)	10
321.3.3	Melting Regimes (650–950 °C to 5 GPa)	11
321.3.3.1	Fluid-saturated (flush) melting	12
321.3.3.2	Fluid-absent melting	12
321.3.4	Dissolution Regime (>5–6 GPa)	15
321.4	How Much H₂O Subducts into the Transition Zone?	16
321.5	Devolatilization in Sediments	16
321.5.1	Pelites + H ₂ O	16
321.5.2	Graywackes and Volcanoclastic Sediments	18
321.5.3	Carbonated Pelites	18
321.5.4	High-Pressure Melting Systematics of Sediments and MORB	18
321.6	Serpentinized Peridotite	20
321.7	Implications for Trace Elements and an Integrated View of the Oceanic Lithosphere	21
321.7.1	Mobile Phase Production and Trace Element Transfer	21
321.7.2	Integrating Fluid Flux over the Entire Subducted Oceanic Crust: An Example	23
321.8	Dents in a Simplified Subduction Model	24
321.8.1	Predicting Element Transfer and the Role of Sediments	24
321.8.2	The Formation of the Volcanic Arc	24
321.8.3	Concluding Remarks	28
References		29

s0010 321.1 Introduction

p0010 Subduction zones constitute the geotectonic environment where the volatile-rich magmas that ultimately yield highly explosive arc volcanoes are generated, where the subarc mantle is refertilized, where many heterogeneities of the deep mantle originate, and where the continental crust is formed. Subduction itself consumes oceanic, and to a more limited extent, continental crust. The recycling of crust replenishes the mantle with a suite of litho- and hydrophile elements that otherwise would, with time, become strongly depleted in the mantle. Subduction has, thus, a major role in maintaining Earth's magmatic environments and tectonic style over geologic history. In order to understand the recycling process, it is necessary to understand the reactions that occur during subduction, in particular, those that allow for transfer of material from the subducting lithosphere to the mantle wedge.

p0015 Prograde metamorphism of subducting oceanic crust causes a series of fluids or melts involving mineralogical reactions that

inevitably result in eclogites that may or may not contain hydrous phases and/or carbonates. Alternating continuous and discontinuous reactions cause devolatilization, yielding a mobile phase. This mobile phase may be a low-density fluid, a high-density solute-rich fluid, a silicate melt, or a carbonatite melt. This chapter reviews the reaction mechanisms and conditions resulting in the generation of the various mobile phases and also examines the restite(s) that are subducted to great depths.

In general, four different regimes can be recognized in the oceanic crust to depth equivalents of 10 GPa that produce fluids or melts (**Figure 1**):

1. *High dehydration rates* at low to medium P , low T (<2.5 GPa, <600 °C), where hydrous phases are abundant and dehydration reactions are often perpendicular to typical subduction geotherms. All subducted lithosphere goes through this first stage, which produces low-density, dominantly aqueous fluids that have small to moderate CO₂ fractions in the presence of carbonates.

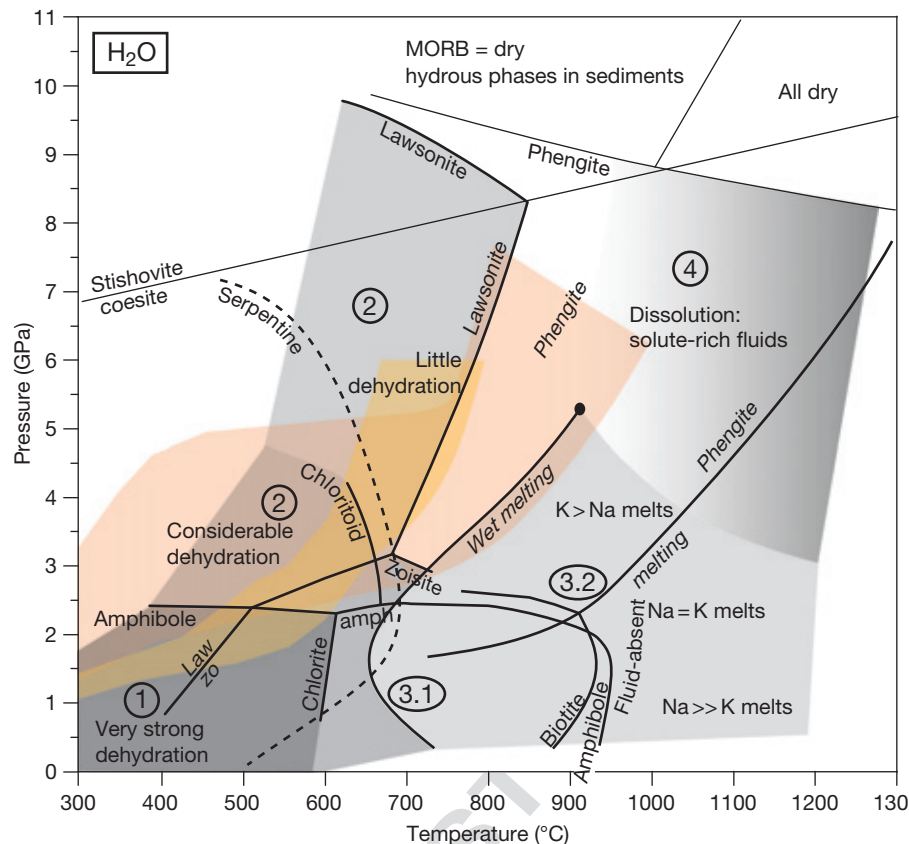


Figure 1 Devolatilization regimes during subduction, mainly based on phase relations in MORB (compare with **Figure 3**). Numbers in ovals refer to the subsections in **Section 321.3**. The P - T region with high dehydration rates (marked 1) is bounded by the amphibole stability and the wet solidus; the P - T region with less dehydration (marked 2) is bounded by zoisite and lawsonite stabilities. H_2O -saturated melting takes place in MORB and sediments at the wet solidus; fluid-absent melting to 2.5 GPa is dominated by amphibole (MORB) or biotite (pelite) and above 2.5 GPa by phengite (only in pelites). The classic melting regime (marked 3) is replaced by a continuous dissolution of hydrous phases in a solute-rich liquid at higher pressures (compare to **Figure 4**). The serpentine stability field in peridotite (dashed line) is given for reference (compare to **Figure 5**). The yellow and orange fields mark P - T paths for average cold (yellow) to intermediate (orange) thermomechanical subduction models of Arcay et al. (2007) and the warm W1300-model of Syracuse et al. (2010), respectively.

- 00015 2. Medium to low dehydration and low decarbonation rates at medium to high P , low T (2.5–10 GPa, 500–800 °C), where hydrous phases are already largely reduced in volume and dehydration reactions are often subparallel to possible slab P - T paths. In this range, fluids become increasingly rich in dissolved matter, but thermodynamic calculations predict very small CO_2 fractions, generally decreasing with increasing pressure.
- 00020 3. Melting, where the amount of melt depends mostly on H_2O availability and the composition of melts is, in addition, strongly pressure sensitive:
 - a. Flush melting (1–4 GPa, 650–850 °C) at temperatures between the wet granite solidus and the fluid-absent amphibole, biotite, and phengite melting curves. In this case, additional fluid is provided from underlying dehydrating lithologies.
 - b. Fluid-absent melting at high temperatures (>800–900 °C). At relatively low P , amphibole and biotite (1–2.5 and 1–3 GPa, respectively) are the principal hydrous phases to melt. Adakitic magmas, that is, slab melts (with $Na > K$), are likely to occur. At medium to high P (>2.5 GPa),

phengite is the principal hydrous phase to melt, and melts have $K > Na$.

- 4. Dissolution at high P , high T (>5–6 GPa, >800 °C), where the solvus between fluid and melt is closed and solute-rich liquids might dissolve hydrous phases.

In the following discussion, the mechanisms of exemplary devolatilization reactions are illustrated, including consideration of ‘real-world’ aspects, such as chemically heterogeneous protoliths and kinetically hindered reaction progress (compared to a chemical homogeneous protolith and an equilibrated ideal situation). We describe and, as far as possible, quantify the four different devolatilization/melting regimes, principally investigating the three major types of bulk compositions of the oceanic lithosphere, that is, pelites, mid-ocean ridge basalts (MORB), and harzburgite with H_2O and CO_2 , as major volatile components. Phase petrology is then applied to understand the behavior of trace elements. Finally, we argue for the necessity of integrating fluid–melt-producing processes over the entire oceanic lithosphere, as pressure–temperature conditions of the different lithologies within a given column

10010

Table 1 Major volatile-carrying phases in subduction zones

Mineral		Chemical formula	H ₂ O (wt%)	Pelite, graywackes	Basalts	Mg-gabbros	Peridotite
Phengite	phe	K(Mg,Fe) _{0.5} Al ₂ Si _{3.5} O ₁₀ (OH) ₂	4.3	+++	+	-	-
Biotite/phlogopite	bt-phl	K(Mg,Fe) _{2.8} Al _{1.4} Si _{2.8} O ₁₀ (OH) ₂	4.1	++	+	-	+
Paragonite	par	NaAl ₃ Si ₃ O ₁₀ (OH) ₂	4.6	+	++	+	-
K-richterite	K-rich	KCa(Mg,Fe) ₄ AlSi ₆ O ₂₂ (OH) ₂	2.0	-	-	-	+
Glaucophane	amp	NaCa(Mg,Fe) ₃ Al ₃ Si ₆ O ₂₂ (OH) ₂	2.2	+	+++	+++	-
Barroisite	amp	Na ₂ (Mg,Fe) ₃ Al ₂ Si ₆ O ₂₂ (OH) ₂					
Hornblende	amp	Ca ₂ (Mg,Fe) ₄ Al ₂ Si ₇ O ₂₂ (OH) ₂	2.2	-	+++	+++	+
Pargasite	amp	NaCa ₂ (Mg,Fe) ₄ Al ₃ Si ₆ O ₂₂ (OH) ₂					
Lawsonite	law	CaAl ₂ Si ₂ O ₇ (OH) ₂ ·H ₂ O	11.2	+	++	++	-
Zoisite/epidote	zo/epi	CaAl ₂ (Al,Fe ³⁺)Si ₃ O ₁₂ (OH)	2.0	+	++	++	-
Chloritoid	cld	(Mg,Fe) ₂ Al ₂ Si ₂ O ₁₀ (OH) ₄	7.5	++	+	++	-
Chlorite	chl	(Fe,Mg) ₅ Al ₂ Si ₃ O ₁₀ (OH) ₈	12.5	++	+++	+++	+
Talc	tc	(Mg,Fe) ₃ Si ₄ O ₁₀ (OH) ₂	4.8	++	+	++	+
in Si-rich veins							+++
Serpentine	serp	(Mg,Fe) ₄₈ Si ₃₄ O ₈₅ (OH) ₆₂	12.3	-	-	+	+++
Phase A	'A'	(Mg,Fe) ₇ Si ₂ O ₈ (OH) ₆	11.8	-	-	?	+++
Phase E	'E'	(Mg,Fe) _{2.2} Si _{1.1} O _{2.8} (OH) _{3.2}	11–18	-	-	?	++
10 Å phase	10A	(Mg,Fe) ₄ Si ₃ O ₁₀ (OH) ₂ ·H ₂ O	8–14	Likely	-	Likely	+
Aragonite/calcite	ara/cc	CaCO ₃	-	+	+	+	-
Dolomite	dol	CaMg(CO ₃) ₂	-	+	+	+	+
Magnesite	mgs	MgCO ₃	-	+	+	+	+

+, <5 vol%; ++, 5–20%; +++, >20%.

of subducted lithosphere are strictly related to each other, and fluid and melt-forming processes are often interdependent (Table 1).

The purpose of this chapter is to give an overview of the mechanisms leading to the transfer of matter from the subducting lithosphere to the mantle wedge and to characterize the oceanic crust residual to the subarc devolatilization and melting processes, which then subducts further and forms chemical heterogeneities in the deeper mantle. The geochemistry of subducted sediments is further reviewed by Plank (2012), and the geochemistry of subduction-zone lithologies is reviewed by Bebout (2012). In addition, Hermann and Rubatto (2012) review the chemical changes accompanying subduction of continental crust, which is directly relevant for material added to the subducting crust through subduction erosion (Section 321.2.2).

321.2 Setting the Scene

321.2.1 The Oceanic Lithosphere Before Subduction

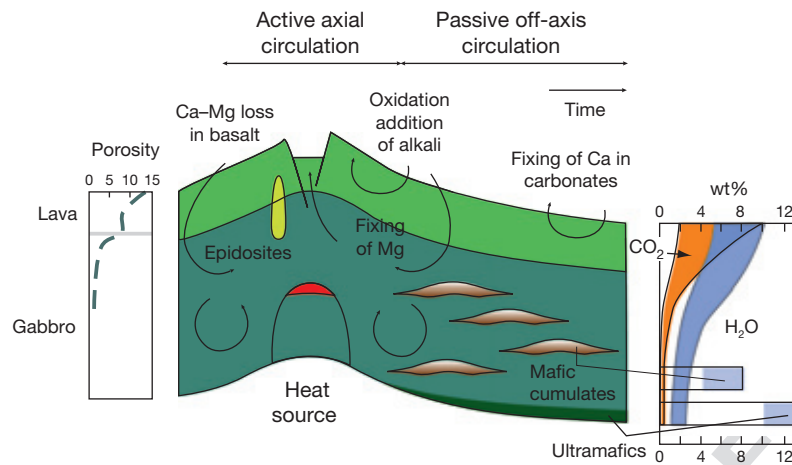
Here, some aspects that are crucial for the production and quantification of mobile phases in the oceanic lithosphere are summarized (Figure 2). The unaltered igneous oceanic crust is described in detail by White and Klein (2012) and Coogan (2012), while the overlying sediments are discussed by Plank (2012) and Li and Schoonmaker (2012) and the alteration processes by Staudigel (2012).

A well-stratified oceanic crust is composed of a sedimentary cover layer (including pelites, carbonates, cherts, and volcanoclastic sediments), a basaltic layer built of pillows and sheeted dikes, and a gabbroic layer with an upper part chemically close to MORB but a lower part mostly composed of differentiated high-Mg gabbros, FeTi gabbros, troctolites, norites, and other

cumulates (Nicolas, 1989). The crust is underlain by a partly serpentinized, depleted, mostly harzburgitic peridotite (Snow and Dick, 1995).

All sediments have some natural porosity and begin expelling fluids during compaction. They generally remain fluid-saturated during prograde metamorphism, and equilibration for major elements can be generally assumed (Carlson, 2002), as field evidence for prograde disequilibrium is essentially absent. Also, eclogites and blueschists having a basaltic precursor generally appear to be fully hydrated during high-pressure metamorphism; thus, assuming fluid saturation and equilibrium during subduction is a reasonable simplification. By contrast, gabbros are mostly only partly hydrated in veins and adjacent alteration zones (Coogan, 2012). Field studies show that, when pervasive alteration of coarse-grained gabbros takes place, hydration reactions are often limited to the grain boundaries. Thus, the gabbroic layer may not generally experience fluid-saturated conditions and may fail to reach equilibrium. Like the gabbros, serpentinization of peridotite is very heterogeneous. Veins and fractures represent important infiltration pathways for fluids, and zones of intensive serpentinization probably alternate with very weakly serpentinized peridotite. Mammerickx (1989) estimated that 20% of the Pacific Ocean floor is affected by fracturing, but for both peridotite and gabbros, quantitative estimates of the volume affected by hydration have been difficult to come by. Additionally, the extent of hydration/carbonatization also depends on the spreading velocity at the mid-ocean ridge (MOR); oceanic lithosphere produced at slow-spreading ridges appears to undergo higher degrees of hydration than that produced at fast-spreading ridges.

Alteration of the igneous parts of the oceanic crust also leads to veins containing carbonates, and although pervasive carbonatization is rare, carbonate contents might be locally



f0015

Figure 2 Schematic representation of hydrothermal alteration of the igneous oceanic crust in a fast-spreading setting. The insert to the right gives H₂O and CO₂ contents in a depth profile of the oceanic crust; the two horizontal bars indicate typical H₂O contents in norites, troctolites, and other cumulates, and in intensively serpentinized ultramafic rocks. In slow-spreading ridges, deep tectonic fragmentation and amagmatic spreading promote exposure of lower crustal sequences and peridotites on the ocean floor. Ophicarbonate breccias are abundant in deep axial valleys.

high in such veins and in their immediate surroundings. Such carbonatization may extend to more than 1000 m below the seafloor (Bach et al., 2001), leading to total amounts of CO₂ of several wt%.

The well-stratified oceanic crust paradigm applies to the circum-Pacific, where 53% of the total length of present Earth's oceanic crust subduction takes place. Fast-spreading Pacific-type oceanic crust, however, is not found in the Atlantic and Indian Oceans, where 4% and 16%, respectively, of present subduction occurs (the remainder being subduction of oceanic crust from comparatively small basins). The slow-spreading Atlantic has an oceanic lithosphere that is more complex structurally, and in which lateral heterogeneity is an important feature (Cannat, 1993; Gente et al., 1995). In the Atlantic, it is common to have serpentinites cropping out on the ocean floor; such bodies are uncommon in the Pacific. Large transforms are often accompanied by the emplacement of ultramafic rocks in the shallowest portions of the lithosphere (Constantin, 1999). The Indian Ocean, where the crustal architecture may be intermediate between Atlantic and Pacific Oceans, currently subducts in the Macran arc, and from Burma to Sunda. Caution is, thus, necessary when applying a simple layered oceanic crust model to infer the geometry of subducted lithologies in the past, and in some present subduction zones as, for example, South-Sandwich, Antilles, or Sumatra.

Determining the state of the oceanic lithosphere before subduction is crucial for understanding how the different lithologies evolve. Most of the alteration takes place close to the mid-ocean ridges; however, it has been shown that some fluid–rock interaction also takes place in older oceanic crust away from the ridge axis (Kelley et al., 2001; Staudigel, 2012), which is especially important for the generation of carbonates (Caldeira, 1995). Fracturing at the seafloor and fractures caused by bending of the subducting lithosphere at the trench provide pathways for fluids and, hence, further possibilities of hydration. The occurrence of double seismic zones in the subducted lithosphere (Yamasaki and Seno, 2003) is commonly regarded as evidence of antigorite or, eventually,

chlorite breakdown in the deep lithospheric mantle of the subducting plate. If the lower seismic zone is related to the presence of such hydrous minerals, hydration of the lithosphere at tens of kilometers depth below the seafloor would be required.

Once the oceanic lithosphere is subducted, continued alteration of the upper layers results from any fluid or melt expelled from deeper levels. Thus, during ongoing subduction, the igneous oceanic crust will interact with fluids passing through it from the serpentinized peridotite, and the sediments will interact with fluids coming from the basaltic and the serpentinized peridotite layers (Gieskes et al., 1990). This process may constitute the main mechanism allowing for melting in the uppermost part of the subducting crust.

The building blocks of the oceanic crust define the major lithologies involved in devolatilization and melting. To a first approximation, the major players are mixed clays and limestones, basalts, and serpentinized harzburgites, including some ophicarbonates. We consider here pelites and carbonates as the main components of the sedimentary layer (see also Plank, 2012). From a phase petrological point of view, graywackes and volcanoclastic sediments of broadly andesitic to dacitic composition can be regarded as intermediate between pelites and basalts.

32.1.2.2 Accretion Versus Erosion

The oceanic crust does not survive the beginning of subduction unmodified: at present, accretionary prisms form over about half of the integrated global trench length. These accumulate 20–30% of the oceanic sediments that enter the trench (Clift and Vannucchi, 2004) and also some mafic oceanic crust. The other half of global trenches does not form accretionary prisms and may undergo subduction erosion (Von Huene and Scholl, 1991); that is, continental material of the overriding plate is mechanically eroded and subducted. Von Huene and Scholl (1991) estimated that, in heavily eroding margins such as N. Japan and Peru, the amount of continental material that is

p0085

p0095

Au8

p0090

p0100

s0025

p0105

AUG scraped off the overriding plate adds several 100 m to the subducting crust; Clift and Vanucchi (2004) suggested that in such margins, eroded forearc crust may exceed the volume of subducted sediments by 20%, doubling the thickness of subducted material with felsic composition.

s0030 321.2.3 Rock Hybridization at the Slab–Mantle Interface

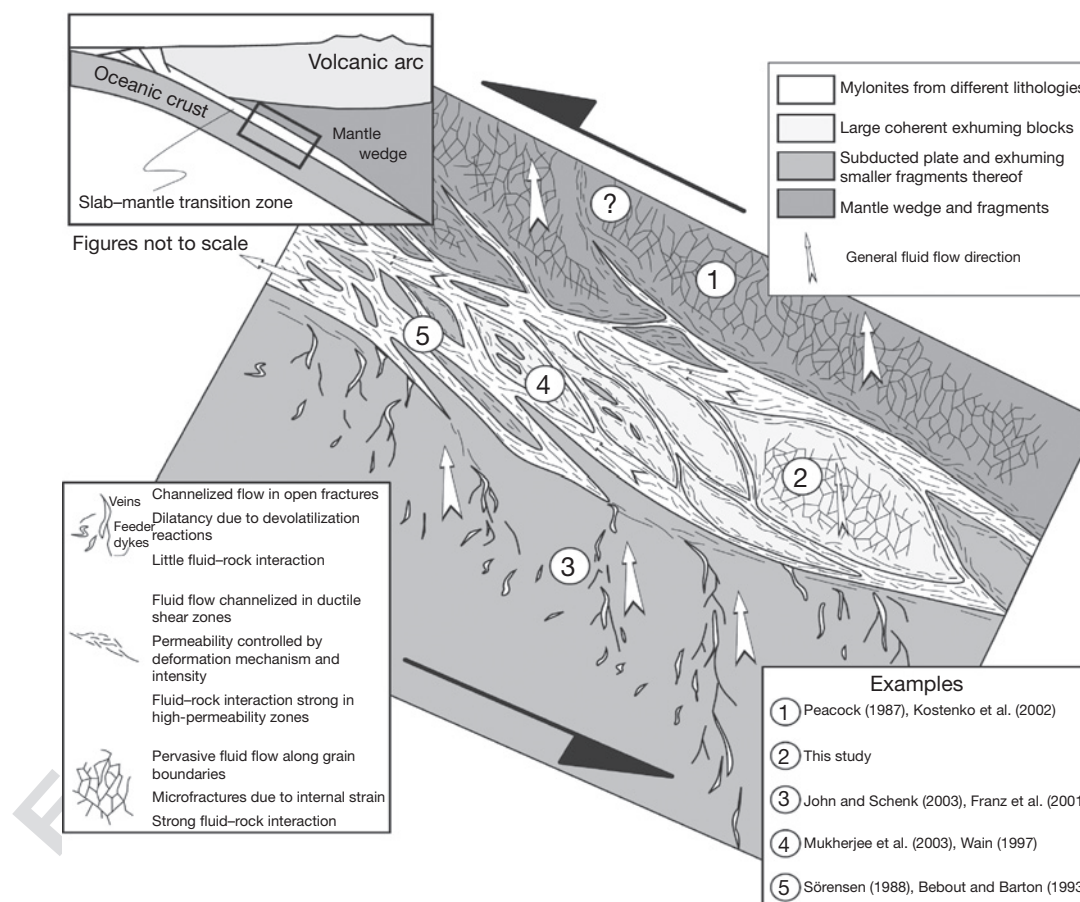
p0110 Field studies increasingly reveal the occurrence of *mélange* complexes at the slab–mantle wedge interface that are attributed to heavy deformation, boudinage, and chemical rehomogenization between the various lithologies involved therein (see review in Bebout, 2012). Rock hybridization is promoted by high strain rates and pervasive fluid flow (Bebout, 2007; Miller et al., 2009; Spandler et al., 2007). Volatile availability, deformation, and fluid–rock interaction lead to phyllosilicate- and, eventually, carbonate-rich rocks, which may approach mono- or bimineralic compositions, such as chlorite schists, talc–magnesite schists, antigorite–magnesite schists, phengite-rich blueschists, and eclogites. Although the

volumes involved in hybridization are still poorly defined, their position is critical in controlling fluid pathways (Konrad-Schmolke et al., 2011) and may act as chromatographic filters fixing or releasing elements at variable *P-T* conditions (Figure 3).

s0035 321.2.4 Continuous Versus Discontinuous Reactions

s0035

p0115 The production of fluids and melts during subduction (the latter occurring in strictly prograde, relatively low-temperature, high-pressure conditions) is dominated by a succession of equally important (in terms of fluid productivity) continuous and discontinuous reactions taking place in both the sedimentary and mafic layers of the oceanic crust. Discontinuous reactions are related to modifications of the stable phase association (terminal and cross reactions) causing abrupt variations in mineral abundances, whereas continuous reactions lead only to change(s) in composition and proportion of the phases already present.



f0020 **Figure 3** Schematic illustration of fluid migration pathways in a subduction zone (used by permission of Oxford University Press from Konrad-Schmolke M, O'Brien PJ, and Zack T (2011) Fluid migration above a subducted slab – Constraints on amount, pathways and major element mobility from partially overprinted eclogite-facies rocks (Sesia Zone, Western Alps). *Journal of Petrology* 52, 482, **Figure 14**). Within the subducted slab, fluid flux is channelized, and in the slab–mantle transition zone, fluid flux is controlled by the extent of viscous deformation. In the mantle wedge immediately overlying the subducting crust, fluid flux is pervasive or might be controlled by viscous deformation. For examples see Bebout and Barton (1993), Franz et al. (2001), John and Schenk (2003), Kostenko et al. (2002), Mukherjee et al. (2003), Peacock (1987), Sørensen (1988), and Wain (1997).

p0120 Extensive solid solutions (amphiboles, micas, pyroxenes, garnets) result in continuous reactions that release fluids over a range of several tens of kilometers' depth. This can be exemplified by the disappearance reactions of amphibole (**Figure 4(a)**) within the amphibole–eclogite facies (Poli, 1993; Poli and Schmidt, 2002). At the minimum pressure necessary for the formation of omphacite in basaltic bulk compositions (1.5 GPa at 650 °C), more than 50% amphibole remains in the eclogitic assemblage: omphacite–garnet–amphibole–epidote–quartz±paragonite. Within this assemblage, amphibole decomposes progressively, forming mainly omphacite and garnet, until 22% amphibole remains at its upper pressure stability at 2.2 GPa. Within this pressure interval, amphibole composition changes from calcic and tschermakite-rich to sodic–calcic and barroisite-rich, and the continuous reaction from 1.5 to 2.2 GPa produces more fluid (i.e., 0.7 wt% H₂O) than the discontinuous terminal amphibole breakdown at 2.2 GPa (i.e., 0.4 wt% H₂O), which results in chloritoid as an additional hydrous phase. As for mafic compositions, amphibole decomposition and abundance in peridotites are controlled by continuous reactions that decompose 50–70% of the amphibole present at 0.5–1 GPa before its terminal breakdown between 3.2 and 3.4 GPa (e.g., Fumagalli et al., 2009; Niida and Green, 1999; **Figure 4(b)**). Experimental studies demonstrate the equal importance of continuous reactions and discontinuous terminal breakdown reactions for amphibole and contradict the earlier models (e.g., Tatsumi, 1986), which related fluid flow and the position of the volcanic front within a subduction zone directly to amphibole breakdown at a given depth.

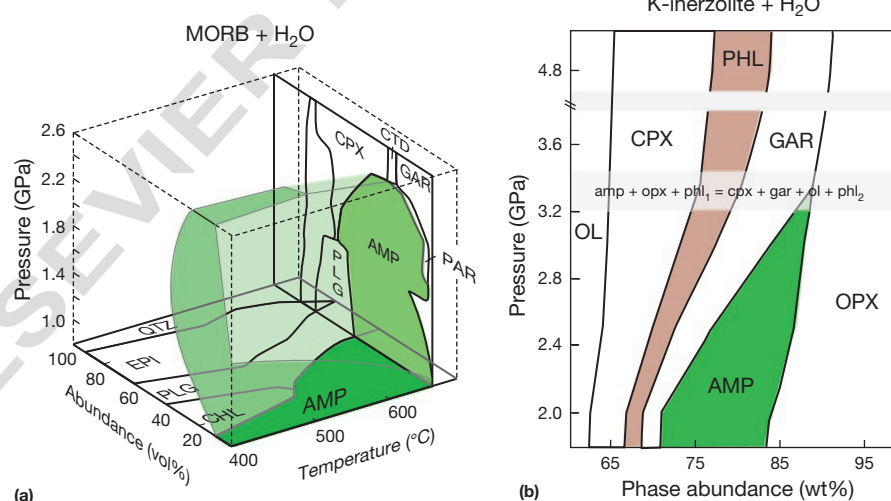
p0125 In sediments and the mafic portion of the subducted crust, all reactions involving hydrous phases and carbonates involve solid solutions whose compositions depend on bulk

composition, pressure, and temperature. Different bulk compositions result in different phase compositions and, thus, cause a given reaction to shift in *P-T* space, that is, to commence in a given bulk composition at shallower or deeper levels. In peridotites, amphibole, and to some extent chlorite, are controlled by continuous *and* discontinuous reactions. However, the other volumetrically important hydrous phases (e.g., brucite, serpentine, talc/10 Å phase, and 'phase A') in altered harzburgites display a relatively restricted compositional range, at least compared to those present in mafic eclogites. As a result, breakdown reactions of hydrous phases in harzburgites are dominated (to a first approximation) by discontinuous reactions taking place over a restricted depth range of only a few kilometers.

321.2.5 Fluid Production

s0040

p0130 There has been a misconception in the literature that hydrous phases will break down in the absence of a free fluid phase and, thus, that the stability fields of hydrous phases are affected by a supposed *lowering of H₂O activity* when the fluid leaves the rock. This is fundamentally wrong: H₂O and CO₂ are chemical species, just like any other species (e.g., SiO₂, Al₂O₃, MgO, etc.). The only difference is that the phase corresponding to the composition of such chemical species (i.e., H₂O, CO₂, etc.) happens to have a physical state (i.e., fluid) that is different from other phases having the exact composition of a chemical species (e.g., quartz, corundum, periclase, etc.). It should be remembered that the thermodynamic treatment of all these phases is identical for the entropy and enthalpy terms, and that they only differ for the *P-V-T* (pressure–volume–temperature) relation adopted. As SiO₂ saturation is not a prerequisite for the stability of the silicates olivine or enstatite, H₂O saturation



f0025 **Figure 4** Continuous versus discontinuous reactions contributing to the disappearance of amphibole in (a) H₂O-saturated, CO₂-free MORB (adapted from Apted MJ and Liou JG (1983) Phase relations among greenschist, epidote-amphibolite, and amphibolite in a basalt system. *American Journal of Science* 283A: 328–356; Poli S (1993) The amphibolite–eclogite transformation: An experimental study on basalt. *American Journal of Science* 293: 1061–1107) and (b) phlogopite-bearing peridotite, where phase abundances up to 3.4 GPa are estimated at 900–1000 °C and data at 4.8 GPa are at 680 °C (reproduced from Fumagalli P, Zanchetta S, and Poli S (2009) Alkali in phlogopite and amphibole and their effects on phase relations in metasomatized peridotites: A high-pressure study. *Contributions to Mineralogy and Petrology* 158: 723–737). AMP, amphibole; CHL, chlorite; CPX, clinopyroxene; CTD, chloritoid; EPI, epidote; GAR, garnet; OL, olivine; OPX, orthopyroxene; PAR, paragonite; PHL, phlogopite; PLG, plagioclase; QTZ, quartz.

is not required for the stability of hydrous phases. In fact, for a given bulk composition and phase assemblage, it is quite possible (when following a suitable $P-T$ trajectory) to pass from a fluid-absent to a fluid-present regime and back again to a fluid-absent regime.

A hydrous fluid is produced only if a given rock volume is already completely hydrated (fluid saturated). If fluid saturation is not realized at the beginning of subduction, a number of fluid-absent reactions will take place. These reactions are of the type $A + V_1 = B + V_2$ (where A, B are volatile-free phases and V_1, V_2 hydrous phases or carbonates), involve hydrates and/or carbonates, and change the mineralogy of a rock volume according to the stability fields of the minerals, but do not liberate a fluid. Prograde subduction-zone metamorphism (as is true for any type of prograde metamorphism) generally reduces the amount of H_2O that can be stored in hydrous minerals with depth. Thus, almost any part of the oceanic crust sooner or later becomes fluid saturated. In an equilibrium situation, the volatile content bound in hydrous phases and carbonates remains constant until fluid saturation occurs. Either continuous or discontinuous reactions might lead to fluid saturation in a rock. The point at which this occurs depends on initial water content and pressure as well as temperature, and, somewhat counterintuitively, initially low water contents do not cause early complete dehydration, but delay the onset of fluid production to high pressures.

Due to heterogeneous alteration (and, thus, varying initial H_2O and CO_2 contents), there is a wide depth range over which different volumes of the oceanic lithosphere become fluid saturated. A second complication arises from the scale at which equilibrium is effective. A few grains may locally form a fluid-saturated environment, but it is questionable whether the fluid produced on a local grain scale is able to escape. Field evidence argues for equilibration of fluids in eclogites on a centimeter to meter scale until they are able to collect and escape in veins (Philippot, 1993; Widmer and Thompson, 2001; Zack et al., 2001; see also Ague, 2012). Most fluid-producing reactions occur in response to an increase in pressure and temperature. At the same time, ascending fluids may change the fluid composition in the overlying layers and cause reactions therein, which may lead to an increase or decrease in their volatile content. Furthermore, fluid pathways, fluid–rock interaction, and the efficiency of metasomatism are expected to vary as a function of strain rate and volume changes related to devolatilization or hydration–carbonation. Konrad-Schmolke et al. (2011, Figure 3) showed that K, Ca, Fe, and Mg in mobilized fluids affect, in a stepwise process, the rock volumes flushed by migrating fluids. In the mantle wedge directly overlying the subducted crust, low strain rates and low permeability, coupled to positive volume changes resulting from metasomatic reactions, may facilitate a pervasive flow and fluid–rock exchange.

s0045 321.2.6 Fluid Availability Versus Multicomponent Fluids

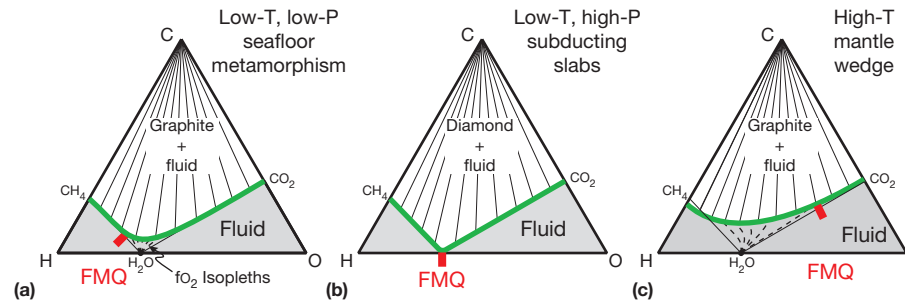
The advent of powerful phase-diagram calculators (Connolly, 1995; de Capitani and Brown, 1987; Holland and Powell, 1998) as well as the widespread application in the last 10 years of forward modeling based on thermodynamic databases has led to a common perception that formation of

hydrous phases, fluid availability, and reaction progress depend on complex paths in a $P-T-nH_2O$ space, where nH_2O stands for the mass proportion of H_2O in a bulk composition (e.g., Clarke et al., 2006; Guiraud et al., 2001). The calculation and analysis of pseudosections in complex multicomponent chemical systems is a powerful tool to inspect variations in mineral assemblages as a function of variable bulk composition, including volatile component abundances. However, when carbonates and/or graphite/diamond occur, such calculations assume that H_2O undersaturation results from the presence of a mixed H_2O-CO_2 fluid. This is not always true.

Thermodynamic calculations based on measured compositions of solid phases yield the chemical potential of H_2O in these phases (nH_2O). Under equilibrium, the chemical potential of H_2O is equal in all phases, and only if some additional constraint implies the presence of a fluid phase (e.g., fluid inclusions), the composition of this fluid phase can be calculated from P, T , and nH_2O . This can be illustrated in the simple system $CaO-Al_2O_3-SiO_2-H_2O-CO_2$, where a given chemical potential of H_2O at a given P and T (4 GPa, 600 °C, Figure 7 in Poli and Schmidt, 1998) may correspond to either a fluid-absent situation (with lawsonite + zoisite + aragonite + coesite + kyanite present) or to the presence of a mixed H_2O-CO_2 fluid phase (with lawsonite + aragonite + coesite + kyanite + fluid present). Note that both cases are described by the (ambivalent) term ' H_2O undersaturated.'

Furthermore, although largely overlooked, graphite (and, in some cases, diamond) is a common accessory phase in a variety of rocks metamorphosed at high-pressure conditions, from metapelites (Sisson et al., 1997) to marbles (Korsakov and Hermann, 2006), felsic gneisses (Stockhert et al., 2001), mafic eclogites (Faryad et al., 2006), serpentinite melanges (Harlow, 1994), and, most notably, in metasomatized peridotites (van Roermund et al., 2002). Graphite may also occur as a 'cryptic' mineral, interlayered on a nanoscale in the phlogopite structure (Ferraris et al., 2004; Finero peridotite body, W. Alps), and, as such, is difficult to detect.

Hydrous minerals, carbonates, graphite/diamond, and mixed H_2O-CO_2 fluid inclusions (Scambelluri and Philippot, 2001) are not the only volatile-bearing species recovered in the geological record. Hydrogen or CH_4 -bearing fluid inclusions (Fu et al., 2003; Peretti et al., 1992; Shi et al., 2005) reveal that redox processes in C–O–H-bearing systems should be carefully evaluated in defining speciation at high-pressure conditions. The chemical system C–O–H is characterized by two large phase fields (Figure 5). In the upper portion of the phase diagram, two phases coexist, a carbon polymorph (at the top) and a fluid phase (given by the green line) saturated in carbon. At lower carbon contents (gray fields), a single fluid phase, with variable abundances of H_2 , CH_4 , H_2O , CO_2 , and CO species, occurs. The boundary that defines the graphite-saturated system is often referred to as the graphite boundary (Holloway and Reese, 1974) or graphite saturation surface (Connolly, 1995). Along the graphite saturation surface, fluid speciation is fixed if a redox condition, fO_2 , is imposed externally. With reference to the common oxygen buffer fayalite–magnetite–quartz (FMQ), Connolly and Cesare (1993) illustrated that, at very low temperatures, fluids are 'reduced,' that is, CH_4 -bearing (red dash on the saturation surface in Figure 5), while at low-temperature, high-pressure conditions



f0030

Figure 5 Schematic isobaric-isothermal composition diagram for the C–O–H system illustrating the displacement of the carbon-saturation surface (green) with pressure and temperature (from (a) to (c)), and the shift of fluid speciation (red dash) at redox conditions buffered by the equilibrium fayalite–magnetite–quartz (FMQ). When FMQ is adopted as a reference, fluids move from ‘reduced’ (methane bearing) in oceanic environments to ‘aqueous’ during devolatilization of the slab at high pressure, and then to ‘oxidized’ (CO_2 bearing) at mantle wedge conditions.

they are nearly ‘aqueous,’ that is, the graphite saturation surface bends very close to the H_2O end member and fluids reach a maximum H_2O content very close to $f\text{O}_2 = \text{FMQ}$, whereas at high temperatures, FMQ-buffered fluids move to an ‘oxidized’ state, that is, they are CO_2 -rich fluids.

Notably, in hydrothermal regimes on the seafloor, methane-bearing vents are observed along the Mid-Atlantic Ridge (Charlou and Donval, 1993; Charlou et al., 2002) and were experimentally reproduced by Berndt et al. (1996) through serpentinization of ultramafic rocks. Coprecipitation of carbon and magnetite (a mineral with 69 wt% Fe_2O_3), together with release of a CH_4 fluid, demonstrates that intuitive concepts of ‘reduced’ and ‘oxidized’ conditions are somewhat arbitrary when qualitatively based on common sense. Following a similar reasoning, Poli et al. (2009) showed that diamond is potentially stable with hematite above 5 GPa at temperatures in the order of 800 °C.

At the high-pressure, low-temperature conditions that are typical for the slab or its hanging wall (the lowermost mantle wedge), oxygen fugacity conditions, fluid speciation, and the oxygen budget are highly variable when carbon is present. Experimental studies, theoretical calculations, and natural findings suggest that the variability in CH_4 or CO_2 contents is modulated on a scale of just a few tens of mole percent across the maximum H_2O condition in C–O–H systems (the bend in the C-saturation surface in **Figure 5**), resulting in nearly aqueous fluids. Whether relatively high oxygen fugacities retrieved from high-pressure, subduction-related samples (Malaspina et al., 2009, 2010) or inferred from arc magmas (Kelley and Cottrell, 2009) are indicative of bulk oxidation, or rather record variations in the chemical potential of oxygen as a function of phase assemblage and variable chemical potential of nonvolatile components, is still to be determined.

The oceanic crust is comparatively oxidized with respect to the mantle wedge. However, to what extent this oxidation may be transferred from the slab to the mantle wedge as well as the extent to which strong redox gradients are preserved is entirely open. Addition of pure H_2O fluid does not lead to oxidation of the mantle wedge; only the transport of oxidized cations, that is, Fe^{3+} , C^{4+} (as CO_2 or HCO_3^-), and oxidized S will lead to wedge oxidation, these three being the only ones with geologically sufficient abundance to cause any major net oxygen transfer.

An oxidized mantle wedge has recently been questioned (Lee et al., 2005, 2010), mostly on the basis of V/Sc and Fe/Zn systematics in arc lavas. In this case, the undoubtedly oxidized nature of typical evolved arc magmas is attributed to the incompatibility of Fe^{3+} with prolonged magma differentiation, similar to the highly differentiated FeTi gabbros in the oceanic crust.

Hydrous subduction-zone fluids are known to dissolve significant quantities of silicates, and complete miscibility between hydrous melts and aqueous solutions may be achieved at ≥ 5 GPa, that is, beyond the ‘second critical endpoint’ of the solidus (see **Section 321.3.4**, which discusses dissolution regimes). At lower pressures and temperatures below the solidus, aqueous fluids in equilibrium with silicates are very dilute solutions. Although increased H_2O ionization and fluid polymerization (Manning et al., 2010) at high P and T enhance solute concentrations (Dolejs and Manning, 2010), subduction-zone fluids bear only two to three times the total dissolved solids of seawater (Manning, 2004). Ligands, such as Cl, promote dissolution, but the range of chlorinities in high-pressure fluids remains unclear (Franz et al., 2001; Scambelluri and Philippot, 2001). As Cl strongly partitions into any fluid present, most Cl is expected to be expelled upon the first squeeze, that is, when porous fluids and fluids from clays and zeolite-pumpellyite facies minerals are expelled from subducted crust. Chlorine in aqueous fluids strongly influences carbonate solubility (Newton and Manning, 2010), but relatively high and, from calculations, unpredicted solubilities of CaCO_3 in pure H_2O (up to 0.6 wt%) were demonstrated by Caciagli and Manning (2003) at 1 GPa, suggesting that carbonate dissolution at high pressure may be a viable mechanism to mobilize carbon in fluids.

321.2.7 Real-World Effects

The compilation of available phase equilibria aims at understanding equilibrium situations in typical (homogeneous) average bulk compositions. However, different ‘real-world effects’ with amplitudes that may depend upon the rock type are to be expected.

In the real world, the following factors contribute to the continuous character of the devolatilization signal from the downgoing slab: highly variable bulk compositions in the

sedimentary and gabbroic layers, as well as possibly different degrees of depletion caused by different amounts of melt extracted in the hydrated peridotitic layer (Constantin, 1999); inhomogeneous distribution of carbonates versus hydrous minerals, resulting in an inhomogeneous X_{CO_2} in the fluid phase (Gillis and Robinson, 1990); large temperature gradients within the subducting lithosphere (Arcay et al., 2007); and, finally, kinetic effects that inhibit reactions and, thus, displace and widen reaction zones. Kinetic effects are mainly related to fluid availability, to effective strain (and thus to deformation history) (Austrheim and Engvik, 1997; Molina et al., 2002), and to thermal retardation of sluggish solid–solid transformations (Schmeling et al., 1999).

All of the above effects lead to release of a fluid–melt ‘pulse’ occurring over a broad depth range. By contrast, the single known focusing mechanism for fluid–melt flow is mechanical: fluids–melts may ascend through channelized flow, hydrofractures, or preexisting fractures, which focus a broadly distributed fluid into distinct pathways. The relative importance of these mechanisms is largely conjectural and whether macroscopic fluid–melt focusing is achieved depends on the extent and spacing of such pathways.

321.3 Devolatilization Regimes in MORB

s0055

Based on phase relations in volatile-bearing MORB, four distinct P – T regions with characteristic mobile-phase production mechanisms can be identified (Figure 1). These are discussed sequentially.

321.3.1 High Dehydration Rates and Fluid Production (Typically to 600 °C, 2.5 GPa)

s0060

Once the oceanic crust starts subducting, most of its remnant porosity will be immediately lost by compaction and its pore fluids expelled. At this stage, zeolites, pumppellyite, and prehnite are the major H_2O -bearing minerals, and H_2O contents of hydrous minerals amount to 8–9 wt% H_2O in the bulk rock (Peacock, 1993). Beyond depths of roughly 15 km, the oceanic crust enters into the blueschist facies, in which the major hydrous minerals are chlorite; Na-rich, Ca-poor amphiboles (glaucophane to barroisite); phengite (white mica); lawsonite or zoisite; and paragonite (e.g., Sorensen, 1986). Bulk water contents at the beginning of the blueschist facies are around 6 wt% (Figure 6(a)). Initially, abundant chlorite has high H_2O

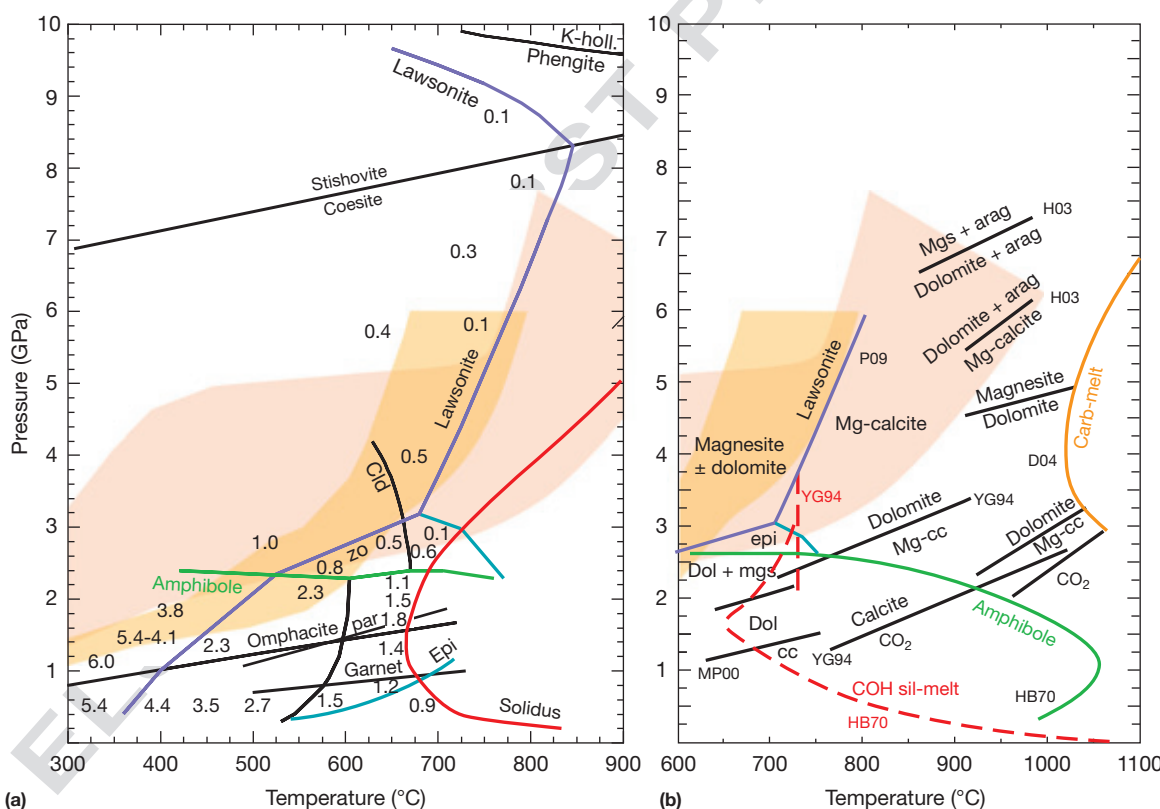


Figure 6 (a) Major phase stability boundaries in H_2O -saturated MORB and H_2O contents (numbers in italics, in wt%) stored in hydrous phases (Schmidt and Poli, 1998). Data below 550 °C are based on natural blueschists and greenschists; all other data are based on experiments. Compare with Figure 1. (b) Phase boundaries in a CO_2 -bearing MORB system; within the lawsonite, epidote, and amphibole stability fields, the coexisting fluid is a C–O–H fluid, with CO_2 contents that vary as a function of redox conditions imposed on the system (see Figure 5). At pressure and/or temperature conditions beyond the stability limit of hydrous phases, the system degenerates to a carbonated MORB, where carbonate species depend on the amount of volatile component and $\text{Ca}/(\text{Mg} + \text{Fe})$ ratio of the bulk composition. The yellow and orange fields mark P – T paths for average cold (yellow) to intermediate (orange) thermomechanical subduction models of Arcay et al. (2007) and the warm W1300-model of Syracuse et al. (2010), respectively. MP00: Molina and Poli (2000); HB70: Hill and Boettcher (1970); YG94: Yaxley and Green (1994); D04: Dasgupta et al. (2004); P09: Poli et al. (2009); HO3: Hammouda (2003).

contents (12 wt%) and decomposes completely in this depth range through various continuous and discontinuous reactions. Lawsonite (11 wt% H₂O) has a maximum abundance of 25 vol% at the onset of blueschist facies metamorphism and decreases to about 10 vol% at the amphibole-out reaction. Anhydrous minerals typically comprise 5–25 vol% (e.g., Okay, 1980; Thurston, 1985) at 5–10 km depth and some 100 °C, grow in volume to about 50 vol% just before the amphibole-out reaction, and increase to >70 vol% at pressures beyond amphibole stability. As a consequence, dehydration rates are considerable within this *P-T* regime; a fully hydrated MORB loses about 4–6 wt% H₂O when passing through the blueschist stage within the forearc region.

At pressures of 2.2–2.4 GPa, that is, the maximum pressure stability of amphibole in MORB (65–70 km), dehydration reactions are numerous, and their orientations in *P-T* space are mostly oblique to a typical subduction-type *P-T* path, resulting in final high dehydration rates for most *P-T* paths. Forneris and Holloway (2003, 2004) observed glaucophane to be stable up to 2.8–3.0 GPa in a relatively Fe-Al-rich basaltic composition at 600–650 °C. However, amphibole at 2.6 GPa, 650 °C, already represents less than 10 vol% in these experiments, and, therefore, has a limited impact on the devolatilization at subarc depth.

Molina and Poli (2000) and Poli et al. (2009) demonstrated the effect of mixed C-O-H fluids on phase relations in mafic compositions (**Figure 6(b)**). With increasing pressure, the stable carbonates at 665–730 °C are calcite (<1.4 GPa), dolomite, and dolomite + magnesite (>2 GPa). Fluids coexisting with calcite are CO₂-rich (^XCO₂=0.4–0.7), but at higher pressures, fluids coexisting with dolomite only have CO₂ mole fractions of 0.02–0.2. This implies that carbon tends to fractionate into the solid with increasing pressure (Kerrick and Connolly, 1998; Molina and Poli, 2000). The effect of CO₂ on the stability of hydrous phases is surprising. In a carbonated system, plagioclase disappears at the same pressures as in the pure H₂O system (~1.5 GPa at 650 °C), but its breakdown does not cause omphacite formation, which is delayed by about 0.5 GPa. Rather, at 680 °C plagioclase breakdown produces ~20 vol% paragonite, which is a hydrous phase. Amphibole breaks down at ~2.5–2.6 GPa (Poli et al., 2009; Yaxley and Green, 1994), that is, 0.3 GPa higher than in the pure H₂O system. The fluid-saturated solidus is located at ~730 °C at 2.2 GPa, as expected in the presence of H₂O-rich fluids at such conditions. Differences in the fluid-saturated solidus at 2.0 GPa, as determined by Hill and Boettcher (1970) (HB70 in **Figure 6(b)**) and by Yaxley and Green (1994) (YG94 in **Figure 6(b)**), can be largely explained by a different speciation of the H₂O-CO₂ mixed fluid, due to different oxygen fugacities attained in the experiments.

The extensive stability of aragonite, dolomite, and magnesite (**Figure 6(b)**) inhibit effective decarbonation at pressures of or above amphibole disappearance, meaning that significant carbon transfer to the mantle wedge is feasible only in the relatively low-pressure field of the forearc region. In experiments buffered at hematite-magnetite-H₂O hydrogen fugacities, relatively high CO₂ proportions can be maintained. However, in such experiments, the source of volatiles is technically unlimited (an unlikely scenario in nature) and the H₂ potential is imposed externally.

Most information concerning amphibole-bearing phase assemblages is obtained from natural occurrences and experiments. Unfortunately, thermodynamic modeling of phase relations in MORB remains unsatisfying when incorporating the amphibole solid solution; both the calculated amounts and stabilities of amphiboles are far from what is observed in nature and experiments. For example, the stability of amphibole in MORB is calculated to 4–5 GPa, instead of the 2.3–3 GPa observed in experiments and deduced from natural eclogites.

Many blueschist minerals contain significant amounts of Fe³⁺ (e.g., Brown and Forbes, 1986; Maruyama et al., 1986). The heterogeneous oxidation within the altered oceanic crust adds another compositional variable, shifts reactions in *P-T* space, and complicates the geochemistry of trace elements having variable oxidation states (e.g., U). The fraction of Fe³⁺/Fe^{tot} is generally highest at the onset of subduction-zone metamorphism, and decreases with increasing grade (Groppo and Castelli, 2010).

Fully hydrated oceanic crust loses about two-thirds of its initial water content in the pressure interval to 2 GPa; most of this fluid will either serpentinize the cold corner of the mantle wedge, or eventually pass through veins to the ocean floor in the forearc region (e.g., Mariana arc, Fryer et al., 1999). The high dehydration rates, in conjunction with a thin mantle wedge close to the trench, should lead to rapid (i.e., within 0.8–3 Ma) and complete serpentinization of the cold corner if fluids percolate pervasively through the mantle wedge (Arcay, 2005; Gerya et al., 2002). The rheological behavior of a serpentinized mantle wedge corner and whether the corner develops counterflows (Davies and Stevenson, 1992), plumes (Gerya and Yuen, 2003) or induces thermal erosion of the lithosphere (Arcay et al., 2005) are still matters of discussion. Such different scenarios have a profound impact on the way we reconstruct volatile pathways in the wedge: Do volatiles stagnate in a cold corner, or are they dragged to the deeper mantle? Do they rapidly percolate to the shallowest levels, or are they advected with buoyant masses?

321.3.2 Low Dehydration Rates and Little Fluid Production (2.5–10 GPa and 500–800 °C)

Until the 1980s, it was believed that oceanic crust is fully dehydrated after pressure-induced amphibole breakdown. However, experiments and natural occurrences of epidote/zoisite, lawsonite, talc, chloritoid, phengite, staurolite, OH-rich topaz, and many other minor hydrous minerals in eclogites that had already lost their amphibole demonstrated that dehydration continues above 2.4 GPa. In particular, the discovery of coesite- and diamond-bearing hydrated eclogites has demonstrated that most of the hydrous minerals listed above are stable at pressures beyond 2.5 GPa (e.g., coesite-lawsonite-bearing eclogites (Tsujimori et al., 2006), some of which occur in xenoliths of the Colorado Plateau (Helmstaedt and Schulze, 1988; Usui et al., 2001)). Generally, the natural occurrence of coesite-, and sometimes diamond-bearing hydrous eclogites (the most famous being Dora Maira, Western Gneiss Region, Dabie Shan, and the Kokchetav Massif; see Liou et al., 1998; Rumble et al., 2003; or Hermann and Rubatto, 2012; for concise reviews) are in good agreement with

experimental findings, and the discussion below is based on experimental *P-T* conditions and mineral abundances.

p0250 Above 2.4 GPa, a maximum of 1.5 wt% H₂O remains stored in hydrous phases of the igneous oceanic crust. The major water hosts are lawsonite, zoisite, chloritoid, talc, and phengite. Lawsonite is the most water-rich of these phases (12 wt% H₂O), and may host >50% of the water present; however, it is restricted to relatively low temperatures (**Figure 6**). Zoisite is stable to about 3.3 GPa, and occurs at the wet solidus until 3 GPa. Talc is only a minor phase in MORB, but becomes abundant in bulk compositions with high X_{Mg} , that is, Mg gabbros. Phengite has an important role, as virtually any K₂O present in the oceanic crust at pressures below 5 GPa will be stored in phengite, irrespective of the bulk composition (Schmidt, 1996). Above this pressure, potassium also enters into clinopyroxene (cpx) (Okamoto and Maruyama, 1998; Schmidt and Poli, 1998) and the relative amounts of phengite, cpx, and coexisting fluid will depend upon the quantity of dissolved potassium and its dissolution rate into the fluid. Above 2.4 GPa, continuous reactions dominate over a few discontinuous ones, and most reactions (including the wet solidus) are subparallel to typical subduction *P-T* paths. As a consequence, a particular rock volume crosses most reactions over wide depth intervals. Thus, dehydration rates are rather low, and the (postamphibole) remnant of 1.5 wt% H₂O is lost over a wide depth range. The pressure–temperature range that defines this ‘low dehydration rate’ regime corresponds to most of the depth interval of the subarc region (**Figures 1** and **6**).

p0255 The hydrous phases in oceanic crust with the widest pressure stability field are lawsonite and phengite, both of which reach into the stishovite field. The breakdown of these two phases corresponds to the ‘end’ of any major dehydration of the oceanic crust.

p0260 Because many reactions are parallel to typical *P-T* paths during subduction, effective H₂O contents, mineral assemblages, and mineral compositions are fairly sensitive to temperature. A K₂O-free MORB passing 600–650 °C at a depth of 100 km has 1 wt% H₂O stored in lawsonite and chloritoid, and will arrive at 200 km with about 0.4 wt% H₂O in lawsonite. Passing 100 km at a temperature of 700 °C causes the loss of the last hydrous phase (zoisite) near this depth, and our MORB volume becomes a dry eclogite and, thus, irrelevant for any further production of mobile phases. On the other hand, if the 100-km depth is achieved at a temperature of 750 °C, MORB is already above the wet solidus, and any fluid infiltrating from below should cause partial melting. As is evident from these considerations, the major difficulty in predicting the type and quantity of mobile phase produced at high-pressure stems from the uncertainty in temperature distribution in the subducting oceanic crust. Unfortunately, a difference of 100 °C has a significant impact.

p0265 Addition of carbonates to the altered MORB compositions does not shrink the stability fields of hydrous phases at >1.5–2 GPa. Somewhat counterintuitively, the temperature stability of lawsonite is increased by approximately 30 °C, due to Ca–Mg partitioning between garnet and carbonates (Poli et al., 2009; **Figure 3**). Hill and Boettcher (1970), who investigated the supersolidus phase relationships of a basaltic composition with mixed H₂O–CO₂ fluids, observed a similar effect for amphibole at 1.0–2.5 GPa. At pressure and temperature

conditions exceeding the stability of lawsonite and epidote, the breakdown of hydrous minerals other than phengite is complete, and carbonates (magnesite, dolomite, or Mg calcite as a function of pressure and of chemographic relationships) are the only volatile-bearing phases, persisting to approximately 1000 °C. Assuming that fluids released from dehydration reactions migrate upward, and almost instantly leave the reactive system, phase relationships in altered H₂O–CO₂-bearing MORB degenerate into the system MORB–CO₂. The latter system is then bound by a carbonatite-forming solidus (see **Section 321.3.3**) at temperatures commonly not achieved in Phanerozoic subduction zones (but which may have been achieved in older subduction zones in a hotter Earth?).

Dissolution of carbonates in aqueous fluids (Caciagli and Manning, 2003; Dolejs and Manning, 2010) generated in the cold, serpentinized peridotitic core of the slab appears to be, as of now, the only viable mechanism by which to transfer carbon to the overlying mantle wedge in this pressure range where decarbonation is inhibited (Gorman et al., 2006). However, the efficiency of this mechanism depends first on fluid production in the subducting peridotite itself, and second on the mode of fluid percolation (channeled vs. pervasive) through the oceanic crust. Further, such a flush dissolution involves variable redox conditions in the reactive lithologies, which still need to be investigated experimentally.

321.3.3 Melting Regimes (650–950 °C to 5 GPa)

s0070

Two principal modes of crust melting may occur in subduction zones: melting at either fluid-saturated or fluid-absent conditions. The principal hydrous phases involved are epidote/zoisite and amphibole, and, to a much lesser extent, biotite, and phengite. If melting of the oceanic crust occurs at pressures below 2.5 GPa, the MORB will not have previously passed through a blueschist and eclogite stage, but through the greenschist and epidote–amphibolite facies at lower pressures (not discussed here).

p0275

Evidence for melting of the oceanic crust is seen in the so-called adakites, which form volcanic suites of andesitic to rhyodacitic composition (Drummond et al., 1996; Kay, 1978) and are interpreted to be partial melts of the oceanic crust that were modified (mainly Mg enriched) during their ascent through the mantle wedge. The interpretation of adakitic suites s.l. is complex, as key trace element ratios (i.e., high La/Yb and Sr/Y, Martin, 1999) reflect an assemblage of garnet+hornblende±plagioclase in the source, and such an assemblage may be produced by a variety of processes, that is, melting of subducted crust (Sen and Dunn, 1994), melting of underplated basalt or lower crust in deep continental arc roots (Atherton and Petford 1993; Jagoutz, 2010), and fractionation of garnet and hornblende within calc-alkaline series magmas (Alonso-Perez et al., 2009; Jagoutz et al., 2011). Nevertheless, a combination of high La/Yb and Sr/Y with anomalously high X_{Mg} values and MgO, Cr, and Ni concentrations (testifying to absorption of olivine during the passage of slab melts through the mantle wedge) at intermediate SiO₂ contents still suggests their origin as slab melts. Melting of subducted crust was possibly predominant on the Archean Earth (Martin et al., 2005), favored by a combination of higher mantle temperatures with more buoyant oceanic plates that were probably thicker, hotter,

and more difficult to subduct (Sleep and Windley, 1982). There is consensus that, on the modern Earth, dehydration dominates in the subducting mafic crust. However, when young, hot crust is subducted when the thermal field within a subduction zone is disturbed at plate boundaries (i.e., at the lateral ends of subducting plates), or when flat slabs form due to ridge subduction, melting of the oceanic crust may also occur.

The compositions of slab melts principally depend on the bulk composition of the oceanic crust, the degree of melting, and the pressure of melting. Nevertheless, at low to moderate melt ratios, where cpx is a major residual mineral, Na/K ratios of the melt mostly depend on pressure. At any pressure in basaltic compositions, potassium is strongly partitioned into the melt. $D_{\text{Na}}^{\text{cpx/melt}}$ partition coefficients are small (<0.5) below 2 GPa, close to unity around 3 GPa, and increase to $D_{\text{Na}}^{\text{cpx/melt}} = 3-7$ at 4 GPa (Schmidt et al., 2004; Thomsen and Schmidt, 2008a). The latter corresponds to 50–70% jadeite component in residual cpx, which, thus, retains most of the Na₂O, but leaves the K₂O for the melt.

As a consequence, melts from amphibole-dominated fluid-absent melting have Na>K as typical for adakites, which, together with the requirement of garnet+hornblende in the residue, thus generally form at 1–2.5 GPa. Even in the relatively K-poor igneous oceanic crust, melts resulting from fluid-present or fluid-absent melting at higher pressures involve phengite and are thus strongly potassic peraluminous granites (with K>Na). Such granites, which would migrate into the mantle wedge at >70 km depth, are not observed at the surface. This is either because they never form or because it is impossible for them to traverse the thick mantle wedge retaining their peculiar chemistry far out of equilibrium with peridotite. Absorption reactions with mantle minerals would largely modify the major element composition of these melts.

There is little consensus on the role of melting at the slab-mantle wedge interface (where most subducted sediments reside, see Section 321.5). *P-T* paths generated from thermal models cover almost the entire *P-T* range. Here, we select two recent models that typify 'very hot' (Syracuse et al., 2010) and 'average cold' (Arcay et al., 2007) thermomechanical models. The 'very hot' type of model (Syracuse et al., 2010) indicates that shear heating and the mechanical coupling of slab and mantle wedge would lead to a relatively abrupt temperature increase of the slab-wedge interface near the coupling depth (50–80 km). Feeding the geometrical parameters of modern subduction zones into their model, Syracuse et al. (2010) obtained a *P-T* path for the slab surface that slightly oversteps the wet pelite solidus in about half the cases. Temperatures of the wet solidus for a K-free MORB are predicted to be attained in only a few modern subduction zones. The 'average cold' *P-T* path (Arcay et al., 2007) incorporates the effects of plate decoupling and thermomechanical ablation of the overriding plate and results in *P-T* paths that only exceptionally would intersect the (wet) minimum solidus of sediments, but not with that of a K-free MORB. We return to the issue of MORB melting after discussing sediment melting.

321.3.3.1 Fluid-saturated (flush) melting

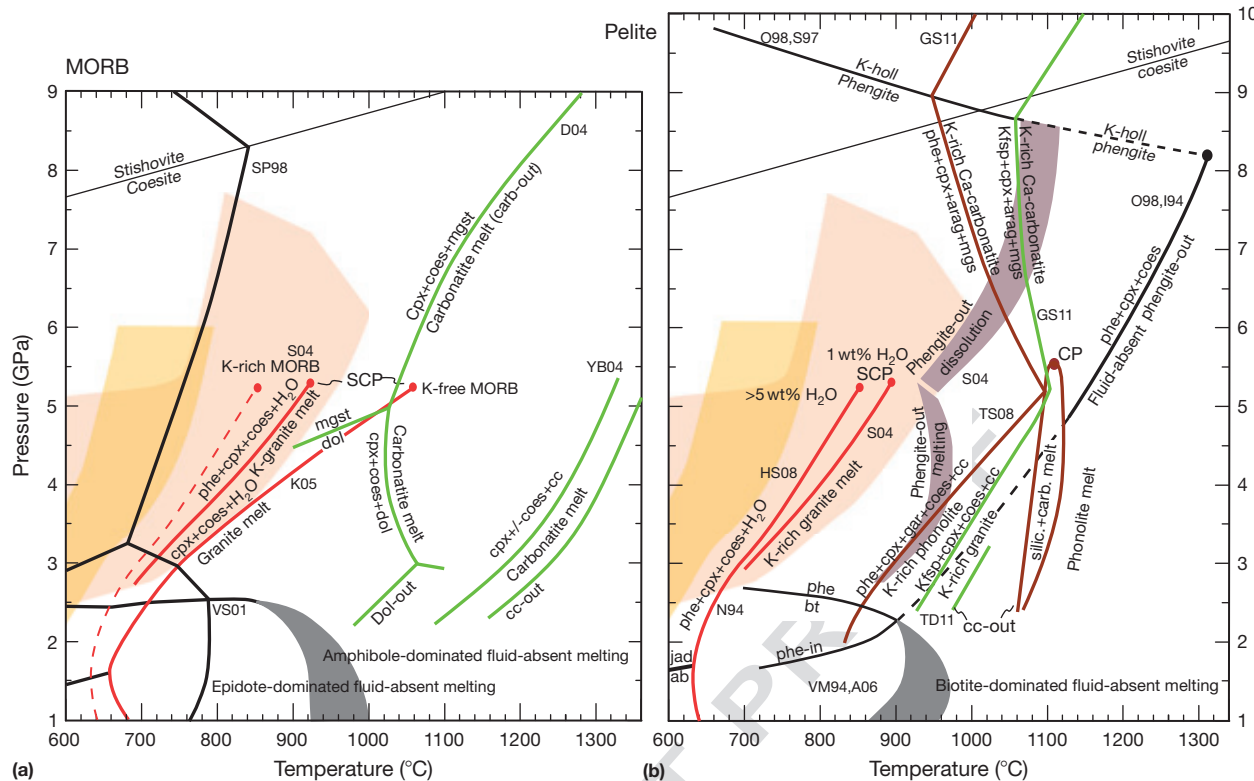
Fluid-saturated melting of K-bearing basaltic crust begins at temperatures of 650 °C at 1.5 GPa, increases to 750 °C at 3 GPa, and ends at ~5.5 GPa, 950 °C (Lambert and Wyllie,

1972; Schmidt et al., 2004; Figure 7(a)). Although a small quantity of free fluid (<0.1 vol%) is likely to be present in any lithology affected by dehydration, such a volume would not be sufficient to produce a significant melt portion through fluid-saturated melting. In subduction zones, fluid-saturated melting could be achieved at relatively low temperatures through flush melting, that is, by addition of aqueous fluid from below. In this case, the melt productivity at the solidus is mainly controlled by the amount of fluid added to the system and may yield 20–30% melt (Kessel et al., 2005b; Klimm et al., 2008; Figure 8). Thus, volumetrically significant melt fractions in MORB will be achieved only by means of added fluids that stem from dehydrating serpentinized peridotite situated below the MORB. Analogously, important sediment melt fractions could result from flushing with fluids from underlying MORB or serpentinized peridotite; these are discussed in Section 321.5.4. For fluid-saturated melting, the wet granite solidus is the most relevant, both for K-bearing mafic systems and for sediments (Schmidt et al., 2004).

321.3.3.2 Fluid-absent melting

Most adakite suites contain andesites that appear to have formed via fluid-absent melting of a basaltic source (but not by melting of mica-dominated sediments only, which would have a lower melting point at any given pressure). Fluid-absent melting is defined as the production of a silicate melt with low water contents from an assemblage that contains hydrous (or carbonate) minerals, but not a separate fluid phase. At pressures below 2.5 GPa, both metapelites and metabasalts contain a pair of hydrous phases with equal water contents (Figure 7). In pelites, phengite (4.3 wt% H₂O) has a lower modal abundance than biotite (4.1 wt% H₂O), but it melts at 100–150 °C lower temperature than biotite. In basaltic compositions, epidote/zoisite (2.0 wt% H₂O, typically 10 vol%) melts approximately 100 °C below amphibole (2.2 wt% H₂O, typically 50–30 vol%, decreasing with increasing pressure; Vielzeuf and Schmidt, 2001; and references therein). In both cases, the first fluid-absent melts are produced through the volumetrically less important phase, that is, phengite in metapelites and epidote/zoisite in metabasalts. These first melts are thought to be dacitic and probably amount to less than 10 vol%. (At fluid-absent conditions, reaction rates are sluggish below ~800 °C, leading to a lack of equilibration during fluid-absent epidote and phengite-dominated melting below 2.5–3 GPa, and hence the lack of experimental data.) It is likely that the primary melts of adakites result from amphibole-dominated fluid-absent melting of MORB, with melt proportions of 20–35 wt%. The garnet+cpx±amph residue thus produced is consistent with the geochemical features of adakites, particularly the strongly fractionated rare-earth element (REE) patterns (Martin, 1999).

Nevertheless, the temperature distribution in a stratified oceanic crust is such that subducted sediments are typically at higher temperatures than the igneous oceanic crust. Thus, if the amphibolites are melted, the overlying sediments must also melt through mica-dominated fluid-absent melting. This complexity needs to be taken into account in geochemical slab-melting models. Fluid-absent melting of amphibolite or metapelite cannot be fully described in a closed system or in a system open only to melt extraction. The temperatures necessary for fluid-absent melting of the MORB layer



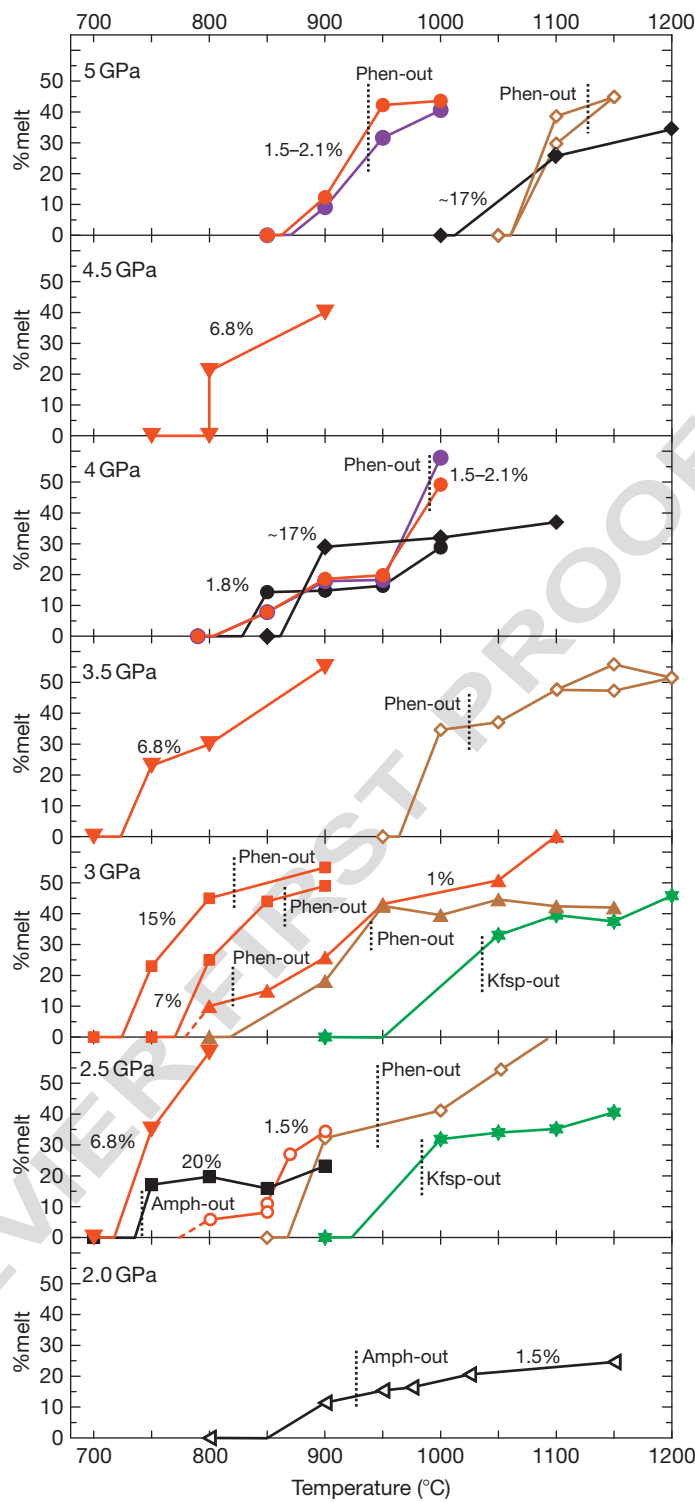
f0040

Figure 7 Compilation of melting reactions in (a) MORB and (b) pelite. (a) Position of the wet solidus (solid red lines) for a K-enriched MORB (Schmidt et al., 2004) and a K-free MORB (Kessel et al., 2005b) with respect to subduction-zone temperatures as modeled by Arcay et al. (2007, yellow field) and Syracuse et al. (2010, orange field). The dashed red line reproduces the wet pelite solidus of panel (b) for reference. Note that the dichotomy of fluid or melt ends at the second critical endpoint (SCP) near 5 GPa, at which pressure a chemical and physical continuum exists between H_2O -rich fluid and silicate-rich melt at the solidus (for details see text). The solidus of K-free MORB below 3 GPa is modified from Lambert and Wyllie (1972). Metabasalts contain two hydrous phases stable above the wet solidus: epidote and amphibole. Both would lead to fluid-absent melting when they break down at low pressures; epidote-dominated fluid-absent melting is expected to produce only a few percent melt, while amphibole-dominated fluid-absent melting is thought to be responsible for adakite generation. Also shown are two solidi for the MORB– CO_2 system (green lines): The lower temperature one, from Dasgupta et al. (2004), is for MORB + CO_2 and has dolomite or magnesite as the stable carbonate at subsolidus conditions. The higher temperature one is for MORB + calcite, from Yaxley and Brey (2004); the shift in $Ca/(Ca + Mg + Fe^{2+})$ resulted in high-Mg calcite as subsolidus carbonate. The most likely first-order explanation for the temperature difference is the nature of the carbonate mineral. At 3–6 GPa, the minimum melting in carbonate systems is near the dolomite composition (Buob et al., 2006; Irving and Wyllie, 1975). Compare subsolidus reactions with **Figure 6**. For comparison, the pelite solidus (b) is reported as dashed red line. (b) Solidi for pelites: red lines are for the wet solidus in a system with >5 wt% excess H_2O (Nichols et al., 1994; to 3 GPa, Hermann and Spandler, 2008; at 3–4.5 GPa) and for a system with <1 wt% excess H_2O (1–1.5 wt% H_2O being bound in phengite, Schmidt et al., 2004). The wet solidus ends slightly above 5 GPa, above which pressure phengite disappears through a continuous solution process (upper reddish gray field) even with less than 1 wt% excess H_2O . The lower reddish gray field locates the melting out of phengite in the <1 wt% excess H_2O (~2 wt% total bulk H_2O) system. The fluid-absent phengite-dominated solidus is unknown. The thick black line denotes the likely location of the phengite-out in fluid-absent systems but is deduced from different experiments (Irfune et al., 1994; Ono, 1998). The brown lines give the melting reactions and the carbonate–silicate melt immiscibility gap for a fluid-absent pelite– H_2O – CO_2 system (Thomsen and Schmidt, 2008a; to 5 GPa, Grassi and Schmidt, 2011a; at >5 GPa). Note that to 5 GPa, a silicate melt forms first, but above 5 GPa, it is a carbonate melt. Compare brown lines to the topology of **Figure 11**. Green lines: interpolated solidus for pelite– CO_2 system (2–3 GPa, Tsuno and Dasgupta, 2011; >5 GPa, Grassi and Schmidt, 2011a). Also in the latter system, a silicate melt forms at 2–3 GPa and a carbonate melt at >5 GPa. At low pressures, fluid-absent melting of biotite would occur (Auzanneau et al., 2006; Vielzeuf and Montel, 1994). A few very warm P–T paths may intersect the wet pelite solidus, but expected melt fractions are small (compare to **Figure 8**) and the efficiency of element transfer at such conditions has recently been questioned (Behn et al., 2011). A06: Auzanneau et al. (2006); D04: Dasgupta et al. (2004); GS11: Grassi and Schmidt (2011a, 2011b); HS08: Hermann and Spandler (2008); I94: Irfune et al. (1994); K05: Kessel et al. (2005a, 2005b); N94: Nichols et al. (1994); O98: Ono (1998); S97: Schmidt (1997); S04: Schmidt et al. (2004); SP98: Schmidt and Poli (1998); TD11: Tsuno and Dasgupta (2011); TS08: Thomsen and Schmidt (2008a, 2008b); VM94: Vielzeuf and Montel (1994); VS01: Vielzeuf and Schmidt (2001); Yaxley and Brey (2004).

Au2

(800–900 °C) are such that the hydrated peridotite below would reach the serpentine stability limit, thus possibly providing a significant amount of fluid. This fluid would strongly increase the melt fractions in amphibolites and metapelites, and might be required to produce a sufficient quantity of

primary melts, which then give rise to adakite suites. This important indirect feedback mechanism, that is, the temperatures necessary for melting in one lithology causing dehydration reactions in an adjacent lithology and thus increasing melt fractions in the former one, has not yet been investigated.



f0045

Figure 8 Silicate melt fractions for fluid-saturated and fluid-absent melting with various combinations of H₂O–CO₂ volatiles present. Red: pelites with H₂O as volatile component, brown: pelites with H₂O + CO₂ as volatile component, green: pelites with CO₂ as volatile component. Purple: graywacke with H₂O as volatile component. Black: MORB with H₂O as volatile component. Closed symbols denote fluid-saturated melting experiments, and open symbols, fluid-absent ones. Bulk H₂O contents (in wt%) are indicated for experiments with H₂O as the only volatile component. Melt fractions for carbonated sediments and basalts that produce carbonatite melts are not shown, as these correspond to the amount of carbonate present at 50–1000 °C above the solidus. Pelites and graywackes: full circles: Schmidt et al. (2004); open circles: Auzanneau et al. (2006); triangles pointing down: Hermann and Spandler (2008); squares: Skora and Blundy (2010); open diamonds: Thomsen and Schmidt (2008a); six-pointed stars: Tsuno and Dasgupta (2011). MORB (black): Full diamonds: Kessel et al. (2005a); full squares: Klimm et al. (2008); open triangle pointing left: Sen and Dunn (1994).

s0085 **321.3.4 Dissolution Regime (>5–6 GPa)**

p0315 The typical low-pressure concept of low-density $\text{H}_2\text{O}-\text{CO}_2$ fluids (with small to moderate amounts of solute) in the subsolidus and high-density silicate liquids above the solidus (with typically 1–15 wt% H_2O dissolved) does not apply to the subduction environment at pressures above 5–6 GPa. At such high pressures, a chemical continuum exists between fluids and melts (Boettcher and Wyllie, 1969), and a continuous dissolution process leaches hydrophile species out of sediments, basalts, and peridotite.

p0320 The fluid–melt dichotomy ends at the ‘second critical endpoint’ (Ricci, 1951) of the solidus, where the critical curve, defined by the (critical) closure points of the fluid–melt miscibility gap, intersects with the fluid-saturated solidus (Figure 9, inspired from Stalder et al., 2000). At crustal pressures, the large

miscibility gap between a low-density aqueous fluid and a high-density hydrous silicate melt leads to ‘fluid’ and ‘melt’ phases with quite distinct chemical and physical properties (e.g., solubilities and composition, viscosity, compressibility). Nevertheless, with increasing pressure, the solubilities of silicates or silicate components in fluids and of H_2O in silicate melts both increase, the miscibility gap between classical ‘fluid’ and ‘melt’ shrinks, the critical curve intersects the solidus, and a chemical continuum between the two extremes – a dry silicate melt and a pure H_2O fluid – is possible (Figure 9). At pressures above this intersection, that is, the critical endpoint of the solidus, the phase boundary between fluid and melt no longer exists, and a single phase field for a supercritical liquid results. This implies a continuum between the chemical and physical properties of former melt and fluid, but does not imply that a

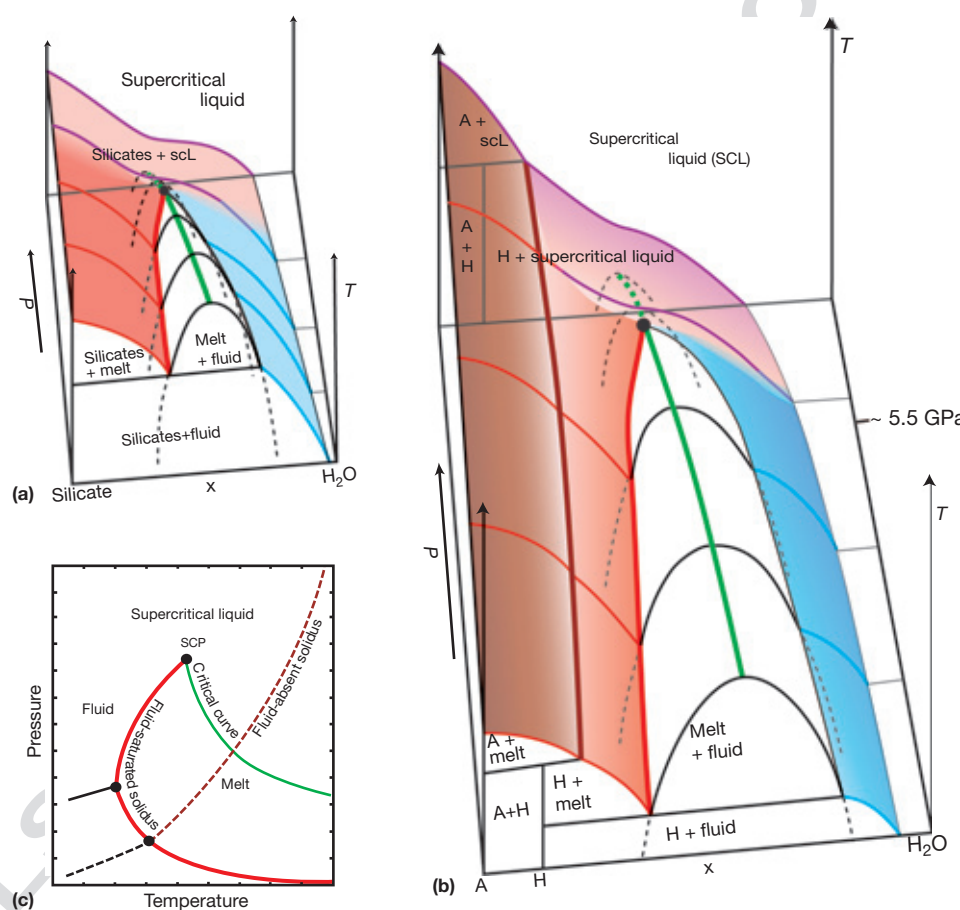


Figure 9 Simplified phase relations at the endpoint of the solidus and the end of the aqueous fluid–hydrous melt dichotomy, where continuum properties of a supercritical liquid exist. (a) With no hydrous phases stable above the solidus (as applicable for MORB at >3 GPa). (b) With hydrous phases (H) stable above the solidus (as applicable for pelites where the hydrous phase is phengite). A, anhydrous silicate. As is characteristic of supercritical liquids, a boundary between a noncritical and a supercritical fluid or melt or liquid cannot be drawn. (c) P – T diagram showing the wet solidus (red line), the critical curve (green line) that corresponds to the crest of the fluid–melt immiscibility gap, and the fluid-absent solidus for a hydrous phase (brown line). At low pressures, a broad miscibility gap exists between a hydrous fluid and an H_2O -bearing melt. With increasing pressure, reciprocal solubilities increase, until the immiscibility gap becomes metastable at the wet solidus. At this point, a continuum between fluid-like and melt-like properties and compositions emerge for all pressures above the solidus’ endpoint. The T – x section on the backside of panels (a) and (b) gives the continuum curve for pressures above the critical endpoint of the solidus. Fluid-absent melting is not affected by the endpoint, and the peritectic reaction $\text{H} = \text{A} + \text{melt}$ is stable at all pressures of (b) and (c). Note that the influence of CO_2 on the critical endpoint of the solidus of natural rock compositions is unknown, but the few available experiments seem to indicate that, in the CO_2 -only system, carbonatite melts form between 3–5 and 23 GPa.

liquid phase with chemical and physical properties otherwise characteristic of lower pressure silicate melts or fluids may not exist at pressures beyond the second critical endpoint. The term 'supercritical fluid' is not adequate to name the liquid phase at pressures above the second critical endpoint, as this term is already used for aqueous/carbonic fluids above the first critical endpoint (at a few 100 bars and °C), which are already supercritical. We thus adopt the term 'supercritical liquid.' Formation of such a supercritical liquid leads to greater dissolution of many key (trace) elements than silicate melt itself, and thus such liquids are effective agents of element transfer from the subducting crust to the mantle wedge (see [Section 321.7](#)).

At conditions of the second critical endpoint, the wet solidus vanishes, the concept of melting loses its definition, and solid assemblages continuously dissolve in an initially volatile-rich but, with increasing temperature, more and more silicate-rich liquid phase. Pressures for this endpoint have been determined to between 1 and 13.5 GPa and strongly depend on the chemical system. However, the exact pressures are still uncertain because of inherent experimental difficulties in identifying complete liquid miscibility versus two coexisting, but increasingly similar, liquids. A variety of experimental strategies based on both *ex situ* (Kennedy et al., 1962; Kessel et al. 2005b; Nakamura and Kushiro, 1974; Paillat et al., 1992; Stalder et al., 2001) and *in situ* (Mibe et al., 2007; Shen and Kepler, 1997) observations have been developed, but none of these resolve all complexities deriving from the behavior of solubility and critical curves in multicomponent systems.

In the simple system $\text{SiO}_2\text{-H}_2\text{O}$, the second critical endpoint is only at 1 GPa 1100 °C (Kennedy et al., 1962); in albite- H_2O , it moves to ca. 1.5 GPa (Stalder et al., 2000); and in $\text{CaO}\text{-SiO}_2\text{-H}_2\text{O}\text{-CO}_2$, it occurs at 3.2 GPa, 500 °C (Boettcher and Wyllie, 1969); however, in the model ultramafic system $\text{MgO}\text{-SiO}_2\text{-H}_2\text{O}$ (MSH), the solidus terminates at ~12 GPa, 1100 °C for compositions in olivine-opx (orthopyroxene)- H_2O (Stalder et al., 2001), and at 13.5 GPa for more magnesian compositions (Melekova et al., 2007). In MORB, graywackes, and pelites, the miscibility gap closes somewhere between 5 and 6 GPa (Hermann and Spandler, 2008; Kessel et al., 2005b; Schmidt et al., 2004). Consequently, up to 5 GPa, a classical sequence of melting reactions and quenched melts is observed in experiments on basalts and pelites, whereas at 6 GPa, initially abundant phengite (in the pelite) becomes less and less abundant until it disappears, and an alkali- and SiO_2 -rich quench precipitate becomes more and more abundant at grain boundaries. In the MORB- H_2O system, the supercritical liquid near the critical endpoint contains between 50 and 30 wt% H_2O and resembles a peralkaline granite when recalculated on a volatile-free basis (Kessel et al., 2005b).

s0090 321.4 How Much H_2O Subducts into the Transition Zone?

It is well known that refertilization of the mantle takes place through transfer of fluids or melts from the subducting lithosphere to the overlying mantle wedge, as described above. A portion of the elements transferred into the mantle wedge is partitioned into partial melts, which ultimately produce arc volcanism and, thus, do not refertilize the deep mantle.

The residue of oceanic crust remaining from this process is subducted to depths of >300 km, where it may ultimately be mechanically mixed with mantle material (Allegre and Turcotte, 1986). Dixon et al. (2002) deduced from the geochemistry of ocean island basalts, which are widely believed to contain some recycled oceanic crust in their sources (see Hofmann, 2012), that dehydration is >92% efficient during subduction.

In order to evaluate how much water is subducted to great depths in the mantle, it is necessary to (i) determine the amount of H_2O stored in peridotite after pressure-induced decomposition of serpentine, and (ii) understand the state of the oceanic crust at pressures just above the phengite breakdown reaction. Any oceanic peridotites that pass beyond 220 km depth and any oceanic crust that passes beyond 300 km depth is unlikely to liberate a liquid phase within the context of ongoing continuous subduction. Only a few hydrous phases may exist beyond 200 and 300 km depth in peridotite and oceanic crust, respectively, and temperature stabilities for these phases ('phase A,' 'phase E,' and 'phase D' in peridotite (Angel et al., 2001; Frost, 1999; Ohtani et al., 2000; Ulmer and Trommsdorff, 1999) and the hydrous aluminosilicates topaz-OH and 'phase egg' in aluminous sediments (Ono, 1998)) increase faster than any subduction geotherm, at least to 20 GPa (see Figure 3 in Ohtani, 2005). Furthermore, hydrous phases become much less important at pressures beyond 10 GPa; the volumetrically dominant, nominally anhydrous phases such as olivine, wadsleyite, garnet, and cpx dissolve considerable amounts of hydrogen at these pressures, and become the principal hydrogen reservoirs at greater depths (3000 ppm OH⁻ in natural cpx from 6 GPa, 1000 °C (Katayama and Nakashima, 2003) up to 3.3 wt% H_2O in wadsleyite (Kohlstedt et al., 1996)).

Whether a significant amount of water is subducted beyond 200 km in peridotitic compositions depends on the exact *P-T* path experienced by the slab. As can be seen in [Figure 10](#), any serpentine-bearing peridotite descending along geotherms that are cooler than 580 °C at 6 GPa (termed the 'choke point' by Kawamoto et al., 1995) will conserve H_2O and form 'phase A' (and subsequently phases E, B, and D). In oceanic lithosphere subducting along geotherms that pass between 580 °C, 6 GPa and 720 °C, 7 GPa, the 10-Å phase forms upon serpentine breakdown (Fumagalli and Poli, 2005; Fumagalli et al., 2001) and holds 0.6 wt% H_2O in the peridotite. Entering the stability field of 'phase A' at greater depths will not lead to a significant increase in the bulk H_2O content of the slab, as most of the fluid produced from serpentine breakdown would have already escaped.

321.5 Devolatilization in Sediments

321.5.1 Pelites + H_2O

While subduction-zone metamorphism leads to a continuous decrease of H_2O stored in MORB, this is not necessarily true for pelites at pressures upto 2.5–3 GPa. By far the most abundant hydrous minerals in metapelites are the potassic micas, phengite, and biotite. The amount of H_2O stored in micas (containing 9–10 wt% K_2O and 4–4.5 wt% H_2O) is easily calculated from the bulk K_2O content. Other important hydrous phases in subduction-zone metapelites are talc, chloritoid, and

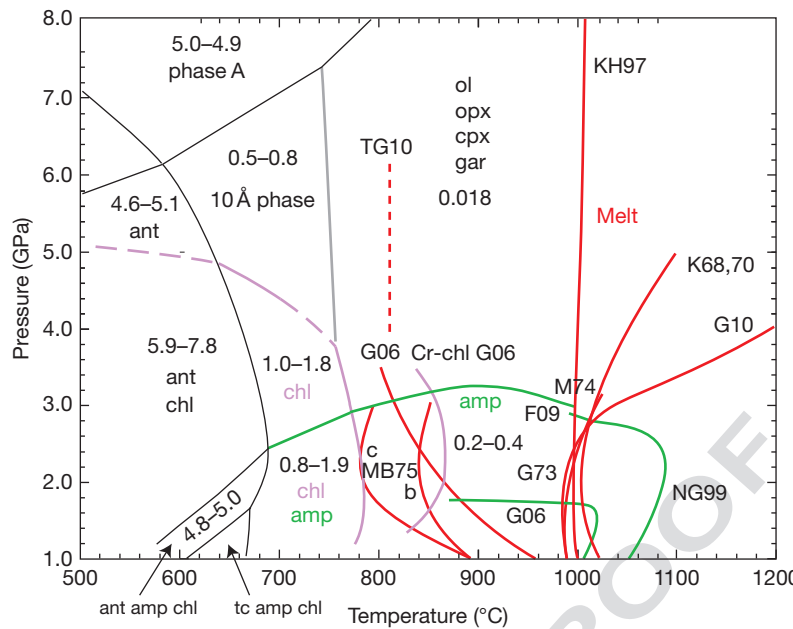


Figure 10 Major phase stability boundaries in H_2O -saturated peridotite and H_2O contents stored in hydrous phases for harzburgite and lherzolite (upper and lower number, respectively, modified from Schmidt MW and Poli S (1998) Experimentally based water budgets for dehydrating slabs and consequences for arc magma generation. *Earth and Planetary Science Letters* 163: 361–379; Fumagalli P and Poli S (2005) Experimentally determined phase relations in hydrous peridotites to 6.5 GPa and their consequences on the dynamics of subduction zones. *Journal of Petrology* 46: 555–578). Red curves are the wet solidi from the various studies; green curves, the amphibole stability limits; and purple curves, the chlorite stability limits. Serpentized peridotite following cold P - T paths will not dehydrate up to transition zone depths, as phase boundaries of ‘phase A’ are flatter in P - T space than typical subduction P - T paths. At high temperatures, for example, in the mantle wedge fluxed by fluids released from the slab, wet melting is still poorly constrained. MB75: Mysen and Boettcher (1975), bulks b and c; G06: Grove et al. (2006); TG10: Till and Grove (2010); G73: Green (1973); F09: Fumagalli et al. (2009); M74: Millholen (1974); M07: Mibe et al. (2007); KH97: Kawamoto and Holloway (1997); K68: Kushiro et al. (1968); G10: Green et al. (2010); NG99: Niida and Green (1999).

chlorite (see compilation in Poli and Schmidt, 2002). The stabilities of these minerals strongly depend on X_{Mg} , which varies in oceanic pelagic sediments from 0.2 to 0.8 (e.g., Plank, 2012; Plank and Langmuir, 1998). Biotite is generally expected to transform to garnet + phengite-bearing assemblages at 2.5–3 GPa (Poli and Schmidt, 2002), but extremely high bulk X_{Mg} values may stabilize biotite to 4 GPa (Hermann, 2002a). By contrast, phengite is stable to 8–9 GPa (Domanik and Holloway, 1996; Ono, 1998).

The absolute amount of hydrous phases, and therefore the maximum amount of H_2O in metapelites, is strongly controlled by the amount of quartz, which is highly variable in mica schists. An average of nine metapelites (containing between 12 and 46 vol% quartz) from the Nome Blueschist Terrane, Alaska (Thurston, 1985) yields 2.7 wt% H_2O stored in phengite, chlorite, paragonite, epidote, and glaucophane. The same average bulk composition would contain about 2.0 wt% H_2O in the hypothetical assemblage phengite-talc-chloritoid-lawsonite (+garnet+coesite), stable at 3 GPa, 600 °C (Chmielowski et al., 2010), and would contain 1.1 wt% H_2O where phengite is the only hydrous phase closer to the solidus. Thus, during subduction from 20 to 80 km depth, 300 m of mica schist would yield only 2–6% of the total mass of H_2O released from 2 km of underlying, fully hydrated MORB. These numbers are fairly approximate, as further experimental work is required to explore the significance of talc, chlorite, and chloritoid in the critical pressure

range of 2–4 GPa. Nevertheless, metapelites contain generally less H_2O than MORB in a low-pressure blueschist stage, but more H_2O at pressures beyond 2.5 GPa.

Typically, only a few 100 m of sediments may be subducted, and the quantity of volatiles stored in pelites is small when compared to MORB and serpentized peridotite. The importance of pelites to subduction-zone geochemistry lies in their relatively high concentration of K_2O and other highly incompatible minor and trace elements, which may be concentrated in accessory phases (typically rutile, allanite, zircon, phosphates, ellenbergerite (Klimm et al., 2008)). Thus, sediments can impart a strong enrichment of incompatible trace elements to slab fluids or melts, which is quite distinct from that derived from the igneous oceanic crust (Plank, 2012). For example, if present, allanite (an LREE-enriched epidote that may be residual during melting) contains more than 90% of the whole rock LREE and Th; rutile contains more than 95% of Ti, Nb, and Ta; zircon contains 95% of the whole rock Zr and Hf; and phengite, at a modal abundance of 20–35%, incorporates more than 95% of the bulk rock Rb, Ba, and Cs (see also Hermann, 2002b). Finally, as discussed above, pelites may strongly impact melting, because carbonate-free pelites have the lowest melting temperature of all subducted lithologies at subarc conditions, and experience the highest temperatures within the subducting oceanic crust.

Like metabasalts, the solidus of wet pelites ends between 5 and 6 GPa (Schmidt et al., 2004). At high pressures, the solvus

between fluid and melt closes and a chemical continuum is realized (**Figure 9**). Estimates of the amount of solute in such liquids above 6–7 GPa range from 50 to 70 wt% (a molar $H_2O : K_2O$ ratio slightly above 1 is, in fact, sufficient for completely dissolving micas), which is close to the solubility of H_2O in water-saturated melts near 3 GPa. Due to the high solubility of K_2O (and probably other components that are less soluble at low pressures), it is expected that only a small part of the subducted potassium and related trace elements would reach great depths. A large portion of the potassium is likely to be transferred to the overlying mantle wedge, where, in a MgO -rich, SiO_2 -poor chemical environment, phlogopite or K-richterite (potassic amphibole) may reprecipitate (Konzett and Ulmer, 1999; Sudo and Tatsumi, 1990; Trønnes, 2002) and then be dragged to greater depths in the mantle directly overlying the subducted slab. The potassium remaining in the oceanic crust after dehydration and leaching is stored in the anhydrous phase K-hollandite ($KAlSi_3O_8$), which is stable to >25 GPa (Grassi and Schmidt, 2011a).

s0105 321.5.2 Graywackes and Volcanoclastic Sediments

p0370 Graywackes and volcanoclastic sediments of andesitic to dacitic composition are a significant component of sedimentary columns at trenches (Plank, 2012; Plank and Langmuir, 1998). Phase diagrams of graywackes and andesites (Schmidt, 1993; Vielzeuf and Montel, 1994) suggest that, for our present purpose, these systems can be viewed as being intermediate between pelites and MORB. The typically 1–3 wt% K_2O in graywackes and volcanoclastic sediments of intermediate composition lead to abundant micas (phengite or biotite) and, thus, they experience reactions and have phases similar to those in pelites. On the other hand, CaO contents are significant enough for the formation of amphibole and zoisite, thus leading to phases and reactions similar to those in intrinsically CaO -rich MORB. Obviously, compared to MORB and pelites, reactions are shifted in the $P-T$ space because of different phase compositions. Furthermore, the proportions of phases are highly variable.

s0110 321.5.3 Carbonated Pelites

p0375 The subducted mass of H_2O in most subduction zones is much larger than that of CO_2 , and at many trenches, the sediments do not contain much carbonate (Rea and Ruff, 1996). Near-trench sediment columns have molar $CO_2 : H_2O$ ratios mostly below 1:3, and a ratio above 1:1 was only found along the middle-American to Peruvian margin (Plank and Langmuir, 1998; Rea and Ruff, 1996; compiled in Poli and Schmidt, 2002). For a more detailed understanding of fluid-producing processes, it is necessary to evaluate the effect of CO_2 on hydrous and carbonate phase stabilities, on fluid and melt-forming reactions, and on melt and fluid compositions.

p0380 Somewhat different from metabasalts, the succession of carbonate minerals in carbonated pelites is expected to be ankeritic calcite → aragonite + magnesite with increasing pressure (**Figure 7(b)**). The calcite–dolomite solvus on the high X_{Mg} side of the $Ca-Mg-Fe$ ternary (relevant for peridotites and MORB) is closed at the low X_{Mg} side (Franzolin et al., 2011), and, thus, a ternary carbonate is generally present in Fe-rich

metasediments (Grassi and Schmidt, 2011a,b; Tsuno and Dasgupta, 2011). In the subsolidus, aragonite + magnesite replace the ternary ankeritic calcite at 5–6.5 GPa. Both calculations (Kerrick and Connolly, 1998, 2001a,b) and experiments (Thomsen and Schmidt, 2008b) show that, at low to intermediate temperatures (up to 800 °C at 4 GPa), a very small amount of CO_2 saturates the system in carbonate, and fluids are buffered to compositions with ≤10 mol% CO_2 , with CO_2 fractions decreasing with increasing pressure.

As x_{CO_2} 's are low in fluids produced from carbonated lithologies during subduction-zone metamorphism, the only efficient decarbonation processes are either flushing with aqueous fluids from below or melting at relatively high temperatures. A scenario describing decarbonation reactions caused by fluid infiltration during subduction would be a layer of carbonaceous sediment overlying hydrated oceanic lithosphere. At any time, the metacarbonate would probably contain a very small amount of equilibrated fluid having 5–15 mol% CO_2 at depths beyond 60 km (the exact CO_2 fraction depending on pressure and temperature (Gorman et al., 2006; Kerrick and Connolly, 2001a,b; Molina and Poli, 2000; Poli et al., 2009)). Aqueous fluid produced in serpentine and basalt below the carbonate layer will migrate upward, replacing the CO_2 -bearing fluid, and then will locally equilibrate, that is, consume carbonate, in order to increase the CO_2 content in the fluid. If the aqueous fluid passes pervasively through a carbonated sediment or limestone, the entire carbonate layer may eventually dissolve, and the fluid migrating into the wedge may transport significant quantities of CO_2 over time.

321.5.4 High-Pressure Melting Systematics of Sediments and MORB

s0115

In some subduction zones, melting of the downgoing oceanic crust might be achieved at pressures above amphibole and biotite stability (>3 GPa). In order to understand which lithologies might melt under high-pressure conditions, it is necessary to compare the melting relations of sediments and MORB under the various fluid-availability conditions. The lowest melting temperatures (at >3 GPa) are achieved for the assemblage phengite + jadeitic cpx + coesite + aqueous fluid, that is, ~700 °C at 3 GPa and ~800 °C at 4.5 GPa (Hermann and Spandler, 2008). Pelitic sediments are highly variable in composition and, apart from fluid availability, melt productivity depends on how closely the bulk sediment composition plots to the peritectic phengite:coesite:cpx ratio. Within 50 °C above the solidus, typical melt fractions of 20–40% are achieved in experiments at ~7 wt% bulk H_2O , while small H_2O excesses of 1–2 wt% yield only 10–15% melt (**Figure 8**, and references therein).

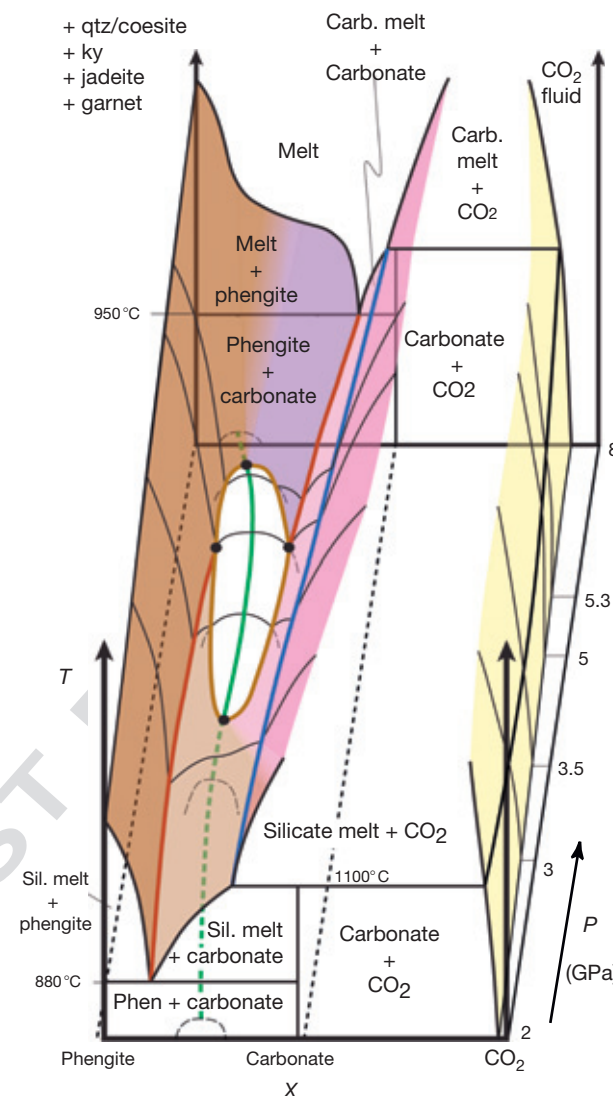
Melting temperatures for K-rich MORB, graywackes, and pelites remain very similar, as long as the phengite + coesite + cpx assemblage is present (Schmidt et al., 2004). The wet MORB solidus is situated 20–50 °C above the wet pelite solidus (**Figure 7(a)** and **7(b)**). All three lithologies melt to produce siliceous granites, which become increasingly potassian with pressure as residual cpx becomes increasingly more abundant and jadeitic (Schmidt et al., 2004). Any carbonate addition results in the presence of ankeritic calcite in the sediments and, in case of fluid saturation, a mixed H_2O-CO_2 fluid phase.

Unfortunately, experiments determining the fluid-saturated solidus for a mixed C–O–H fluid are not yet available. It is speculated that the addition of carbonates to the system causes only a small increase in melting temperatures: $x\text{CO}_2$ in the fluid, which increases the solidus temperature, remains low at >3 GPa, but CO_2 solubilities in silicate melt, which decrease the solidus temperature, become significant. Thus, these effects may almost cancel out.

p0400 An interesting feature of melting at pressures above 3 GPa arises from the fact that MORB (Okamoto and Maruyama, 1999; Schmidt, 1996), pelites (Domanik and Holloway, 1996; Ono, 1998), and also intermediate andesite (Poli and Schmidt, 1995), graywacke (Schmidt et al., 2004) and continental crust compositions, (Hermann and Green, 2001) all contain garnet, cpx, phengite, and coesite (Schmidt et al., 2004). Peraluminous graywackes and pelites also have kyanite. Thus, all the lithologies of the oceanic crust contain the same assemblage, and fluid-saturated melting occurs through the identical reaction $\text{phengite} + \text{cpx} + \text{coesite} + \text{H}_2\text{O} = \text{melt} \pm \text{garnet}$. If a significant amount of free water is not available, only minor melting might occur at the wet solidus, and the production of major melt fractions occurs only through $\text{phengite} + \text{cpx} + \text{coesite} = \text{garnet} + \text{melt} \pm \text{kyanite}$. This reaction takes place about 150–200 °C above the wet solidus (at 3 to at least 5 GPa) and leads to 20–30 wt% melt in the metasediments, and to a few percent melt in the mafic rocks (dependent on the bulk K₂O content, Figure 8). In MORB, phengite is immediately consumed upon melting, and the temperature must rise by >100 °C to significantly increase melt fractions through the reaction $\text{cpx} = \text{garnet} + \text{melt}$ (25–30% melt). Nevertheless, temperatures necessary for these high-pressure melting reactions are high and unrealistic at the slab–mantle interface (for discussion see Section 321.8).

p0405 At truly fluid-absent conditions, melting temperatures for the assemblages $\text{phengite} + \text{jadeite} + \text{coesite}$, $\text{phengite} + \text{calcite} + \text{jadeite} + \text{coesite}$, and $\text{K-feldspar} + \text{calcite} + \text{jadeite} + \text{coesite}$ become exceedingly high: 910–960 °C at 3 GPa and 1030–1100 °C at 4.5 GPa (Thomsen and Schmidt, 2008a; Tsuno and Dasgupta, 2011). As might be expected, the $\text{H}_2\text{O} + \text{CO}_2$ -bearing fluid-absent system with $\text{phengite} + \text{calcite}$ melts at lower temperatures than the H_2O -free, CO_2 -bearing system with $\text{Kfsp} + \text{calcite}$. The fluid-absent solidus in the H_2O -only system, with phengite as the only volatile-bearing phase, has not been determined yet. It is approximated indirectly from other experiments in Figure 7(b) (Irfune et al., 1994; Ono, 1998). The temperatures necessary for fluid-absent melting, for any combination of H_2O and CO_2 as volatiles, are not predicted by any model for the slab surface. Thus, fluid-absent sediment melting is not expected to occur, unless cold diapirs involving metasedimentary material rise from the slab surface into the mantle wedge (Gerya and Yuen, 2003; see discussion below).

Au15 p0410 An interesting feature of $\text{CO}_2 + \text{H}_2\text{O}$ -bearing carbonated sediments occurs at ~ 5 GPa, when the solidus reaction yielding a phonolitic silicate melt changes to one that yields an alkali-rich carbonate melt (Figures 7(b) and 11). The high-pressure solidi at >5 GPa (with or without H_2O), which lead to carbonate melts, have negative slopes in the P – T space for both the H_2O -bearing and H_2O -free systems (Grassi and Schmidt, 2011a,b). Thus, they could be intersected by hot slab P – T paths (Figure 7(b)). Such alkali-rich carbonatites from carbonated pelites would form between 6 and 9 GPa, that is, beyond the



subarc pressure range. Due to their low viscosity and good wetting properties, these carbonatite melts are expected to travel into the mantle, but probably enter into a larger mantle cycle than represented by the subduction system.

In order to achieve flush melting of the sediments, a concomitant dehydration within the underlying hydrated layers (MORB + ultramafics) is required. This scenario requires a very particular thermal regime: first, the sediments have to pass through the temperature range of 700–800 °C at 3.0–4.0 GPa (subarc region) and, second, the temperature within the lower part of the oceanic crust and serpentized mantle must be high enough to provide a significant quantity of fluid via lawsonite (MORB) or antigorite or chlorite breakdown reactions (peridotite). Within the temperature range where flush melting occurs in the sediments, in a ‘normal’ temperature gradient within the slab (i.e., temperatures decreasing with depth in the oceanic crust by almost 200 °C within 10 km, see **Figure 6** in Arcay et al., 2007), mafic eclogites would retain H₂O in lawsonite and serpentized peridotites would remain in the chlorite + serpentine stability field and, thus, not produce any fluid. For the same reason, flush melting of MORB near the wet solidus by fluids derived from underlying serpentinite is improbable in the depth range of interest (compare with **Figure 1**, see Syracuse et al., 2010). Warmer regimes, where extensive dehydration of serpentinite promotes fluid flow, are therefore expected to result in (unrealistic) sediment melting at forearc conditions.

The combined conditions necessary for significant flush melting to occur might well be realized in some subduction zones; however, the large range of calculated P-T paths demonstrates that realization of these conditions will not be the general case, and that it is not expected for most of the fast subduction zones that dominate the Pacific rim. For these, thermal models predict temperatures too low for melting in the 3–4 GPa depth range (Gerya et al., 2002; Kincaid and Sacks, 1997; Syracuse et al., 2010).

Fluid-absent melting at lower pressure conditions, involving biotite in sediments or amphibole in MORB, produces melts with distinct compositions at different P-T conditions (**Figure 7**), with different pressure dependencies of the melting reactions. The amphibole-melting reaction bends strongly backward around 2 GPa and, near the solidus, amphibole disappears at 2.4 GPa (**Figure 7(a)**). In MORB, epidote/zoisite remains stable at the solidus to ~3 GPa, allowing for minor fluid-absent melting up to these pressures. Any fluid-absent but H₂O-present melting in MORB at higher pressures depends on the K₂O content of MORB and the related presence of minor biotite/phengite. In average metapelites and graywackes, biotite is completely replaced by phengite around 2.5–2.8 GPa (Auzanneau et al., 2006; Vielzeuf and Schmidt, 2001), but at high Mg/(Mg+Fe), biotite stability extends to ~4 GPa (Hermann, 2002a).

321.6 Serpentized Peridotite

The serpentized peridotite layer that lies just below the igneous oceanic crust (and is often brought to the surface in slow-spreading oceans such as the Atlantic) constitutes a H₂O reservoir in the subducted lithosphere comparative in mass to

the oceanic crust. The degree of serpentization in this layer is difficult to quantify because it is highly variable both on a regional and local scale, as distinctly localized hydrothermal systems near the ridge and transform faults of all dimensions are the primary sites of hydration. Hydration has also been suggested to occur in extensional faults that parallel the trench and are caused by bending of the subducting plate at the onset of subduction (Peacock, 2001). Our best estimate is an average of 20% serpentization to a few kilometers’ depth (Schmidt and Poli, 1998). Although there might be some localized serpentization along faults much deeper in the oceanic lithosphere, large-scale serpentization and the resulting low-density peridotite (2.3–2.5 g cm⁻³) would cause a buoyancy problem during subduction.

While a number of reactions at intermediate to elevated temperatures are important for hydration of peridotite in the overlying mantle wedge directly adjacent to the top of the oceanic crust (**Figure 10**), almost any subduction P-T path will keep the slab in the serpentine stability field to at least >2 GPa (Ulmer and Trommsdorff, 1995). As a consequence, hydrated peridotite in the downgoing lithosphere will contain serpentine and chlorite (+ olivine + cpx), while a multitude of reactions are taking place in the oceanic crust above. The serpentized peridotite layer of the oceanic lithosphere will not produce any significant fluid to pressures of 3–6 GPa, at which, depending on temperature, serpentine breakdown may occur (**Figure 10**). The H₂O contents of **Figure 10** are calculated for average harzburgite. However, oceanic alteration not only adds H₂O but also removes MgO. Peridotite sitting just above the slab surface experiences metasomatism by fluids that derived or passed through generally quartz- or coesite-saturated sediments and MORB, and, thus, these fluids are most likely somewhat SiO₂-enriched. If the MgO/(MgO + SiO₂) ratio in the peridotite is shifted from between olivine and serpentine to a value between serpentine and talc, then talc stabilizes to higher pressures (talc + serpentine reaction; Bailey and Holloway, 2000; Ulmer and Trommsdorff, 1999). In monomineralic veins, talc might persist to its maximum pressure stability limit at 4.5–5.0 GPa (Pawley and Wood, 1995). Potassium addition and formation of phlogopite has long been considered a feature of fluid-related metasomatism in mantle wedge peridotites (Sekine and Wyllie, 1982; Wyllie and Sekine, 1982). Fumagalli et al. (2009) have shown that the mineral chemistry of phlogopite can be highly variable at very high pressures and temperatures below 900 °C. The ‘talc/10-Å phase’ substitution ([v]SiAl_{1-K-1}) promotes increased modal proportions of a ‘potassium-deficient’ phlogopite beyond the stability of talc (**Figure 4(b)**), and therefore H₂O transfer in wedge peridotite that is dragged downward by the slab. The transformation of phlogopite to K-richterite, an amphibole with a K/OH ratio very similar to phlogopite, at >6 GPa (Konzett and Ulmer, 1999) is responsible for further H₂O fixation in the solid, for limited fluid release, and for inhibition of melting in this setting.

With respect to the subducting lithospheric peridotite, subduction zones can be divided into two types: those with hotter geotherms where the serpentine-out reaction overstepped below 6 GPa (and major dehydration of serpentized peridotite occurs), and those with cooler geotherms where the serpentine stability boundary is overstepped at >6 GPa.

As discussed above, almost no fluid production is expected when serpentine reacts directly to 'phase A' (see **Figure 10**) and the H₂O stored in the hydrated peridotite subducts deeply. By contrast, if the stabilities of serpentine and 'phase A' do not overlap along a given slab geotherm, a significant flushing zone (over 20–30 km depth) is expected due to the reactions: serpentine–chlorite peridotite → chlorite peridotite → anhydrous garnet peridotite. The width of such a zone is controlled by the stability of chlorite, which is stable at least 100 °C higher than serpentine in complex systems approaching natural rocks (Fumagalli and Poli, 2005). Up to 3.5 GPa, chromium appears to enlarge the temperature stability of chlorite (Grove et al., 2006), although the roles of chlorite and the wet peridotite solidus are still heavily debated (**Figure 10**; see below).

p0445 The above dehydration sequence changes along a cooler *P-T* path, producing the succession serpentine → 10-Å phase → 'phase A' (Dvir et al., 2011; Fumagalli and Poli, 2005). In this case, a moderate amount (max. 0.8 wt%) of H₂O subducts to great depth, while >75% of the initially subducted H₂O of the serpentized peridotite is lost via dehydration.

p0450 In a number of arcs (NE Japan–Kuriles–Kamchatka, Aleutians, N. Chile), the so-called double seismic zones are observed. Whereas the upper seismic zone is located within the oceanic crust, it has been suggested (Peacock, 2001; Seno and Yamanaka, 1996) that the lower seismic zone corresponds to the limit of serpentine stability in the lower part of the oceanic lithosphere (see **Figure 10**). Lower seismic zone earthquakes are triggered by reactivation of ancient faults due to fluid saturation, where the fluids derive from serpentine or, in some cases, chlorite dehydration (Dorbat et al., 2008).

p0455 It has recently been suggested that the wet solidus of peridotite occurs at temperatures sufficiently low to intersect chlorite stability at subarc depths (Grove et al., 2006). As a result, flush hydration and melting of the hanging mantle wall of the slab has been proposed as a possible mechanism for the production of arc magmas (Grove et al., 2006). However, discrepancies in experimental determination of the wet peridotite solidus at 2.0–3.5 GPa are dramatic and amount to 300 °C (Fumagalli et al., 2009; Green, 1973; Green et al., 2010; Grove et al., 2006; Kawamoto and Holloway, 1997; Kushiro, 1970; Kushiro et al., 1968; Millholen et al., 1974; Mysen and Boettcher, 1975). Such differences in the location of the solidus correlate with differences in the pressure stability of pargasitic amphibole, which is 1.8 GPa for Grove et al. (2006) and 3.0 GPa for Niida and Green (1999) and Fumagalli et al. (2009). Differences are even more extreme at higher pressures. At 6 GPa, Till and Grove (2010) suggested the occurrence of a wet solidus for peridotite at 810 °C, whereas Green et al. (2010) found the wet solidus at 1370 °C. Green et al. (2010) suggested that these discrepancies could be mostly ascribed to the amount of H₂O added to the run charge, to Na partitioning into the fluid phase, and to the interpretation of the amorphous quench phase found in the experimental charges. This phase has been variably interpreted as a melt or a precipitate from a solute-rich high-pressure fluid. However, as discussed in the context of the critical endpoint of the solidus, a reliable determination of the physical state(s) of the liquid (melt, fluid, or both, or supercritical liquid) cannot be obtained from textural observation of interstitial quench products from H₂O-rich melts or solute-rich fluids.

Furthermore, if chlorite would occur on the wet solidus, fluid-absent melting of chlorite must exist. No evidence for this is observed either in nature or in the MgO–Al₂O₃–SiO₂–H₂O system. Nevertheless, addition of CaO and/or FeO might shift the solidus and, thus, intersection of the chlorite+cpx/opx stability field with the solidus may occur in the CFMASH **Au16** system. Such a possibility should be experimentally explored. We further note that an 800 °C solidus of peridotite would lead to melting in orogenic peridotites metamorphosed to granulite facies, such as Beni-Bousera (Kornprobst, 1969) and/or peridotite bodies in the Western Gneiss Region (Norway) (Carswell and van Roermund, 2005), and that such melting has not yet been described.

Addition of carbonates, as in ophiocarbonate breccias, is not expected to alter significantly the picture described above at temperatures below 950 °C, although the details of phase relationships for the H₂O+CO₂-present solidus are still debated (Olafsson and Eggerl, 1983; Tumiati et al., 2009; Wallace and Green, 1988).

321.7 Implications for Trace Elements and an Integrated View of the Oceanic Lithosphere **s0125**

Trace elements and isotopes such as ¹⁰Be, B, Li, Ba, Cs, and elements of the U–Th series provide important information on element transfer processes in arcs and are reviewed in Morris and Ryan (2012), Kelemen et al. (2012), and Plank (2012). Such studies may allow one to distinguish between a sediment and an altered MORB signal in island arc volcanic rocks (Morris et al., 1990) to deduce across-arc variations as a function of slab depth (Ishikawa and Nakamura, 1994; Moriguti and Nakamura, 1998; Ryan et al., 1995), yield time constraints on element transfer (Sigmarsson et al., 1990; see Turner et al., 2003; for review), and might allow a distinction between dehydration and melting processes (Martin et al., 2005; Sigmarsson et al., 1998). On the other hand, the correct interpretation of trace element concentrations and their spatial distributions rely on major element phase relations and on the understanding of the nature and quantity of the mobile phase, as discussed in this chapter.

321.7.1 Mobile Phase Production and Trace Element Transfer **s0130**

Devolatilization of the oceanic crust is a process that combines continuous and discontinuous reactions in a variety of heterogeneous bulk compositions. In addition, within a vertical column, the sedimentary, mafic, and serpentized peridotite layers, all experience a significant thermal gradient. The result is a continuous, but not constant, production of a fluid or melt, with the rate of mobile phase production generally decreasing with depth. Peaks in the volatile flux result from significant discontinuous reactions. However, despite the continuous fluid flux, trace elements may not necessarily be released continuously.

All dehydration reactions in oceanic lithosphere take place at temperatures where diffusion rates in most minerals are insignificant compared to the available time span for fluid production in subduction zones. Thus, in terms of trace

element partitioning, it is necessary to distinguish between the mineral mode in a given bulk composition and the reactive volume, which will be much smaller. For example, an altered MORB at 4 GPa, 700 °C has 48 vol% garnet, 39 vol% cpx, 5 vol% lawsonite, 2 vol% phengite, and 6 vol% coesite. The breakdown of lawsonite can be modeled via the reaction lawsonite + cpx + garnet₁ = garnet₂ (grossular enriched) + H₂O, which produces about 8 vol% garnet in the rock (Schmidt and Poli, 1998). The garnet that grows from the breakdown of lawsonite is in equilibrium with the fluid, while the preexisting garnet is not. Diffusion rates at 700 °C for garnet and cpx are so slow that, in the available time span (several tens of thousands of years, based on radioactive disequilibrium, see review by Turner et al., 2003), the volumes of the nonreacting garnet and cpx affected by diffusion are negligible (< 0.1 vol%). Thus, the trace elements formerly residing

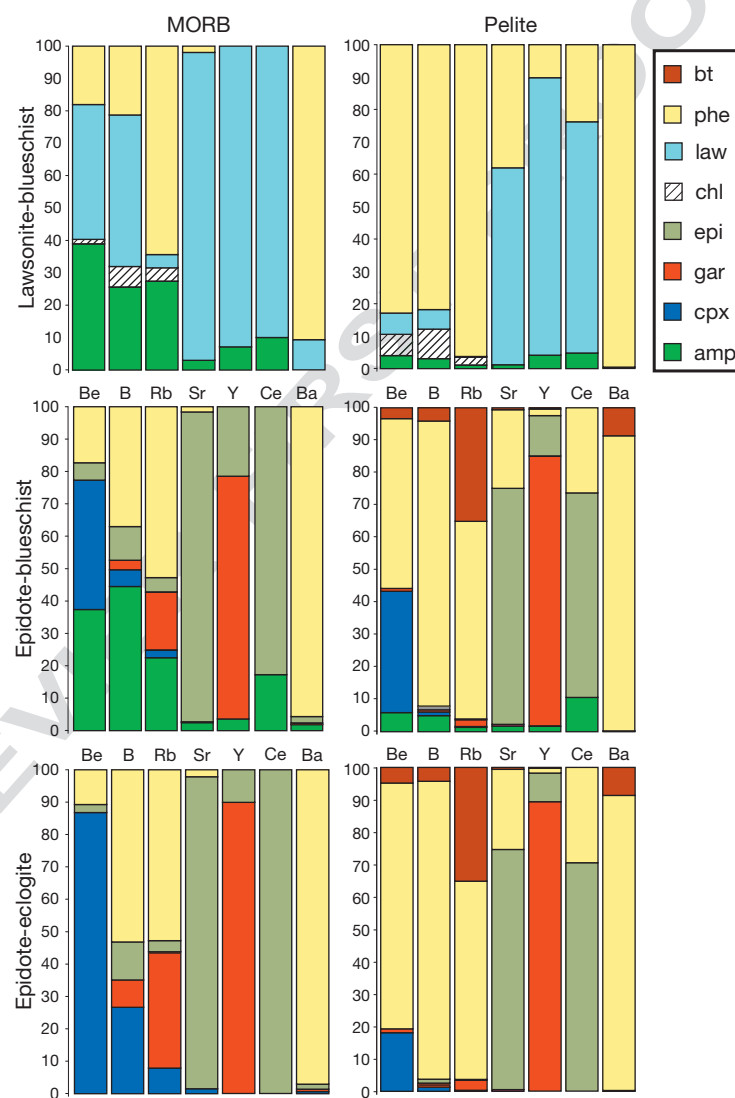
in lawsonite and the 3 vol% of cpx that decompose with lawsonite are redistributed between the newly formed garnet and fluid. More than 85 vol% of the rock remains unequilibrated and, thus, cannot be included when calculating geochemical residua or trace element contents of the fluid. As a consequence of slow solid-state diffusion, in most cases, the only elements that may be mobilized are those hosted in minerals that decompose, and it is necessary to quantify the trace element redistribution among the minerals in subduction-zone lithologies (Figure 12).

The following cases may be distinguished:

p0485

- Highly soluble elements (e.g., B, Cs, or Rb; Ryan et al., 1995; Figure 13) where the mineral/fluid partition coefficient is ≪ 1. The concentration of such elements may continuously decrease in the fluid with increasing depth.

u0010



0065 **Figure 12** Distribution of Be, B, Rb, Sr, Y, Ce, and Ba between minerals of average MORB and pelite in blueschist and eclogite facies (assuming representative mineral modes for natural blueschists and experimental epidote-eclogite; trace element concentration data mostly from Domanik et al., 1993). At subsolidus temperatures, diffusive equilibration is ineffective (except for micas) and the equilibrating volume that needs to be taken into account for trace element modeling is defined by the reacting minerals. Thus, a given trace element equilibrates with the fluid only when its host phase(s) break(s) down.

Concentrations might already be very low in fluids produced at moderate depths due to the effective removal from the subducting crust at shallow levels. Such behavior is also expected for any salt that is present in the altered oceanic crust.

- u0015 • Elements with partition coefficients close to 1 (e.g., Be; Marschall et al., 2007). In this case, the concentration in the fluid does not change as subduction progresses (**Figure 13**).
- u0020 • Elements that partition strongly into a particular hydrous phase (e.g., La, Ce, Sr into lawsonite or epidote, the latter also hosting most of the Th, **Figure 6**) and have only moderate to low cpx/fluid and gar/fluid partition coefficients. These elements will quantitatively enter into the fluid at the breakdown reaction(s) of the given mineral, and cause a pulse in their concentrations that is not at all proportional to the fluid flux. The transfer of such elements to the mantle wedge is much more effective than in a bulk equilibrium situation.

- Elements that partition strongly into mica (e.g., Ba and, to some extent, Be in the sediments). As mica dissolves with increasing depth and temperature, these elements enter into the fluid only at greater depth, its flux at low temperature and pressure being small.
- Elements that strongly partition into cpx or garnet (HREE) or into accessory minerals that are stable during devolatilization (e.g., rutile, zircon, monazite, allanite; Hermann and Rubatto, 2009; Klimm et al., 2008). Such elements will be returned to replenish the deep mantle trace element reservoir.

321.7.2 Integrating Fluid Flux over the Entire Subducted Oceanic Crust: An Example

The layered structure of oceanic lithosphere originating from fast-spreading ridges, combined with temperature gradients within the subducting lithosphere, defines the relationship between the amount and depth range of fluids and/or melts

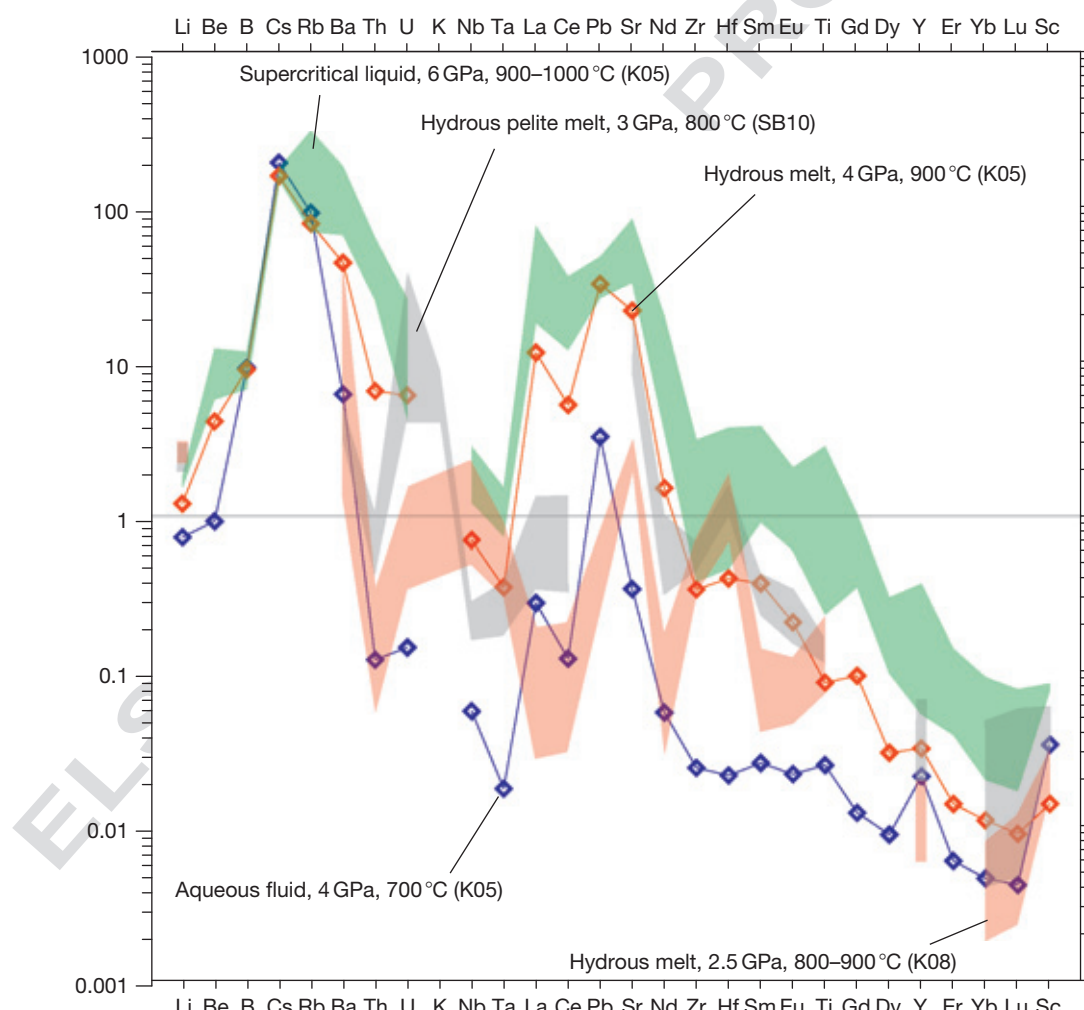


Figure 13 Liquid/solid residue partition coefficients for fluid/MORB (blue diamonds), melt/MORB (red diamonds and red array), supercritical liquid/MORB (green array), and melt/pelite (gray array). In all cases, the residue is composed of garnet + cpx ± quartz/coesite with rutile + epidote/allanite for the gray melt/MORB field, and with phengite + ilmenite + rutile for the red melt/pelite field. Data from Kessel et al. (2005a) – K05: diamonds and green array, Klimm et al. (2008) – K08: red array, and Skora and Blundy (2010) – SB10: gray array.

generated by devolatilization in the sedimentary and mafic layers and fluids generated from the ultramafic layer. The interdependence between sediment and MORB melting and dehydration in serpentized peridotite was illustrated in **Section 321.3.3**. Here, an example of the effects on trace element transfer as a function of fluid to rock ratios is illustrated. The layered structure of the oceanic lithosphere may cause the fluid to rock ratio in the sedimentary layer to be greater than 1 (as fluids from the underlying mafic and peridotitic layers must rise through the sediments). Thus, some of the trace elements commonly considered to be efficiently mobilized only by melts (e.g., Be, Th) could also be quite effectively mobilized by fluids, if the entire subducted lithosphere is considered.

p0520 An apparent contradiction was put forward to argue for melting of sediments contemporaneously with dehydration of MORB. It was estimated that >30–40% of the subducted Be and Th, which are strongly enriched in sediments, are recycled into the mantle and extracted via arc volcanism (Johnson and Plank, 1999, and references therein). At the same time, B, which is strongly enriched in altered MORB, and U appear to be effectively recycled into arc magmas by fluids. Based on bulk partition coefficients $x_{\text{tl}}/\text{fluid}D$ of 2–4.8 and $x_{\text{tl}}/\text{melt}D$ of 0.7–1.5 for Be and Th, Johnson and Plank (1999) argued that recycling of >30–40% is possible only when sediments melt, while MORB dehydrates (mobilizing B and U). It was then shown by thermal modeling that such a temperature distribution is possible (van Keken et al., 2002). However, this scenario treats sediments, MORB, and hydrated peridotite as independent systems. Considering that the bulk partition coefficients for Be and Th are not extremely high, that is, <2–5, that most of the Be partitions into phengite, and that phengite is the only phase where diffusive reequilibration at subsolidus temperatures is possible, it follows that an elevated fluid to rock ratio can dissolve >80% of the Be (and probably Th) in the sediments if pervasive fluid infiltration from the lower layers occurs. Employing the above partition coefficients, the fluid produced from MORB dehydration below 3 GPa would be sufficient for leaching 60% of Be (and possibly Th) out of 200 m of pelagic sediments. Thus, sufficient Be could be mobilized before typical melting depths are reached. This estimate is conservative in that partition coefficients for relatively low-pressure fluids are employed. Solute-rich, high-pressure fluids and continuous dissolution of phengite would greatly facilitate the transfer of Be to the mantle wedge and, in fact, significant mobilization of Be could simply be taken as evidence that micas dissolve away in a dissolution regime.

p0525 Finally, trace element transport by supercritical solute-rich liquids is more efficient than by silicate melts: a comparison of liquid/bulk residue partition coefficients (**Figure 13**) for fluids, silicate melts, and supercritical liquids (Kessel et al., 2005a; Klimm et al., 2008; Skora and Blundy 2010) demonstrates that liquid/residue partition coefficients of supercritical liquids are greater than for melts, which in turn are greater than for fluids. Unfortunately, full sets of mineral/liquid partition coefficients that allow calculation of liquid/bulk residue partition coefficients are rare and, thus, the comparison of **Figure 13** is limited to few datasets. The partition coefficients express a somewhat relative mobility of characteristic elements, which has to be modified considering the reactive volumes and limited bulk equilibration during devolatilization.

321.8 Dents in a Simplified Subduction Model

s0140

This chapter is a plea for geocomplexity (Holloway, pers. comm.). Petrology provides a geochemical toolbox that contains mineral phases and reactions, which produce mobile phases that have well-defined major and trace element characteristics. For each type of subduction zone, a few ingredients have to be chosen from this toolbox, ultimately leading to different mechanical properties of the rock volumes under consideration and to distinct chemical characteristics of the mobile phase as a function of lithological input and P - T paths.

321.8.1 Predicting Element Transfer and the Role of Sediments

s0145

Natural processes, that is, heterogeneous bulk compositions, heterogeneous volatile distribution, equilibrium on different scales, and kinetic effects, give rise to complexities in individual subduction zones. Nevertheless, there is no reason for pessimism. Today, the dehydration and decarbonation behaviors of the two volumetrically predominant lithologies, basalt and peridotite, are fairly predictable. The resulting mobile component then has a sediment signal added. This signal can be predicted when the composition of the subducting column of sediments and the temperatures to which these sediments are exposed are well known. There is geochemical evidence for a correlation between the subducted sediment composition and the ‘sediment signal’ in arc magmas (e.g., Morris and Ryan, 2003; Plank, 2012; Plank and Langmuir, 1993; Turner et al., 2003). Nevertheless, the temperatures necessary for effective extraction of trace elements from sediments are very much under discussion.

Traditionally, petrologists, geochemists, and modelers have always liked clear and sharp boundaries between the subducting plate and the overlying mantle wedge. Nevertheless, this need not be so, and an interesting class of models (Gerya and Yuen, 2003) removes this conceptual boundary (see also **Figure 3**), allowing for sediment diapirs rising into the mantle wedge. Moving crustal material into the mantle wedge leads to temperatures characteristic for the mantle, thus enabling large-degree melting in such diapirs. Behn et al. (2011) argue, on the basis of natural metapelites, that the mobility of trace elements that are characteristic of sediments (Th, Be, Nd, Pb) is negligible until temperatures of 1050 °C are reached. Thus, even if the slab surface temperature might slightly exceed temperatures of the fluid-saturated solidus of sediments, a different mechanism to achieve high temperatures would be needed, making the case for sediment-containing diapirs into the mantle wedge. The rise of such diapirs would be facilitated through partial melting, as long as the melts do not escape.

321.8.2 The Formation of the Volcanic Arc

s0150

The complexity of natural processes in subducting slabs is reflected by the complex distribution of volcanic emissions in subduction zones. First, it should be emphasized that only 69% of modern subduction zones on Earth (totaling 40 900 km trench length; Schmidt and Poli, 2003) show active volcanism in the Quaternary. The rest (18 500 km) are not volcanic

because of either unfavorable thermomechanical environments (e.g., flat slabs, initiation of subduction, etc.) or possibly the lack of a sufficient amount of volatiles released at depths where melting could take place.

p0550 Even though we believe there is no straightforward relationship between the location of fluid release in the slab and volcanic emissions, the variability of reaction patterns illustrated in this chapter is recorded by a large variability in the distribution of volcanic arcs on Earth's surface (Figure 14, see also England et al., 2004). The spatial onset of volcanism, the arc, is probably primarily controlled by the thermal structure in the mantle wedge, that is, when a sufficient thickness and convection intensity in the mantle wedge is reached in order to allow temperatures necessary for the formation of primitive arc magmas (Kushiro, 1987; Schmidt and Poli, 1998). The depth of the slab below the volcanic front was often regarded as a relevant parameter to characterize petrologic processes occurring in subduction zones (Gill, 1981; Tatsumi, 1986). This parameter has often been expressed as single values with some sort of standard deviation (128 ± 38 km (Gill, 1981), 110 ± 38 km (Tatsumi, 1986), 108 ± 14 km (trench-side chain), 173 ± 12 km (backarc-side chain) Tatsumi and Eggins, 1995) on the basis of a fairly arbitrary 'volcano counting' in selected arcs. On the contrary, our compilation (Schmidt and Poli, 2003) is based on the available slab surface tomographies and on the spatial extent of volcanic activity and shows that, although some maximum is found at ~ 100 km depth, a continuum in the 'depth of the slab surface below the volcanic front' is observed (Figure 14(a) and 14(b)). Again, despite the fact that a majority of volcanic arcs are fairly well focused on the surface (< 50 km wide), volcanic activity across more than 100 km of arc width is not unusual (Figure 14(c)). Such an arc width corresponds to a comparative depth range of the slab surface.

p0555 As a first-order observation, the 'depth of the slab below the arc front' has a clear distribution maximum in the histogram for continental arcs, while such a maximum is absent in that for intraoceanic arcs. This somewhat surprising observation suggests that the crust of the overriding plate may play an important role in the focusing of melts from the mantle wedge. In fact, in some continental arcs (e.g., Sumatra, the Southern Volcanic Zone in the Andes, Figure 15), a narrow volcanic arc is the result of virtually all volcanoes being situated on a major fault oriented subparallel to the trench. In such a case, it appears likely that the volcano distribution is not directly related to processes taking place below the lithosphere of the overriding plate.

p0560 For many decades, a correlation between petrological and geochemical processes at depth and geometric subduction parameters (convergence or burying velocity, slab dip, etc.) was sought with the volcano distribution at the surface. The only robust correlation observed so far is a negative one between the width of the volcanic arc and the subduction angle. This correlation can be interpreted as a simple geometric correspondence of a slab depth interval with a surface width. It is beyond the scope of this review to discuss in detail the statistical parameters of subduction zones, but the absence of other correlations and the wide range of slab surface depths below the volcanic front (Figure 14(a) and 14(b)) suggest that conditions attained in subducting slabs are highly variable, even for

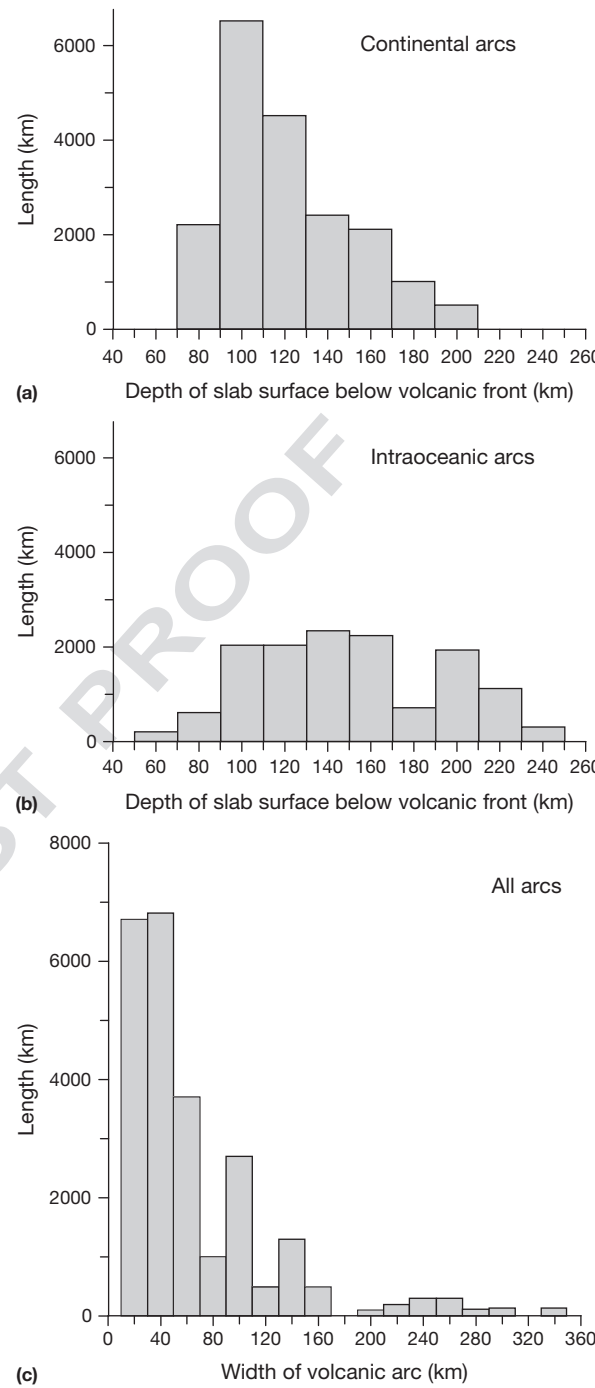
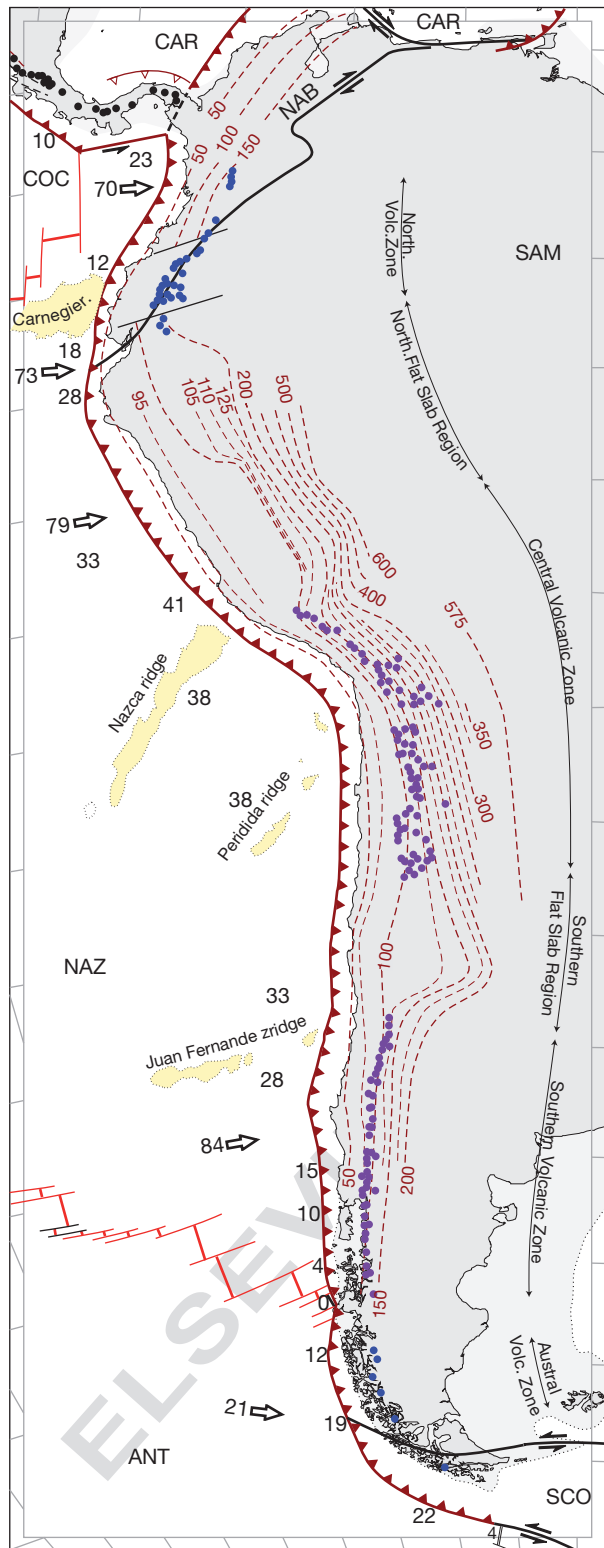


Figure 14 Subduction-zone statistics: histograms of depths of the slab surface below the volcanic front subdivided into (a) continental arcs and (b) intraoceanic arcs. (c) Histogram of the width of volcanic arcs. The vertical axis denotes arc lengths in km measured at the trench. This is our own compilation (unpublished) based on locations of quaternary volcanoes and slab surfaces from tomography (if available), otherwise earthquake depths. f0075

similar convergence parameters, and that the interplay between thermomechanical properties and reaction paths is responsible for a complex pattern of fluid release and magma genesis.



f0080

Figure 15 Compilation of arc volcanoes, slab surface isobaths, and selected tectonic features for the South American subduction zone, which represents a relatively simple geometry. Although subduction-related volcanism is known in South America since the Ordovician, volcanically active sectors and the geometry of the slab continuously change at present; this is mostly due to (aseismic and mid-oceanic) ridge subduction. See text for further details and references.

There is general agreement that, in most arcs, the parental melts form by melting in the mantle wedge (Kushiro, 1987). Thus, arcs that differentiate from a primitive basaltic parent are the surface manifestation of volatile-assisted decompression melting in the mantle wedge (Grove et al., 2006) and of mantle flow, rather than volatile transfer from the subducted lithosphere. In this spirit, the volcanic arc forms where mantle melting is sufficiently important to cause surface volcanism (Schmidt and Poli, 1998). An assumption tacitly built into a correlation between (subduction) kinematics and temperature distribution (in the mantle wedge) is that the kinematics directly governs the temperature distribution, that is, that subduction zones are in steady state. The down drag of the subducting lithosphere on the mantle wedge plays a major role in convection in the wedge, and the coupling depth between slab and mantle wedge is crucial in all models (e.g., Arcay et al., 2007; Syracuse et al., 2010). Nevertheless, a correlation between the (orthogonal) subducting plate velocity or the (orthogonal vertical) burying velocity and the 'height of the volcanic front above the slab' is either weak and can be identified for only a selected set of arcs (England and Katz, 2010), or is completely absent (our unpublished compilation, and Syracuse and Abers, 2006). It is important to emphasize that both of these studies concur with the concept that anhydrous melting in the mantle wedge governs the primary melt production in arcs.

p0565

Why is it that a correlation between kinematic parameters, thought to govern the thermal field in the mantle wedge, and the position of the volcanic arc, resulting from melting in the mantle wedge, is mostly absent? Most likely this is because the present-day kinematics has not been constant long enough in time to achieve a close correspondence between the present-day kinematics and the present-day thermal field. In other words, subduction zones are unlikely to achieve steady-state kinematics and thermal structure as (i) geometrical changes occur on faster time scales than those on which steady state could be achieved, and (ii) part of the flow in the mantle wedge results from Rayleigh–Taylor instabilities, which are not stable over time (Gerya et al., 2003).

p0570

From a petrological perspective, the approach to a thermo-mechanical steady-state condition requires a stable three-dimensional geometry of the subducted lithosphere and constant kinematic response of the overriding plate for periods on the order of tens of million years. This is not the case for most subduction zones.

Au18

p0575

In the Andes, two segments produce adakitic magmatism (Martin et al., 2005), while the Central and Southern volcanic zones produce calc–alkaline suites that derive from primitive mantle basalts (Figure 15). One adakite segment is in Ecuador, where the subducting aseismic Carnegie Ridge, formed from the Galapagos hotspot, causes a flat slab style subduction (Gutscher et al., 1999) resulting in the melting of the Carnegie Ridge (Beate et al., 2001). The second adakitic segment is the Austral volcanic zone (e.g., Sigmarsdóttir et al., 1998), where subduction of the MOR separating the Nazca and Antarctic plates is considered responsible for anomalously high temperatures in the subducting lithosphere. In between the volcanic segments are two nonvolcanic segments with flat slabs, which are thought to result from subduction of the Juan Fernandez and Nazca ridges (Figure 15). This enormous along-strike

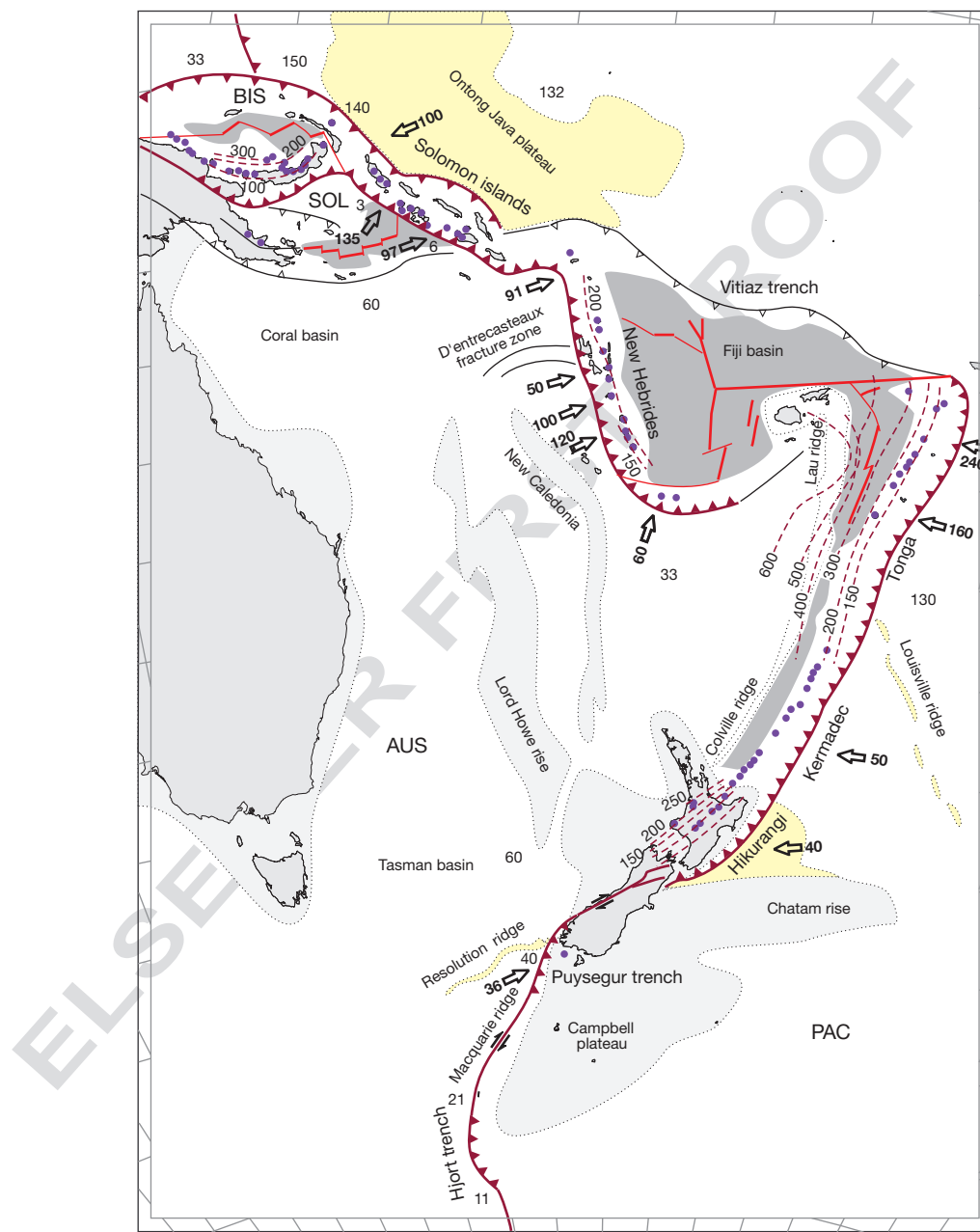
p0580

variation in the Andes, where subduction has been occurring since several 100 Ma in a relatively simple geometry, underlines the degree to which regional scale plate configurations influence the surface volcanism. To understand this surface volcanism, mass transfer from the subducting plate to the mantle wedge is one key player, but certainly not the only one.

In the Southwest Pacific (Figure 16), more than 9000-km-long subduction systems from the Puysegur and Hjort trenches in the South to the Bismarck plate in the NW are heavily influenced by movements of the Australian and Zealandia continental blocks, by the impact of some of the largest of

the large igneous provinces (LIPs) and, consequently, by some of the fastest reversals in subduction polarity and opening of back-arc basins.

In the North Island, New Zealand, complexities in volcanic activity, shifting in space from subduction-related to intraplate and anorogenic magmatism, are attributed to the interplay of W-directed subduction of oceanic crust, to the subduction of the Hikurangi LIP, and to the behavior of sutured Zealandia blocks. The volcanic activity along the Tonga-Kermadec system has a large gap corresponding to the intersection between the subduction trench, the Louisville Ridge (a track of the



f0085

Figure 16 Compilation of arc volcanoes, slab surface isobaths, and selected tectonic features of the South Pacific subduction zones. Reversals in subduction polarity, gaps in volcanic activity, and location of volcanic fronts are heavily influenced by movements of continental blocks, subduction of oceanic plateaus, and fragmentation of oceanic crust inherited from its history, from the mid-ocean ridge to the trench. See text for further comments and references.

hotspots presently located near the intersection of the Eltanin Fracture Zone, and the Southwest Pacific–Antarctica Ridge) and the Osborn Trough, which is a portion of the spreading system rifting apart the Hikurangi and Manihiki plateaus. Extreme variations in short-range convergence rates along the Tonga–Kermadec subduction zone are coupled to a profoundly variable behavior of back-arc basins. The spreading rates range from 85 to 92 mm year⁻¹ in the Central Lau Spreading Center to 40 mm year⁻¹ at the southern end of the Eastern Lau Spreading Center (Taylor and Martinez, 2003), down to 27 mm year⁻¹ in the Havre trough (Campbell et al., 2006), west of Kermadec. Moving to another complex sector of the Southwest Pacific, the structure of Vanuatu arc is the result of the collision with several major submarine ridges (West Torres Massif, d'Entrecasteaux Ridge, the Loyalty Island Ridge) and of the spreading of the North Fiji Basin. Further North, the Solomon Islands arc experienced the collision of the Ontong Java Plateau (Mann and Taira, 2004), the initiation of a second subduction zone, and the subduction of a young oceanic spreading ridge. These processes have led to volcanism on the plate being subducted and, in the forearc, the production of picritic magmas and of high magnesian andesites and adakites, as well as of alkaline magmas (Schuth et al., 2009; Smith et al., 2009).

Au19

Variability in the constituents of the oceanic crust inherited during the long journey from the MOR to the trench and the involvement of wandering continental terranes are not a unique feature of the Southwest Pacific and Andes, but occur at most subduction zones. Complexities in the lithological structure and in the devolatilization pattern of the subducted material are therefore the rule rather than the exception. Thermomechanical modeling and phase-diagram framework should be applied to transient specific geological scenarios, as overly generalized schemes are expected to fail in explaining natural complexities.

p0600

At present, the resolution of thermal models for the oceanic crust, with its large temperature gradients, is not sufficient. This is because the thermal field strongly depends on the flow field and on the degree of mechanical coupling between the subducting slab and the mantle wedge (e.g., Syracuse et al., 2010), which, in turn, depend on the viscosity of the materials at the slab–wedge interface, which is a function of *P* and *T* and the materials present. The latter then depend on the chemical reactions taking place, which, in turn, depend on the temperature field. Determining a temperature distribution model is, thus, a fairly complex problem and needs input from a large variety of disciplines.

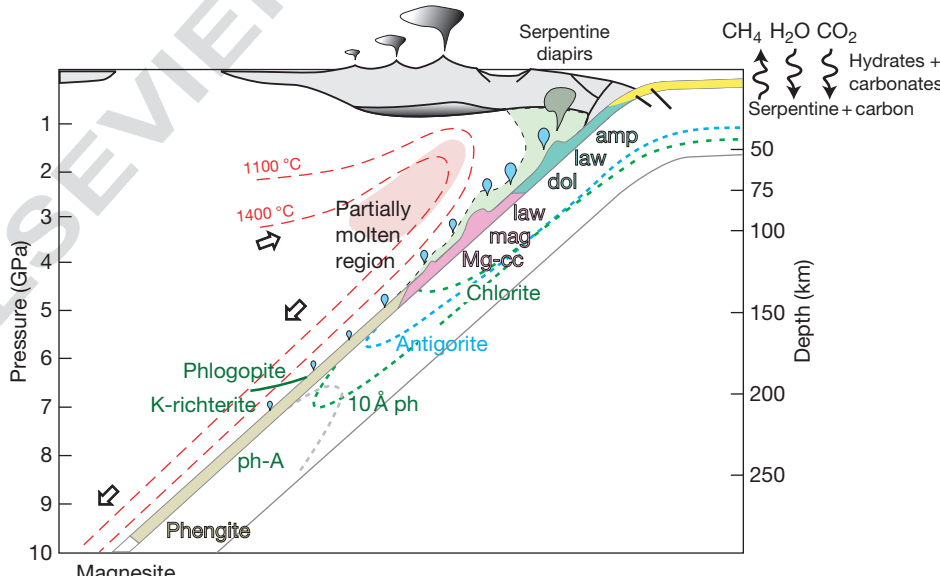
p0605

An example of feedback between temperature field and phase petrology is serpentinization in the mantle wedge directly overlying the subducted slab (Gerya et al., 2002). First, the calculated temperature distribution from thermomechanical models results in a pressure–temperature region where serpentine would be potentially stable. Second, dehydration rates and fluid transport mechanisms (pervasive vs. channeled flow) allow one to model the amount of serpentine formed. However, the serpentinized peridotite has 4–6 orders of magnitude lower viscosity than dry peridotite. This strongly influences the coupling of the subducting slab and convection in the mantle wedge. It also influences the possible amount of shear heating at the slab surface. If convection patterns change

p0610

s0155 321.8.3 Concluding Remarks

The general picture of mass transfer in subduction zones (**Figure 17**) includes the devolatilization of the downgoing lithosphere, the variable mode of mass transfer to the mantle wedge, melting in the mantle wedge intimately linked to convection, and the rise of these melts to the base and into the crust of the overriding plate, where they differentiate into the typical intermediate to felsic arc magmas and where new continental crust is formed.



f0090

Figure 17 Cartoon of events in a typical cold subduction zone in which melting of the oceanic crust does not occur. Modified from Poli S and Schmidt MW (2002) Petrology of subducted slabs. *Annual Review of Earth and Planetary Sciences* 30: 207–235.

due to a modified rheology caused by phase transformations, the temperature field as well as the permissible region for the serpentine changes. We thus require more complex models in which these parameters are varied simultaneously.

p0615 Upward-directed interaction between the different lithologies largely depends on the temperature gradient within the oceanic lithosphere, which is among the most difficult parameters to model. Thus, at present, a pure forward model for mass transfer in a given subduction zone is not reliable, and geochemical information on the subduction output (Kelemen et al., 2012; Morris and Ryan, 2012; Plank, 2012) is necessary to constrain likely mass transfer processes.

References

- Agué JJ (2012) Fluid flow in the deep crust. In: Rudnick RL (ed.) *The Crust*, 2nd edn. In: Holland HD and Turekian KK (eds.) *Treatise on Geochemistry*, vol. 3. Oxford: Elsevier-Pergamon.
- Allegre CJ and Turcotte DL (1986) Implications of a 2-component marble–cake mantle. *Nature* 323: 123–127.
- Alonso-Perez R, Muntener O, and Ulmer P (2009) Igneous garnet and amphibole fractionation in the roots of island arcs: Experimental constraints on andesitic liquids. *Contributions to Mineralogy and Petrology* 157: 541–558.
- Angel RJ, Frost DJ, Ross NL, and Hemley R (2001) Stabilities and equations of state of dense hydrous magnesium silicates. *Physics of the Earth and Planetary Interiors* 127: 181–196.
- Apred MJ and Liou JG (1983) Phase relations among greenschist, epidote–amphibolite, and amphibolite in a basalt system. *American Journal of Science* 283A: 328–356.
- Arcay D, Tric E, and Doin MP (2005) Numerical simulations of subduction zones: Effect of slab dehydration on the mantle wedge dynamics. *Physics of the Earth and Planetary Interiors* 149: 133–153.
- Arcay D, Tric E, and Doin MP (2007) Slab surface temperature in subduction zones: Influence of the interpolate decoupling depth and upper plate thinning processes. *Earth and Planetary Science Letters* 255: 324–338.
- Atherton PD and Petford N (1993) Generation of sodium-rich magmas from newly underplated basaltic crust. *Nature* 362: 144–146.
- Austrheim H and Engvik A (1997) Fluid transport, deformation and metamorphism at depth in a collision zone. In: Jamtveit B and Yardley BWD (eds.) *Fluid Flow and Transport in Rocks*, pp. 123–135. London: Chapman & Hall.
- Auzanneau E, Vielzeuf D, and Schmidt MW (2006) Experimental evidence of decompression melting during exhumation of subducted continental crust. *Contributions to Mineralogy and Petrology* 152: 125–148.
- Bach W, Alt JC, Niu Y, Humphris SE, Erzinger J, and Dick HJB (2001) The geochemical consequences of late-stage low-grade alteration of lower ocean crust at the SW Indian Ridge: Results from ODP Hole 735B (Leg 176). *Geochimica et Cosmochimica Acta* 65: 3267–3287.
- Bailey E and Holloway JR (2000) Experimental determination of elastic properties of talc to 800 °C, 0.5 GPa; calculations of the effect on hydrated peridotite, and implications for cold subduction zones. *Earth and Planetary Science Letters* 183: 487–498.
- Beate B, Monzier M, Spikings R, et al. (2001) Mio-Pliocene adakite generation related to flat subduction in southern Ecuador: The Quimsacocha volcanic center. *Earth and Planetary Science Letters* 192: 561–570.
- Bebout GE (2007) Metamorphic chemical geodynamics of subduction zones. *Earth and Planetary Science Letters* 260: 373–393.
- Bebout GE (2012) In: Rudnick RL (ed.) *The Crust*, 2nd edn. In: Holland HD and Turekian KK (eds.) *Treatise on Geochemistry*, vol. 3. Oxford: Elsevier-Pergamon.
- Bebout GE and Barton MD (1993) Metasomatism during subduction: Products and possible paths in the Catalina schist, California. *Chemical Geology* 108: 61–92.
- Behn MD, Kelemen PB, Hirth G, Hacker BR, and Massone HJ (2011) Diapirs as the source of the sediment signature in arc lavas. *Nature Geoscience* 4: 641–646.
- Berndt EM, Allen DE, and Seyfried WE (1996) Reduction of CO₂ during serpentinization of olivine at 300 °C and 500 bar. *Geology* 4: 351–354.
- Boettcher AL and Wyllie PJ (1969) The system CaO–SiO₂–CO₂–H₂O: III. Second critical end-point on the melting curve. *Geochimica et Cosmochimica Acta* 33: 611–632.
- Brown EH and Forbes RB (1986) Geology of the Shuksan Suite, North Cascades, Washington, USA. In: Evans BW and Brown EH (eds.) *Blueschists and Eclogites*, Memoir 164, pp. 143–167. Boulder, CO: Geological Society of America.
- Bub A, Luth RB, Schmidt MW, and Ulmer P (2006) Experiments on CaCO₃–MgCO₃ solid solutions at high pressure and temperature. *American Mineralogist* 91: 435–440.
- Caciagli NC and Manning CE (2003) The solubility of calcite in water at 6–16 kbar and 500–800 °C. *Contributions to Mineralogy and Petrology* 146: 275–285.
- Caldeira K (1995) Long-term control of atmospheric carbon dioxide: Low-temperature seafloor alteration or terrestrial silicate-rock weathering? *American Journal of Science* 295: 1077–1114.
- Campbell ME, Rowland JV, Wright IC, and Smith IEM (2006) Oblique rifting along the central and southern Kermadec Arc front (30 degrees–36 degrees S), SW Pacific. *Geochemistry, Geophysics, Geosystems* 8: Q01007.
- Cannat M (1993) Emplacement of mantle rocks in the seafloor at mid-ocean ridges. *Journal of Geophysical Research* 98: 4163–4172.
- Carlson WD (2002) Scales of disequilibrium and rates of equilibration during metamorphism. *American Mineralogist* 87: 185–204.
- Carswell DA and van Roermund HLM (2005) On multi-phase mineral inclusions associated with microdiamond formation in mantle-derived peridotite lens at Bardane on Fjørtoft, west Norway. *European Journal of Mineralogy* 17: 31–42.
- Charlou JL and Donval JP (1993) Hydrothermal methane venting between 12-degrees-N and 26-degrees-N along the Mid-Atlantic Ridge. *Journal of Geophysical Research* 98: 9625–9642.
- Charlou JL, Donval JP, Fouquet Y, Jean-Baptiste P, and Holm N (2002) Geochemistry of high H₂ and CH₄ vent fluids issuing from ultramafic rocks at the Rainbow hydrothermal field (36°14'N, MAR). *Chemical Geology* 191: 345–359.
- Chmielowski RM, Poli S, and Fumagalli P (2010) Experiments to constrain the garnet-talc join for metapelitic material at eclogite-facies conditions. *Geophysical Research Abstracts* 12: EGU2010-9544.
- Clarke GL, Powell R, and Fitzherbert JA (2006) The lawsonite paradox: A comparison of field evidence and mineral equilibria modelling. *Journal of Metamorphic Geology* 24: 715–725.
- Clift P and Vannucchi P (2004) Controls on tectonic accretion versus erosion in subduction zones: Implications for the origin and recycling of the continental crust. *Reviews of Geophysics* 42: 1–31.
- Connolly JAD (1995) Phase-diagram methods for graphitic rocks and application to the system C–O–H–FeO₂–SiO₂. *Contributions to Mineralogy and Petrology* 119: 94–116.
- Connolly JAD (2005) Computation of phase equilibria by linear programming: A tool for geodynamic modeling and its application to subduction zone decarbonation. *Earth and Planetary Science Letters* 236: 524–541.
- Connolly JAD and Cesare B (1993) C–O–H–S fluid composition and oxygen fugacity in graphitic metapelites. *Journal of Metamorphic Geology* 11: 379–388.
- Constantin M (1999) Gabbroic intrusions and magmatic metasomatism in harzburgites from the Garrett transform fault: Implications for the nature of the mantle–crust transition at fast spreading ridges. *Contributions of Mineralogy and Petrology* 136: 111–130.
- Coogan LA (2012) The lower oceanic crust. In: Rudnick RL (ed.) *The Crust*, 2nd edn. In: Holland HD and Turekian KK (eds.) *Treatise on Geochemistry*, vol. 3. Oxford: Elsevier-Pergamon.
- Dasgupta R, Hirschmann MM, and Withers AC (2004) Deep global cycling of carbon constrained by the solidus of anhydrous, carbonated eclogite under upper mantle conditions. *Earth and Planetary Science Letters* 227: 73–85.
- Davies HJ and Stevenson DJ (1992) Physical model of source region of subduction zone volcanics. *Journal of Geophysical Research* 97: 2037–2070.
- De Capitani C and Brown TH (1987) The computation of chemical-equilibrium in complex systems containing nonideal solutions. *Geochimica et Cosmochimica Acta* 51: 2639–2652.
- Dixon JE, Leist L, Langmuir C, and Schilling JG (2002) Recycled dehydrated lithosphere observed in plume-influenced mid-ocean-ridge basalt. *Nature* 420: 385–389.
- Dolejs D and Manning CE (2010) Thermodynamic model for mineral solubility in aqueous fluids: Theory, calibration and application to model fluid-flow systems. *Geofluids* 10: 20–40.
- Domanik KJ, Hervig RL, and Peacock SM (1993) Beryllium and boron in subduction zone minerals: An ion microprobe study. *Geochimica et Cosmochimica Acta* 57: 4997–5010.
- Domanik KJ and Holloway JR (1996) The stability and composition of phengitic muscovite and associated phases from 5.5 to 11 GPa: Implications for deeply subducted sediments. *Geochimica et Cosmochimica Acta* 60: 4133–4150.
- Dorbat C, Gerbault M, Carlier G, and Guiraud M (2008) Double seismic zone of the Nazca plate in northern Chile: High-resolution velocity structure, petrological implications, and thermomechanical modeling. *Geochimica et Cosmochimica Acta* 72: 4071–4088.

Au20

Au21

- Drummond MS, Defant MJ, and Kepezhinskas PK (1996) Petrogenesis of slab-derived trondjemite-tonalite-dacite/adakite magmas. *Transactions of the Royal Society of Edinburgh: Earth Sciences* 87: 205–215.
- Dvir O, Pettke T, Fumagalli P, and Kessel R (2011) Fluids in the peridotite–water system up to 6 GPa and 800°C: New experimental constraints on dehydration reactions. *Contributions to Mineralogy and Petrology* 161: 829–844.
- England PC, Engdahl R, and Thatcher W (2004) Systematic variation in the depths of slabs beneath arc volcanoes. *Geophysical Journal International* 156: 377–408.
- England PC and Katz RF (2010) Melting above the anhydrous solidus controls the location of volcanic arcs. *Nature* 467: 700–705.
- Faryad SW, Perraki M, and Vrana S (2006) P–T evolution and reaction textures in retrogressed eclogites from Svetlik, the Moldanubian Zone (Czech Republic). *Mineralogy and Petrology* 88: 297–319.
- Ferraris C, Grobety B, Früh-Green GL, and Wessicken R (2004) Intergrowth of graphite within phlogopite from Finero ultramafic complex (Italian Western Alps): Implications for mantle crystallization of primary-texture mica. *European Journal of Mineralogy* 16: 899–908.
- Forneris JF and Holloway JR (2003) Phase equilibria in subducting basaltic crust: Implications for H₂O release from the slab. *Earth and Planetary Science Letters* 214: 187–201.
- Forneris JF and Holloway JR (2004) Evolution of mineral compositions during eclogitization of subducting basaltic crust. *American Mineralogist* 89: 1516–1524.
- Franz L, Romer RL, Klemd R, et al. (2001) Eclogite-facies quartz veins within metabasites of the Dabie Shan (eastern China): Pressure–temperature–time–deformation path, composition of the fluid phase and fluid flow during exhumation of high-pressure rocks. *Contributions to Mineralogy and Petrology* 141: 322–346.
- Franzolin E, Schmidt MW, and Poli S (2011) Ternary Ca–Fe–Mg carbonates: Subsolidus phase relations at 3.5 GPa and a thermodynamic solid solution model including order/disorder. *Contributions to Mineralogy and Petrology* 161: 213–227.
- Frost DJ (1999) The stability of dense hydrous magnesium silicates in Earth's transition zone and lower mantle. In: Fei Y, Bertka CM, and Mysen BO (eds.) *Mantle Petrology: Field Observations and High-Pressure Experimentation*, pp. 283–296. Houston, TX: Geochemical Society, Special Publication No. 6.
- Frost DJ (2001) The stability of dense hydrous magnesium silicates in Earth's transition zone and lower mantle. In: Fei Y, Bertka CM, and Mysen BO (eds.) *Mantle Petrology: Field Observations and High Pressure Experimentation*, pp. 283–296. Houston, TX: Geochemical Society, Special Publication No. 6.
- Fryer P, Wheat CG, and Mott MJ (1999) Mariana blueschist mud volcanism: Implications for conditions within the subduction zone. *Geology* 27: 103–106.
- Fu B, Touret JLR, and Zheng Y-F (2003) Remnants of premetamorphic fluid and oxygen isotopic signatures in eclogites and garnet clinopyroxenite from the Dabie–Sulu terranes, eastern China. *Journal of Metamorphic Geology* 21: 561–578.
- Fumagalli P and Poli S (2005) Experimentally determined phase relations in hydrous peridotites to 6.5 GPa and their consequences on the dynamics of subduction zones. *Journal of Petrology* 46: 555–578.
- Fumagalli P, Stixrude L, Poli S, and Snyder D (2001) The 10 Å phase: A high-pressure expandable sheet silicate stable during subduction of hydrated lithosphere. *Earth and Planetary Science Letters* 186: 125–141.
- Fumagalli P, Zanchetta S, and Poli S (2009) Alkali in phlogopite and amphibole and their effects on phase relations in metasomatized peridotites: A high-pressure study. *Contributions to Mineralogy and Petrology* 158: 723–737.
- Gente P, Pockalny RA, Durand C, et al. (1995) Characteristics and evolution of the segmentation of the mid-atlantic ridge between 20° N and 24° N during the last 10 million years. *Earth and Planetary Science Letters* 129: 55–71.
- Gerya TV, Connolly JAD, Yuen DA, Gorczyk W, and Capel AM (2006) Seismic implications of mantle wedge plumes. *Physics of the Earth and Planetary Interiors* 156: 59–74.
- Gerya TV, Stöckhert B, and Perchuk AL (2002) Exhumation of high-pressure metamorphic rocks in a subduction channel: A numerical simulation. *Tectonics* 21(6): 1056.
- Gerya TV and Yuen DA (2003) Rayleigh–Taylor instabilities from hydration and melting propel 'cold plumes' at subduction zones. *Earth and Planetary Science Letters* 212: 47–62.
- Gieskes JM, Vrolijk P, and Blanc G (1990) Hydrogeochemistry of the northern Barbados accretionary complex transect: Ocean Drilling Project Leg 110. *Journal of Geophysical Research* 95: 8809–8818.
- Gill J (1981) *Orogenic Andesites and Plate Tectonics*, 390 pp. New York: Springer-Verlag.
- Gillis KM and Robinson PT (1990) Patterns and processes of alteration in the lavas and dykes of the Troodos Ophiolite Cyprus. *Journal of Geophysical Research* 95: 21523–21548.
- Gorman PJ, Kerrick DM, and Connolly JAD (2006) Modeling open system metamorphic decarbonation of subducting slabs. *Geochemistry, Geophysics, Geosystems* 7: Q04007.
- Grassi D and Schmidt MW (2011a) The melting of carbonated pelites from 70 to 700 km depth. *Journal of Petrology* 52: 765–789.
- Grassi D and Schmidt MW (2011b) Melting of carbonated pelites at 8–13 GPa: Generating K-rich carbonatites for mantle metasomatism. *Contributions to Mineralogy and Petrology*. doi:10.1007/s00410-010-0589-9. [Au22]
- Green DH (1973) Experimental melting studies on a model upper mantle composition at high-pressure under water-saturated and water-undersaturated conditions. *Earth and Planetary Science Letters* 19: 37–53.
- Green DH, Hibberson WO, Kovacs I, and Rosenthal A (2010) Water and its influence on the lithosphere–asthenosphere boundary. *Nature* 467: 448–497.
- Groppi C and Castelli D (2010) Prograde P–T evolution of a lawsonite eclogite from the Monviso meta-ophiolite (Western Alps): Dehydration and redox reactions during subduction of oceanic FeTi-oxide gabbro. *Journal of Petrology* 51: 2489–2514.
- Grove TL, Chatterjee N, Parman SW, et al. (2006) The influence of H₂O on mantle wedge melting. *Earth and Planetary Science Letters* 249: 74–89.
- Guiraud M, Powell R, and Rebay G (2001) H₂O in metamorphism and unexpected behavior in the preservation of metamorphic mineral assemblages. *Journal of Metamorphic Geology* 19: 445–454.
- Gutscher MA, Malavieille J, Lallemand S, and Collot JY (1999) Tectonic segmentation of the North Andean margin: Impact of the Carnegie Ridge collision. *Earth and Planetary Science Letters* 168: 255–270.
- Hammouda T (2003) High-pressure melting of carbonated eclogite and experimental constraints on carbon recycling and storage in the mantle. *Earth and Planetary Science Letters* 124: 357–368.
- Harlow GE (1994) Jadeites, albitites and related rocks from the Motagua Fault Zone Guatemala. *Journal of Metamorphic Geology* 12: 49–68.
- Heimstaedt H and Schulze DJ (1988) Eclogite-facies ultramafic xenoliths from Colorado Plateau diatreme breccias: Comparison with eclogites in crustal environments, evaluation of the subduction hypothesis, and implications for eclogite xenoliths from diamondiferous kimberlites. In: Smith DC (ed.) *Eclogite and Eclogite Facies Rocks*, pp. 387–450. New York: Elsevier.
- Hermann J (2002a) Experimental constraints on phase relations in subduction continental crust. *Contributions to Mineralogy and Petrology* 143: 219–235.
- Hermann J (2002b) Allanite: Thorium and light rare earth element carrier in subducted crust. *Chemical Geology* 192: 289–306.
- Hermann J and Green DH (2001) Experimental constraints on high pressure melting in subducted crust. *Earth and Planetary Science Letters* 188: 149–168.
- Hermann J and Rubatto D (2009) Accessory phase control on the trace element signature of sediment melts in subduction zones. *Chemical Geology* 265: 512–526.
- Hermann J and Rubatto D (2012) In: Rudnick RL (ed.) *The Crust*, 2nd edn. In: Holland HD and Turekian KK (eds.) *Treatise on Geochemistry*, vol. 3. Oxford: Elsevier-Pergamon. [Au23]
- Hermann J and Spandler CJ (2008) Sediments at sub-arc depths: An experimental study. *Journal of Petrology* 49: 717–740.
- Hill RET and Boettcher AL (1970) Water in Earth's mantle, melting curves of basalt–water and basalt–water–carbon dioxide. *Science* 167: 980.
- Hofmann AW (2012) Sampling mantle heterogeneity through oceanic basalts: Isotopes and trace elements. In: Carlson RW (ed.) *The Mantle and Core*, 2nd edn. In: Holland HD and Turekian KK (eds.) *Treatise on Geochemistry*, vol. 2. Oxford: Elsevier-Pergamon.
- Holland TJB and Powell R (1998) An internally consistent thermodynamic data set for phases of petrological interest. *Journal of Metamorphic Geology* 16: 309–343.
- Holloway JR and Reese RL (1974) Generation of N₂–CO₂–H₂O fluids for use in hydrothermal experimentation. 1. Experimental-method and equilibrium calculation in C–O–H–N system. *American Mineralogist* 59: 587–597.
- Irlifne T, Ringwood AE, and Hibberson WO (1994) Subduction of continental-crust and terrigenous and pelagic sediments – an experimental-study. *Earth and Planetary Science Letters* 126: 351–368.
- Irving AJ and Wyllie PJ (1975) Subsolidus and melting relationships for calcite magnesite and join CaCO₃–MgCO₃ to 36 kb. *Geochimica et Cosmochimica Acta* 39: 35–53.
- Ishikawa T and Nakamura E (1994) Origin of the slab component in arc lavas from across-arc variation of B and Pb isotopes. *Nature* 370: 205–208.
- Jagoutz O (2010) Construction of the granitoid crust of an island arc, Part II: A quantitative petrogenetic model. *Contributions to Mineralogy and Petrology* 160: 359–381.
- Jagoutz O, Muntener O, Schmidt MW, and Burg JP (2011) The roles of flux- and decompression melting and their respective fractionation lines for continental crust formation: Evidence from the Kohistan arc. *Earth and Planetary Science Letters* 303: 25–36.

- John T and Schenk V (2003) Partial eclogitisation of gabbroic rocks in a late Precambrian subduction zone (Zambia): Prograde metamorphism triggered by fluid infiltration. *Contributions to Mineralogy and Petrology* 146: 174–191.
- Johnson MC and Plank T (1999) Dehydration and melting experiments constraints the fate of subducted sediments. *Geochemistry, Geophysics, Geosystems* 1.
- Katayama I and Nakashima S (2003) Hydroxyl in clinopyroxene from the deep subducted crust: Evidence for H₂O transport into the mantle. *American Mineralogist* 88: 229–234.
- Kawamoto T and Holloway JR (1997) Melting temperature and partial melt chemistry of H₂O-saturated mantle peridotite to 11 GPa. *Science* 276: 240–243.
- Kawamoto T, Leinenweber K, Hervig RL, and Holloway JR (1995) Stability of hydrous phases in an H₂O-saturated KLB-1 peridotite up to 15 GPa. *Volatile in the Earth and Solar System*, 229–239.
- Kay RW (1978) Aleutian Magnesian andesites: Melts from subducted Pacific Ocean Crust. *Journal of Volcanology and Geothermal Research* 4: 117–132.
- Kelemen PB, Hanghøj K, and Greene AR (2012) One view of the geochemistry of subduction-related magmatic arcs, with an emphasis on primitive andesite and lower crust. In: Rudnick RL (ed.) *The Crust*, 2nd edn. In: Holland HD and Turekian KK (eds.) *Treatise on Geochemistry*, vol. 3. Oxford: Elsevier-Pergamon.
- Kelley KA and Cottrell E (2009) Water and the oxidation state of subduction zone magmas. *Science* 325: 605–607.
- Kelley DS, Karson JA, Blackman DK, et al. (2001) An off-axis hydrothermal vent field near the Mid-Atlantic Ridge at 30° N. *Nature* 412: 145–149.
- Kennedy GC, Wasserburg GJ, Heard HC, and Newton RC (1962) The upper three-phase region in the system SiO₂-H₂O. *American Journal of Science* 260: 501–521.
- Kerrick DM and Connolly JAD (1998) Subduction of ophiocarbonates and recycling of CO₂ and H₂O. *Geology* 26: 375–378.
- Kerrick DM and Connolly JAD (2001a) Metamorphic devolatilization of subducted oceanic metabasalts: Implications for seismicity, arc magmatism and volatile recycling. *Earth and Planetary Science Letters* 189: 19–29.
- Kerrick DM and Connolly JAD (2001b) Metamorphic devolatilization of subducted marine sediments and the transport of volatiles into the Earth's mantle. *Nature* 411: 293–296.
- Kessel R, Schmidt MW, Pettke T, and Ulmer P (2005) Trace element signature of subduction-zone fluids, melts, and supercritical liquids at 120–180 km depth. *Nature* 437: 724–727.
- Kessel R, Ulmer P, Pettke T, Schmidt MW, and Thompson AB (2005) The water-basalt system at 4 to 6 GPa: Phase relations and the second critical endpoint in a K-free eclogite at 700–1400 °C. *Earth and Planetary Science Letters* 237: 873–892.
- Kincaid C and Sacks IS (1997) Thermal and dynamical evolution of the upper mantle in subduction zones. *Journal of Geophysical Research* 102: 12295–12315.
- Klein E (2012) Oceanic crust: MORB, gabbros and cumulates. *Treatise of Geochemistry*, vol. 3.
- Klimm K, Blundy JD, and Green TH (2008) Trace element partitioning and accessory phase saturation during H₂O-saturated melting of basalt with implications for subduction zone chemical fluxes. *Journal of Petrology* 49: 523–553.
- Kohlstedt DL, Keppler H, and Rubie DC (1996) Solubility of water in the α, β, and γ-phases of (Mg, Fe)₂SiO₄. *Contributions to Mineralogy and Petrology* 123: 345–357.
- Konrad-Schmalke M, O'Brien PJ, and Zack T (2011) Fluid migration above a subducted slab – Constraints on amount, pathways and major element mobility from partially overprinted eclogite-facies rocks (Sesia Zone, Western Alps). *Journal of Petrology* 52: 457–486.
- Konzett J and Ulmer P (1999) The stability of hydrous potassic phases in Iherzolite mantle – An experimental study to 9.5 GPa in simplified and natural bulk compositions. *Journal of Petrology* 40: 629–652.
- Kornprobst J (1969) Le massif ultrabasique de Beni Bousera (Rif interne, Maroc): Étude des pélédites de haute température et de haute pression, et des pyroxénolites, à grenat ou sans grenat, qui leur sont associées. *Contributions to Mineralogy and Petrology* 23: 283–322.
- Korsakov AV and Hermann J (2006) Silicate and carbonate melt inclusions associated with diamonds in deeply subducted carbonate rocks. *Earth and Planetary Science Letters* 241: 104–118.
- Kostenko O, Jamtveit B, Austrheim H, Pollock K, and Putnis C (2002) The mechanism of fluid infiltration in peridotites at Almklovdalen, Western Norway. *Geofluids* 2: 203–215.
- Kushiro I (1970) Stability of amphibole and phlogopite in the upper mantle. *Carnegie Institute of Washington Yearbook* 68: 245–247.
- Kushiro I (1987) A petrological model for the mantle wedge and lower crust in the Japanese island arcs. In: Mysen BO (ed.) *Magmatic Processes: Physicochemical principles*, pp. 165–181. Houston, TX: Geochemical Society. Special Publication No. 1.
- Kushiro I, Syono Y, and Akimoto S (1968) Melting of a peridotite nodule at high pressures and high water pressures. *Journal of Geophysical Research* 73: 6023–6029.
- Lambert IB and Wyllie PJ (1972) Melting of gabbro (quartz eclogite) with excess water to 35 kilobars, with geological applications. *Journal of Geology* 80: 693–708.
- Lee C-TA, Leeman WP, Canil D, and Li Z-XA (2005) Similar V/Sc systematics in MORB and arc basalts: Implications for the oxygen fugacities of their mantle source regions. *Journal of Petrology* 46: 2313–2336.
- Lee C-TA, Luffi P, Le Roux V, Dasgupta R, Albare F, and Leeman WP (2010) The redox state of arc mantle using Zn/Fe systematics. *Nature* 468: 681–685.
- Li Y-H and Schoonmaker JE (2012) Chemical composition and mineralogy of marine sediments. In: Rudnick RL (ed.) *The Crust*, 2nd edn. In: Holland HD and Turekian KK (eds.) *Treatise on Geochemistry*, vol. 3. Oxford: Elsevier-Pergamon.
- Liou JG, Zhang RY, Ernst WG, Rumble D III, and Maruyama S (1998) High pressure minerals from deeply subducted metamorphic rocks. *Reviews in Mineralogy* 37: 33–96.
- Malaspina N, Poli S, and Fumagalli P (2009) The oxidation state of metasomatized mantle wedge: Insights from C-O-H bearing garnet peridotite. *Journal of Petrology* 50: 1533–1552.
- Malaspina N, Scambelluri M, Poli S, et al. (2010) The oxidation state of mantle wedge majoritic garnet websterites metasomatised by C-bearing subduction fluids. *Earth and Planetary Science Letters* 298: 417–426.
- Mammerickx J (1989) Large scale undersea features on the north-east Pacific. In: Winterer EL, Hussong DM, and Decker RW (eds.) *The Eastern Pacific Ocean and Hawaii, The Geology of North America*, pp. 5–13. Boulder, CO: Geological Society of America.
- Mann P and Taira A (2004) Global tectonic significance of the Solomon Islands and Ontong Java Plateau convergent zone. *Tectonophysics* 389: 137–190.
- Manning CE (2004) The chemistry of subduction-zone fluids. *Earth and Planetary Science Letters* 223: 1–16.
- Manning CE, Antignano A, and Lin HA (2010) Premelting polymerization of crustal and mantle fluids, as indicated by the solubility of albite plus paragonite plus quartz in H₂O at 1 GPa and 350–620 °C. *Earth and Planetary Science Letters* 292: 325–336.
- Marschall HR, Altherr R, and Rupke L (2007) Squeezing out the slab – Modeling the release of Li, Be and B during progressive high-pressure metamorphism. *Chemical Geology* 239: 323–335.
- Martin H (1999) Adakitic magmas: Modern analogues of Archaean granitoids. *Lithos* 46: 411–429.
- Martin H, Smithies RH, Rapp R, et al. (2005) An overview of adakite, tonalite-trondhjemite-granodiorite (TTG) and sanukitoid: Relationships and some implications for crustal evolution. *Lithos* 79: 1–24.
- Maruyama S, Cho M, and Liou JG (1986) Experimental investigations of blueschist–greenschist transition equilibria: Pressure dependence of Al₂O₃ contents in sodic amphiboles – A new geobarometer. In: Evans BW and Brown EH (eds.) *Blueschists and Eclogites, Memoir 164*, pp. 1–16. Boulder, CO: Geological Society of America.
- Melekhova E, Schmidt MW, Ulmer P, and Pettke T (2007) The composition of liquids coexisting with dense hydrous magnesium silicates at 11–13.5 GPa and the endpoints of the solidi in the MgO–SiO₂–H₂O system. *Geochimica et Cosmochimica Acta* 71: 3348–3360.
- Mibe K, Kanazaki M, Kawamoto T, Matsukage KN, Fei Y, and Ono S (2007) Second critical endpoint in the peridotite–H₂O system. *Journal of Geophysical Research* 112: B03201. doi:10.1029/2005JB004125.
- Miller DP, Marschall HR, and Schumacher JC (2009) Metasomatic formation and petrology of blueschist-facies hybrid rocks from Syros (Greece): Implications for reactions at the slab–mantle interface. *Lithos* 107: 53–67.
- Millhollen GL, Irving AJ, and Wyllie PJ (1974) Melting interval of peridotite with 5.7 per cent water to 30 kilobars. *Journal of Geology* 82: 575–587.
- Molina JF, Austrheim H, Giordani J, and Rusin A (2002) The eclogites of the Marun-Keu complex, Polar Urals (Russia): Fluid control on reaction kinetics and metasomatism during high P metamorphism. *Lithos* 61: 55–78.
- Molina JF and Poli S (2000) Carbonate stability and fluid composition in subducted oceanic crust: An experimental study on H₂O-CO₂-bearing basalts. *Earth and Planetary Science Letters* 176: 295–310.
- Moriguti T and Nakamura E (1998) Across-arc variation of Li isotopes in lavas and implications for crust/mantle recycling at subduction zones. *Earth and Planetary Science Letters* 163: 167–174.
- Morris JD, Leeman WP, and Tera F (1990) The subducted component in island arc lavas: Constraints from Be isotopes and B-Be systematics. *Nature* 344: 31–36.
- Morris JD and Ryan JG (2012) Subduction zone processes and implications for changing composition of the upper and lower mantle. In: Carlson RW (ed.) *The Mantle and Core*, 2nd edn. In: Holland HD and Turekian KK (eds.) *Treatise on Geochemistry*, vol. 2. Oxford: Elsevier-Pergamon.

- Mukherjee BK, Sachan HK, Ogasawara Y, Muko A, and Yoshioka N (2003) Carbonate-bearing UHPM rocks from the Tso-Morari region, Ladakh, India: Petrological implications. *International Geology Review* 45: 49–69.
- Mysen BO and Boettcher AL (1975) Melting of a hydrous mantle. 1. Phase relations of natural peridotite at high-pressure and temperatures with controlled activities of water, carbon-dioxide, and hydrogen. *Journal of Petrology* 16: 520–548.
- Nakamura Y and Kushiro I (1974) Composition of the gas phase in $Mg_2SiO_4-SiO_2-H_2O$ at 15 kbar. *Carnegie Institute of Washington Yearbook* 73: 255–258.
- Newton RC and Manning CE (2010) Role of saline fluids in deep-crustal and upper mantle metasomatism: Insights from experimental studies. *Geofluids* 10: 58–72.
- Nichols GT, Wyllie PJ, and Stern CR (1994) Subduction zone-melting of pelagic sediments constrained by melting experiments. *Nature* 371: 785–788.
- Nicolas A (1989) *Structures of Ophiolites and Dynamics of Oceanic Lithosphere*. Dordrecht: Kluwer.
- Niida K and Green DH (1999) Stability and chemical composition of paragasic amphibole in MORB pyrolite under upper mantle conditions. *Contributions to Mineralogy and Petrology* 135: 18–40.
- Ohtani E (2005) Water in the mantle. *Elements* 1: 25–30.
- Ohtani E, Mizobata H, and Yurimoto H (2000) Stability of dense hydrous magnesium silicate phases in the systems $Mg_2SiO_4-H_2O$ and $MgSiO_3-H_2O$ at pressures up to 27 GPa. *Physical and Chemistry of Minerals* 27: 533–544.
- Okamoto K and Maruyama S (1998) Multi-anvil re-equilibration experiments of a Dabie Shan ultrahigh pressure eclogite within the diamond-stability fields. *The Island Arc* 7: 52–69.
- Okamoto K and Maruyama S (1999) The high-pressure synthesis of lawsonite in the MORB+H₂O system. *American Mineralogist* 84: 362–373.
- Okay AI (1980) Mineralogy, petrology, and phase relations of glaucophane-lawsonite zone blueschists from the Tavsan region, Northwest Turkey. *Contributions to Mineralogy and Petrology* 72: 243–255.
- Olafsson M and Eggler EH (1983) Phase relations of amphibole, amphibole-carbonate, and phlogopite-carbonate peridotite – Petrologic constraints on the asthenosphere. *Earth and Planetary Science Letters* 64: 305–315.
- Ono S (1998) Stability limits of hydrous minerals in sediment and mid-ocean ridge basalt compositions: Implications for water transport in subduction zones. *Journal of Geophysical Research* 103: 18253–18267.
- Paillat O, Elphick SC, and Brown WL (1992) The solubility of water in NaAlSi₃O₈ melts: A re-examination of Ab-H₂O phase relationships and critical behaviour at high pressures. *Contributions to Mineralogy and Petrology* 112: 490–500.
- Pawley AR and Wood BJ (1995) The high-pressure stability of talc and 10 Å phase: Potential storage sites for H₂O in subduction zones. *American Mineralogist* 80: 998–1003.
- Peacock SM (1987) Serpentization and infiltration metasomatism in the Trinity peridotite, Klamath Province, northern California: Implications for subduction zones. *Contributions to Mineralogy and Petrology* 95: 55–70.
- Peacock SM (1993) The importance of blueschist to eclogite dehydration reactions in subducting oceanic crust. *Geological Society of America Bulletin* 105: 684–694.
- Peacock S (2001) Are the lower planes of double seismic zones caused by serpentine dehydration in subducting oceanic mantle? *Geology* 29: 299–302.
- Peretti A, Dubessy J, and Mullis J (1992) Highly reducing conditions during alpine metamorphism of the Malenco peridotite (Sondrio, Northern Italy) indicated by mineral paragenesis and H₂ in fluid inclusions. *Contributions to Mineralogy and Petrology* 112: 329–340.
- Philipott P (1993) Fluid–melt–rock interaction in mafic eclogites and coesite bearing sediments: Constraints on volatile recycling during subduction. *Chemical Geology* 108: 93–112.
- Plank T (2012) The chemical composition of subducting sediments. In: Rudnick RL (ed.) *The Crust*, 2nd edn. In: Holland HD and Turekian KK (eds.) *Treatise on Geochemistry*, vol. 3. Oxford: Elsevier-Pergamon.
- Plank T and Langmuir CH (1993) Tracing trace elements from sediment input to volcanic output at subduction zones. *Nature* 362: 739–743.
- Plank T and Langmuir CH (1998) The chemical composition of subducting sediment and its consequences of the crust and mantle. *Chemical Geology* 145: 325–394.
- Poli S (1993) The amphibolite-eclogite transformation: An experimental study on basalt. *American Journal of Science* 293: 1061–1107.
- Poli S, Franzolin E, and Fumagalli P (2009) The transport of carbon and hydrogen in subducted oceanic crust: An experimental study to 5 GPa. *Earth and Planetary Science Letters* 278: 350–360.
- Poli S and Schmidt MW (1995) H₂O transport and release in subduction zones – Experimental constraints on basaltic and andesitic systems. *Journal of Geophysical Research* 100: 22299–22314.
- Poli S and Schmidt MW (1998) The high-pressure stability of zoisite and phase relationships of zoisite-bearing assemblages. *Contributions to Mineralogy and Petrology* 130: 162–175.
- Poli S and Schmidt MW (2002) Petrology of subducted slabs. *Annual Review of Earth and Planetary Sciences* 30: 207–235.
- Poli S and Schmidt MW (2004) Experimental subsolidus studies on epidote minerals. *Reviews in Mineralogy and Geochemistry* 56: 171–195.
- Rea DK and Ruff LJ (1996) Composition and mass flux of sediment entering the world's subduction zones: Implications for global sediment budgets, great earthquakes, and volcanism. *Earth and Planetary Science Letters* 140: 1–12.
- Ricci JE (1951) *The Phase Rule and Heterogeneous Equilibrium*, p. 504. New York: Dover.
- Rumble D, Liou JG, and Jahn BM (2003) Continental crust subduction and ultrahigh pressure metamorphism. *Treatise of Geochemistry* 3: 293–320.
- Ryan JG, Morris J, Tera F, Leeman WP, and Tsvetkov A (1995) Cross-arc geochemical variations in the Kurile Arc as a function of slab depth. *Science* 270: 625–627.
- Scambelluri M and Philipott P (2001) Deep fluids in subduction zones. *Lithos* 55: 213–227.
- Schmelz H, Monz R, and Rubie DC (1999) The influence of olivine metastability on the dynamics of subduction. *Earth and Planetary Science Letters* 165: 55–66.
- Schmidt MW (1993) Phase relations and compositions in tonalite as a function of pressure: An experimental study at 650°C. *American Journal of Science* 293: 1011–1060.
- Schmidt MW (1996) Experimental constraints of recycling of potassium from subducted oceanic crust. *Science* 272: 1927–1930.
- Schmidt MW and Poli S (1998) Experimentally based water budgets for dehydrating slabs and consequences for arc magma generation. *Earth and Planetary Science Letters* 163: 361–379.
- Schmidt MW and Poli S (2003) Generation of mobile components during subduction of oceanic crust. *Treatise of Geochemistry*, vol. 3, pp. 567–591. New York: Elsevier. (10 vols).
- Schmidt MW, Vielzeuf D, and Auzanneau E (2004) Melting and dissolution of subducting crust at high pressures: The key role of white micas. *Earth and Planetary Science Letters* 228: 65–84.
- Schuth S, Münker C, König S, et al. (2009) Petrogenesis of lavas along the Solomon Island Arc, SW Pacific: Coupling of compositional variations and subduction zone geometry. *Journal of Petrology* 50: 781–821.
- Sekine T and Wyllie PJ (1982) Phase-relationships in the system $KaSiO_4-Mg_2SiO_4-SiO_2-H_2O$ as a model for hybridization between hydrous siliceous melts and peridotite. *Contributions to Mineralogy and Petrology* 79: 368–374.
- Sen C and Dunn T (1994) Dehydration melting of a basaltic composition amphibolite at 1.5 and 2.0 GPa – Implications for the origin of adakites. *Contributions to Mineralogy and Petrology* 117: 394–409.
- Seno T and Yamanaka Y (1996) Double seismic zones, compressional deep trench-outer rise events, and superplumes. In: Bebout E, Schol DW, Kirby SH, and Blatt JP (eds.) *Subduction: Top to Bottom Geophysical Monograph*, vol. 96, pp. 347–355. Washington, DC: American Geophysical Union.
- Shen AH and Keppler H (1997) Direct observation of complete miscibility in the albite-H₂O system. *Nature* 385: 710–712.
- Shi GU, Tropper P, Cui WY, Tan J, and Wang CQ (2005) Methane, (CH₄)-bearing fluid inclusions in the Myanmar jadeite. *Geochemical Journal* 39: 503–516.
- Sigmarsdóttir O, Condoinnes M, Morris JD, and Harmon RS (1990) Uranium and ¹⁰Be enrichments by fluids in the Andean arc magmas. *Nature* 346: 163–165.
- Sigmarsdóttir O, Martin H, and Knowles J (1998) Melting of a subducting oceanic crust from U-Th disequilibria in austral Andean lavas. *Nature* 394: 566–569.
- Sisson VB, Ertan IE, and Lallement HGA (1997) High-pressure (approximate to 2000 MPa) kyanite- and glaucophane-bearing pelitic schist and eclogite from Cordillera de la Costa belt, Venezuela. *Journal of Petrology* 38: 65–83.
- Skora S and Blundy J (2010) High-pressure hydrous phase relations of radiolarian clay and implications for the involvement of subducted sediment in arc magmatism. *Journal of Petrology* 51: 2211–2243.
- Sleep NH and Windley BF (1982) Archean plate tectonics: Constraints and inferences. *Journal of Geology* 90: 363–379.
- Smith DJ, Petterson MG, Saunders AD, et al. (2009) The petrogenesis of sodic island arc magmas at Savo volcano, Solomon Islands. *Contributions to Mineralogy and Petrology* 158: 785–801.
- Snow JE and Dick HJB (1995) Pervasive magnesium loss by marine weathering of peridotite. *Geochimica et Cosmochimica Acta* 59: 4219–4235.
- Sorensen SS (1986) Petrologic and geochemical comparison of the blueschist and greenschist units of the Catalina Schist terrane, southern California. In: Evans BW and Brown EH (eds.) *Blueschists and Eclogites Memoir* 164, pp. 59–75. Boulder, CO: Geological Society of America.
- Sorensen SS (1988) Petrology of amphibolite-facies mafic and ultramafic rocks from the Catalina schist, southern California: Metasomatism and migmatization in a subduction zone metamorphic setting. *Journal of Metamorphic Geology* 6: 405–435.

- Spandler C, Mavrogenes J, and Hermann J (2007) Experimental constraints on element mobility from subducted sediments using high-P synthetic fluid/melt inclusions. *Chemical Geology* 239: 228–249.
- Stalder R, Ulmer P, Thompson AB, and Günther D (2000) Experimental approach to constrain second critical end points in fluid/silicate systems: Near-solidus fluids and melts in the system albite-H₂O. *American Mineralogist* 85: 68–77.
- Stalder R, Ulmer P, Thompson AB, and Gunther D (2001) High pressure fluids in the system MgO-SiO₂-H₂O under upper mantle conditions. *Contributions to Mineralogy and Petrology* 140: 607–618.
- Au27** Staudigel H (2012) Hydrothermal alteration processes. *Treatise of Geochemistry*, vol. 3.
- Stockert B, Duyster J, Trepmann C, and Massonne HJ (2001) Microdiamond daughter crystals precipitated from supercritical CO₂ plus silicate fluids included in garnet, Erzgebirge, Germany. *Geology* 29: 391–394.
- Sudo A and Tatsumi Y (1990) Phlogopite and K-amphibole in the upper mantle: Implication for magma genesis in subduction zones. *Geophysical Research Letters* 17: 29–32.
- Syracuse EM and Abers GA (2006) Global compilation of variations in slab depth beneath arc volcanoes and implications. *Geochemistry, Geophysics, Geosystems* 7: Q05017.
- Syracuse EM, van Keken PE, and Abers GA (2010) The global range of subduction zone thermal models. *Physics of the Earth and Planetary Interiors* 183: 73–90.
- Tatsumi Y (1986) Formation of the volcanic front in subduction zones. *Geophysical Research Letters* 13: 717–720.
- Tatsumi Y and Eggins S (1995) *Subduction Zone Magmatism Frontiers in Earth Sciences*, p. 211. Cambridge, MA: Blackwell Science.
- Taylor B and Martinez F (2003) Back-arc basin basalt systematics. *Earth and Planetary Science Letters* 210: 481–497.
- Thomsen TB and Schmidt MW (2008a) Melting of carbonated pelites at 2.5–5.0 GPa, silicate-carbonatite liquid immiscibility, and potassium–carbon metasomatism of the mantle. *Earth and Planetary Science Letters* 267: 17–31.
- Thomsen TB and Schmidt MW (2008b) The biotite to phengite reaction and mica-dominated melting in fluid + carbonate-saturated pelites at high pressures. *Journal of Petrology* 49: 1889–1914.
- Thurston SP (1985) Structure, petrology, and metamorphic history of the Nome Group blueschist terrane, Salmon Lake area, Seward Peninsula, Alaska. *Geological Society of America Bulletin* 96: 600–617.
- Till CB and Grove TL (2010) *Experimental Insights into the Subduction Filter Presented at 2010 Fall Meeting, 13–17 December*. San Francisco, CA: AGU. Abstract V12B-04.
- Trønnes RG (2002) Stability range and decomposition of potassio richterite and phlogopite end members at 5–15 GPa. *Mineralogy and Petrology* 74: 129–148.
- Tsujimori T, Sisson VB, Liou JG, Harlow GE, and Sorensen SS (2006) Very-low-temperature record of the subduction process: A review of worldwide lawsonite eclogites. *Lithos* 92: 609–624.
- Tsunoo K and Dasgupta R (2011) Melting phase relation of nominally anhydrous, carbonated pelitic-eclogite at 2.5–3.0 GPa and deep cycling of sedimentary carbon. *Contributions to Mineralogy and Petrology* 161: 743–763.
- Tumiati S, Fumagalli P, and Poli S (2009) Carbonate-silicate equilibria in upper-mantle peridotites saturated with C-O-H fluids. *Geochimica et Cosmochimica Acta* 73: A1352.
- Turner S, Bourdon B, and Gill J (2003) Insights into magma genesis at convergent margins from U-series isotopes. *Reviews in Mineralogy and Geochemistry* 52: 255–315.
- Ulmer P and Trommsdorff V (1995) Serpentine stability to mantle depths and subduction-related magmatism. *Science* 268: 858–861.
- Ulmer P and Trommsdorff V (1999) Phase relations of hydrous mantle subducting to 300 km. In: Fei YW, Bertka C, and Mysen BO (eds.) *Mantle Petrology: Field Observations and High Pressure Experimentation: A Tribute to Francis R. (Joe) Boyd*, pp. 259–281. Houston, TX: The Geochemical Society. Special Publication No. 6.
- Usui T, Nakamura E, Kobayashi K, Maruyama S, and Helmstaedt H (2001) Petrology and trace element geochemistry of eclogite xenoliths from the Colorado Plateau. In: Ito E, et al. (ed.) *Transport of Materials in the Dynamic Earth*, p. 46. Misasa: Institute for Study of the Earth's Interior.
- Van Keken PE, Kiefer B, and Peacock S (2002) High-resolution models of subduction zones: Implications for mineral dehydration reactions and the transport of water into the deep mantle. *Geochemistry, Geophysics, Geosystems* 3.
- Au28** van Roermund HLM, Carswell DA, Drury MR, and Heijboer TC (2002) Microdiamonds in a megacrystic garnet websterite pod from Bardane on the island of Fjørtoft, western Norway: Evidence for diamond formation in mantle rocks during deep continental subduction. *Geology* 30: 959–962.
- Vielzeuf D and Montel JM (1994) Partial melting of Al-metagreywackes. Part I: Fluid-absent experiments and phase relationships. *Contributions to Mineralogy and Petrology* 117: 375–393.
- Vielzeuf D and Schmidt MW (2001) Melting relations in hydrous systems revisited: Application to metapelites, metagreywackes and metabasalts. *Contributions to Mineralogy and Petrology* 141: 251–267.
- Von Huene R and Scholl DW (1991) Observations at convergent margins concerning sediment subduction, subduction erosion, and the growth of continental crust. *Reviews of Geophysics* 29: 279–316.
- Wain A (1997) New evidence for coesite in eclogite and gneisses: Defining an ultrahigh-pressure province in the Western Gneiss region of Norway. *Geology* 25: 927–930.
- Wallace ME and Green DH (1988) An experimental-determination of primary carbonatite magma composition. *Nature* 335: 343–346.
- White WM and Klein EM (2012) The oceanic crust. In: Rudnick RL (ed.) *The Crust*, 2nd edn. In: Holland HD and Turekian KK (eds.) *Treatise on Geochemistry*, vol. 3. Oxford: Elsevier-Pergamon.
- Widmer T and Thompson AB (2001) Local origin of high pressure vein material in eclogite facies rocks of the Zermatt-Saas zone, Switzerland. *American Journal of Science* 301: 627–656.
- Wyllie PJ and Sekine T (1982) The formation of mantle phlogopite in subduction zone hybridization. *Contributions to Mineralogy and Petrology* 79: 375–380.
- Yamasaki T and Seno T (2003) Double seismic zone and dehydration embrittlement of the subducting slab. *Journal of Geophysical Research Solid Earth* 108(B4). Article Number 2212.
- Yaxley GM and Brey GP (2004) Phase relations of carbonate-bearing eclogite assemblages from 2.5 to 5.5 GPa: Implications for petrogenesis of carbonatites. *Contributions to Mineralogy and Petrology* 146: 606–619.
- Yaxley GM and Green DH (1994) Experimental demonstration of refractory carbonate-bearing eclogite and siliceous melt in the subduction regime. *Earth and Planetary Science Letters* 128: 313–325.
- Zack T, Rivers T, and Foley SF (2001) Cs-Rb-Ba systematics in phenite and amphibole: An assessment of fluid mobility at 2.0 GPa in eclogites from Tescolmen (Central Alps). *Contributions to Mineralogy and Petrology* 140: 651–669.